GEOMORPHOLOGY, STRATIGRAPHY, AND RADIOCARBON CHRONOLOGY OF LLANQUIHUE DRIFT IN THE AREA OF THE SOUTHERN LAKE DISTRICT, SENO RELONCAVÍ, AND ISLA GRANDE DE CHILOÉ, CHILE

BY
G.H. DENTON[1], T.V. LOWELL[2], C.J. HEUSSER[3], C. SCHLÜCHTER[4], B.G. ANDERSEN[5], LINDA E. HEUSSER[6], P.I. MORENO[7], and D.R. MARCHANT[8]

[1]Department of Geological Sciences and Institute for Quaternary Studies, Bryand Global Sciences Center, University of Maine, Orono, Maine, USA
[2]Department of Geology, University of Cincinnati, Cincinnati, Ohio, USA
[3]100 Clinton Road, Tuxedo, New York, USA
[4]Institute of Geology, University of Bern, Bern, Switzerland
[5]Institute for Geology, University of Oslo, Oslo, Norway
[6]Lamont-Doherty Earth Observatory, Palisades, New York, USA
[7]Institute for Quaternary Studies, University of Maine, Orono, Maine, USA
[8]Department of Geology, Boston University, Boston, Massachusetts, USA

Denton, G.H., Lowell, T.V., Heusser, C.J., Schlüchter, C., Andersen, B.G., Heusser, Linda E., Moreno, P.I. and Marchant, D.R., 1999: Geomorphology, stratigraphy, and radiocarbon chronology of Llanquihue drift in the area of the southern Lake District, Seno Reloncaví, and Isla Grande de Chiloé, Chile. *Geogr. Ann.*, 81 A (2): 167–229.

ABSTRACT. Glacial geomorphologic features composed of (or cut into) Llanquihue drift delineate former Andean piedmont glaciers in the region of the southern Chilean Lake District, Seno Reloncaví, Golfo de Ancud, and northern Golfo Corcovado during the last glaciation. These landforms include extensive moraine belts, main and subsidiary outwash plains, kame terraces, and meltwater spillways. Numerous radiocarbon dates document Andean ice advances into the moraine belts during the last glacial maximum (LGM) at 29,363–29,385 ^{14}C yr BP, 26,797 ^{14}C yr BP, 22,295–22,570 ^{14}C yr BP, and 14,805–14,869 ^{14}C yr BP. Advances may also have culminated at close to 21,000 ^{14}C yr BP, shortly before 17,800 ^{14}C yr BP, and shortly before 15,730 ^{14}C yr BP. The maximum at 22,295–22,567 ^{14}C yr BP was probably the most extensive of the LGM in the northern part of the field area, whereas that at 14,805–14,869 ^{14}C yr BP was the most extensive in the southern part. Snowline depression during these maxima was about 1000 m. Andean piedmont glaciers did not advance into the outer Llanquihue moraine belts during the portion of middle Llanquihue time between 29,385 ^{14}C yr BP and more than 39,660 ^{14}C yr BP. In the southern part of the field area, the Golfo de Ancud lobe, as well as the Golfo Corcovado lobe, achieved a maximum at the outermost Llanquihue moraine prior to 49,892 ^{14}C yr BP. Pollen analysis of the Taiquemó mire, which is located on this moraine, suggests that the old Llanquihue advance probably corresponds to the time of marine isotope stage 4. The implication is that the Andean snowline was then depressed as much as during the LGM. A Llanquihue-age glacier expansion into the outer moraine belts also occurred more than about 40,000 ^{14}C yr BP for the Lago Llanquihue piedmont glacier.

Introduction

This paper presents the geomorphology, stratigraphy, and radiocarbon chronology of extensive moraine belts deposited in the region of the southern Chilean Lake District and Seno Reloncaví, as well as on Isla Grande de Chiloé, by Andean piedmont ice lobes during the last glaciation. Along with the associated drift morphology and stratigraphy, the chronology establishes the duration of the last glacial maximum (LGM) and reveals the structure of the last glacial/interglacial transition. Integration of these middle-latitude Southern Hemisphere data into a global network of detailed paleoclimate records emerging from ice cores in both polar regions (Sowers and Bender 1995; Blunier *et al.* 1998; Steig *et al.* 1998), from deep-sea cores in the North Atlantic Ocean (Bond and Lotti 1995), and from the classic European late-glacial paleoclimate record may clarify mechanisms responsible for ice-age climate changes, as discussed in Denton *et al.* (1999).

The field area is in the north–south trending Valle Central at the western edge of the Cordillera

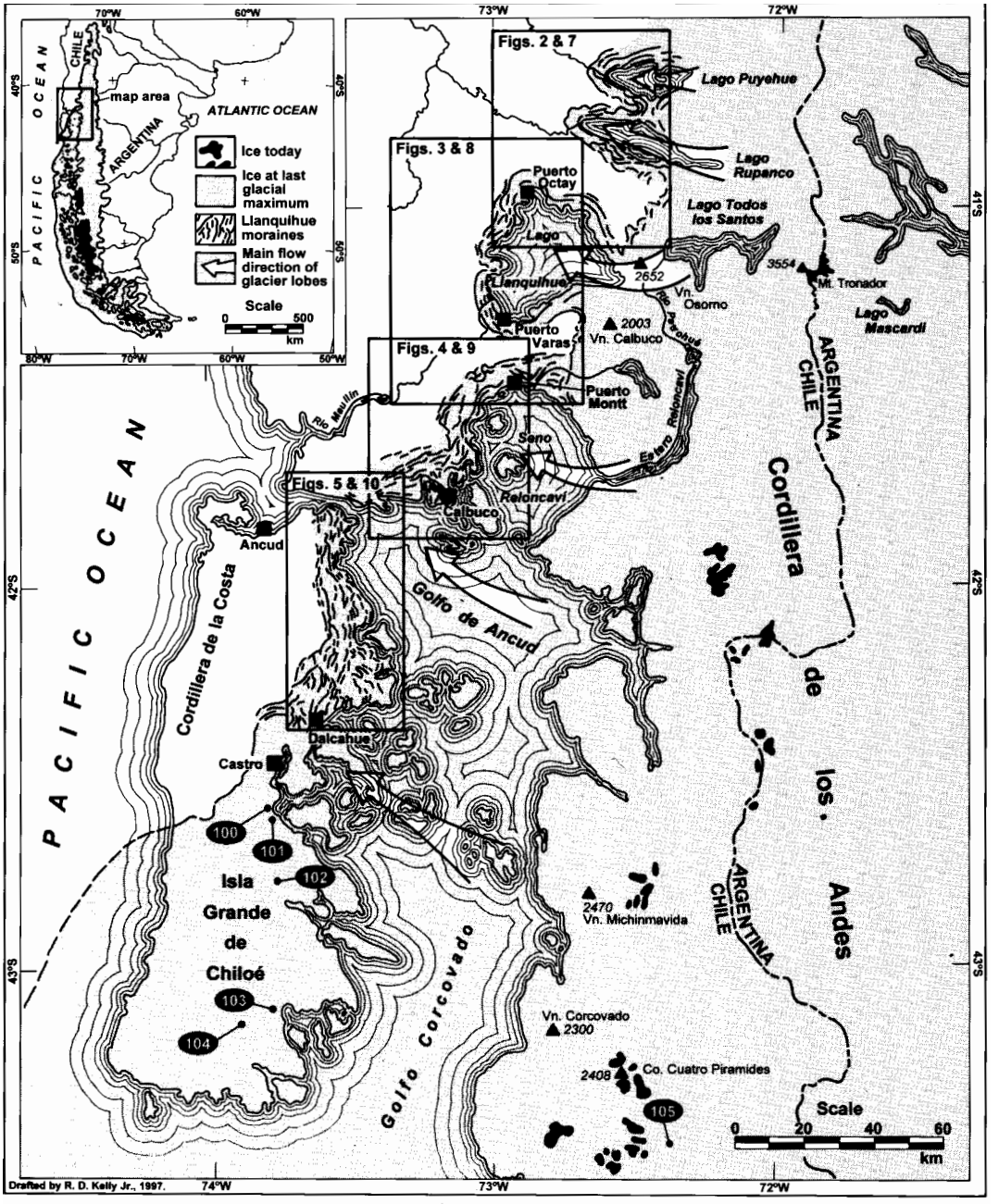

Fig. 1. Index map of the southern Lake District, Seno Reloncaví, and Isla Grande de Chiloé, Chile. The boxes show the locations of the glacial geomorphologic maps in Andersen *et al.* (1999) and in Figs 2–5. Valle Central is a large north-south trending depression in the center of the map occupied by the lakes and gulfs. The numbered sites refer to Table 1.

de los Andes between 40°30' and 42°25'S (Fig. 1). This sector of the Andes has a widespread low portion, with average summit elevations of 1500–2000 m, composed chiefly of crystalline rocks. Large volcanoes with summit elevations of 1900–3200 m form the highest peaks. The volcanoes above 2000 m elevation have extensive mantles of glacier ice, but only small glaciers are scattered on the lower crystalline peaks. The modern snowline in an east–west transect across the Andes at the latitude of Lago Llanquihue (41°15'S), estimated by Porter (1981) from the median elevation of glaciers on high volcanic peaks, rises inland from about 1900 m elevation at Volcán Calbuco alongside Lago Llanquihue to 2250 m elevation in the Argentine Andes.

The Cordillera de la Costa forms the western margin of Valle Central. The summits are generally 350–800 m in elevation, but in places are as much as 950 m. Today the Cordillera de la Costa is free of glacier ice.

Valle Central is largely above sea level and is about 80 km wide in the northern half of the field area. The dominant topographic features are large, deep lakes in basins occupied at the LGM by piedmont ice lobes emanating from the Andes. These lakes include Lago Puyehue (185 m elevation), Lago Rupanco (115 m), and Lago Llanquihue (51 m). Lago Llanquihue is commonly more than 200 m deep, with a maximum depth of 320 m. Moraine belts and outwash plains dating to the LGM fringe the western margins of these lakes. Separating the lakes are outwash plains and moraine belts, also largely dating to the LGM. Farther west, Valle Central features older moraine belts and associated outwash plains. The lakes drain westward through deep spillways. In the case of Lago Rupanco and Lago Llanquihue, the elevations of the outlets, and hence of the lake levels, are controlled by indurated, waterlain till deposits. Basalt bedrock controls outflow from Lago Puyehue. Río Pilmaiquén is the outlet for Lago Puyehue, and Río Rahue for Lago Rupanco. Río Maullín now drains Lago Llanquihue southwestward through moraine belts and outwash plains to the Pacific Ocean. A former eastern outlet for Lago Llanquihue extends into Río Petrohué, which flows into Estero Reloncaví.

In the southern half of the field area, Valle Central is about 120 km wide and dominated by marine embayments. Seno Reloncaví is commonly well over 250 m deep, with maximum depths of more than 450 m near Estero Reloncaví. At the LGM this embayment was filled by a piedmont glacier fed through Estero Reloncaví. Scallop-shaped bays mark the western shore. Islands separated from the mainland by sinuous channels occur near the western shore. Islands divided by short, straight channels nearly close off the southern margin of Seno Reloncaví.

South of Seno Reloncaví there is an abrupt increase in the size of marine gulfs that contained piedmont glaciers at the LGM. Seno Reloncaví is about the size of Lago Llanquihue, which in turn is larger than either Lago Rupanco or Lago Puyehue. But Golfo de Ancud, south of Seno Reloncaví, is much bigger than any of the water bodies farther north. It is commonly more than 250 m deep, and in places exceeds 300 m in depth. Just as with Seno Reloncaví, southern Golfo de Ancud is fringed by dissected islands of glacial deposits.

Northern Golfo Corcovado, with Isla Grande de Chiloé at its western edge, is relatively shallow with numerous islands of glacial deposits. Andean ice flowed across the gulf, around the southern end of Cordillera de la Costa, and over southern Isla Grande de Chiloé onto the Pacific continental shelf.

The southern part of the field area has characteristics of a drowned terrain. Canal de Chacao is likely the spillway of a former glacial lake in Golfo de Ancud. The canals and scallop-shaped bays along the western margins of Seno Reloncaví and Golfo de Ancud were probably eroded by former ice-marginal rivers that converged on Canal de Chacao. Taken together, Paso Tautil and Canal Calbuco represent the former outlet for a glacial lake in Seno Reloncaví. Marine channels between dissected islands along the southern margin of Seno Reloncaví may also have been spillways of a former glacial lake in Seno Reloncaví. In similar fashion, the canals and marine passes that separate numerous islands of glacial drift south of Golfo de Ancud may have originally been cut by rivers flowing between former lakes in present-day Golfo de Ancud and Golfo Corcovado. The drowned landscape must be partially due to the sea-level rise of the last deglaciation. But many submerged features are too deep to be explained entirely in this manner. The implication is of tectonic subsidence, consistent with submerged alerce (*Fitzroya cupressoides*) stumps on the north shore of Seno Reloncaví (Porter 1981).

The natural vegetation in the southern Lake District is illustrated along a transect from the southern Lake District inland across the Andes (see Heusser *et al.* 1999; Moreno *et al.* 1999). Here Lowland De-

ciduous Forest (up to 200 m elevation) is succeeded by Valdivian Evergreen Forest (200–600 m), North Patagonian Evergreen Forest (600–1000 m), and Subantarctic Deciduous Beech Forest (1000–1250 m) (Heusser 1974, 1981). The shrub-like beech *Nothofagus antarctica* occurs at tree line and in isolated locations to 1370 m. Above tree line is parkland and tundra consisting principally of grasses and ericaceous shrubs and herbs. Patches of Magellanic Moorland exist above 700 m in the coast range west of the southern Lake District. On the east slope of the coast range on Isla Grande de Chiloé, Valdivian Evergreen Forest extends to 250 m elevation and the North Patagonian Evergreen Forest extends from 250 to 450 m (Villagrán 1988; Heusser *et al.* 1996). Above 450 m elevation the vegetation becomes more open and North Patagonian tree species occur as enclaves in a Magellanic Moorland complex.

The evergreen forests and the high-elevation Magellanic Moorland complex reflect a cool-temperate wet climate that results from the cold, offshore Humboldt Current combined with the Southern Hemisphere westerlies. Cyclonic depressions are frequent throughout the year, resulting in high precipitation and extensive cloudiness. Close to sea level at Puerto Montt on the northern shore of Seno Reloncaví, mean annual temperature is 11.2°C, with a range from a winter mean of 7.7°C to a summer mean of 15.1°C; mean annual precipitation is 2341 mm (Hajek and di Castri 1975).

Previous work

In early studies Brüggen (1950), Weischet (1958, 1964), and Olivares (1967) recognized multiple moraine belts of different ages west of Lago Puyehue, Lago Rupanco, and Lago Llanquihue. Mercer (1972, 1976), and Laugenie and Mercer (1973) differentiated four moraine belts west of Lago Llanquihue, the younger three of which had been previously recognized by Brüggen (1950) and Olivares (1967). The drifts associated with these moraine belts were named, from youngest to oldest, the Llanquihue (Heusser 1974), Casma, Colegual, and Río Frío (Mercer 1976). Relative age characteristics suggest that these four drifts represent at least three, and perhaps four, glaciations. A radiocarbon chronology shows that only Llanquihue drift represents the last glaciation. Llanquihue drift is little weathered, with near-surface volcanic clasts exhibiting rinds of 0.5 mm or less. The permeable portions of the Casma and Colegual drifts both contain volcanic clasts with weathering rinds of about 2 cm and therefore may represent a single glaciation (Mercer 1976). Volcanic clasts in permeable portions of Río Frío drift have weathering rinds of 4 cm. Mercer (1976) suggested that the outermost group of Llanquihue moraines and outwash plains dates to >40,000 ^{14}C yr BP and is probably early Llanquihue in age. The late Llanquihue ice limit was placed well behind early Llanquihue moraines near Puerto Varas, at the outer edge of Llanquihue moraines near Frutillar Alto, and on the peninsula at the mouth of Bahía Muñoz Gamero (Mercer 1976). A reworked peat clast in outwash graded to the outermost late Llanquihue moraine near Frutillar Alto yielded an age of 20,100±550 ^{14}C yr BP (RL-116) (Mercer 1976). Basal peat from the Canal de Chanchán (named by Laugenie 1982) spillway channel yielded a date of 17,370±670 ^{14}C yr BP (RL-120) (Mercer 1976); a subsequent date of basal peat of 18,170±650 ^{14}C yr BP (GX-5274) is a minimum value for recession of ice lobe from the moraine at the mouth of Bahía Muñoz Gamero (J.H. Mercer, pers. comm. in Porter 1981). Thus the late Llanquihue advance of the Lago Llanquihue piedmont glacier was bracketed between 20,100 and 18,170 ^{14}C yr BP. For the adjacent Lago Rupanco piedmont lobe, dates of 19,450±350 ^{14}C yr BP (I-5679) and 21,360±840 ^{14}C yr BP (I-5678) (Mercer 1976; Heusser 1974) apply to ashy peat below till on the outer late Llanquihue moraine.

The subsequent history of the Lago Llanquihue ice lobe was reconstructed from lake-level fluctuations associated with the two main outlets (Brüggen 1950). One of these is the present-day Río Maullín outlet, anchored at about 51 m elevation by indurated waterlain till on the western lake shore. The former eastern outlet is now plugged by a lahar fan from Volcán Calbuco, but is still less than 10 m above present-day lake level (Mercer 1972, 1976). In a prominent terrace near Lago Llanquihue at Puerto Varas, organic beds are exposed in lakeside cliffs, in a road cut beside Calle Santa Rosa, and beneath the railroad bridge over Route V-50. The thin laminated lacustrine silt and clay on these organic beds are overlain first by thick deposits of unsorted pebbles and cobbles in a sandy matrix and then by ash and pumice washed onto the terrace by the lake (Mercer 1976). This sequence was interpreted as indicating ice recession from the eastern outlet of Lago Llanquihue in order for the lake level to drop enough for accumulation of organic sediments on the exposed terrace surface (Mercer 1976). Accumulation of organic sedi-

ments ended when a readvancing piedmont glacier lobe again blocked the eastern outlet, causing a rise in lake level and deposition of lacustrine sediments on the Puerto Varas terrace. This readvance extended to undated moraine ridges located on the southern margin of the lake 25 km from the western shore. The interval of deposition of the organic sediment, termed the Varas interstade by Mercer (1972, 1976), was originally estimated to have begun before 16,270±360 ^{14}C yr BP (RL-113) (wood fragment at base of organic silt at the railroad bridge site) and to have ended about 14,820±230 ^{14}C yr BP (I-5033) (top 5 mm of the organic bed at the Calle Santa Rosa site) (Mercer 1972). The end of organic accumulation, and hence lake-level rise, was subsequently revised to about 13,300 ^{14}C yr BP on the basis of three dates of peat and wood from the prominent organic bed at the railroad bridge site (13,300±550 ^{14}C yr BP, GX-2947; 13,200±320 ^{14}C yr BP, GX-4169; and 13,750±295 ^{14}C yr BP, GX-4170) (Heusser 1974, Mercer 1976).

In a delineation of moraine belts and drift sheets different from that of Mercer (1976), Porter (1981) recognized four drift sheets, each dominated by till, deposited by the Lago Llanquihue piedmont ice lobe; from youngest to oldest these were named the Llanquihue, Santa María, Río Llico, and Carocol. A type section was assigned for each drift sheet. Only the little-weathered Llanquihue drift was recognized as having distinctive morainal topography. The three older drift sheets were distinguished by relative weathering criteria. A wide belt of Santa María drift was mapped across most of the lowland west of the outer edge of Llanquihue drift. Santa María drift is more weathered than Llanquihue drift, in that it has a yellowish-brown color from limonite that coats clasts and penetrates fissures. Rind thicknesses on volcanic clasts near the surface of Santa María drift have a mean value of 2 mm. The broad crests within the Santa María drift sheet were described as moraine ridges or dissected remnants of a drift plain (Porter 1981). In any case, the Santa María drift includes the Río Frío, Casma, and Colegual drifts of Mercer (1976). Lying west of the Santa María drift, and exposed in a 10-km-wide surface belt near the Cordillera de la Costa, is the Río Llico drift. Till of this drift is weathered to clay, and volcanic clasts have mean weathering rinds of 10 mm. Carocol drift is largely buried by younger drifts and is highly weathered, with rinds on volcanic clasts having a mean thickness of 17 mm.

Porter (1981) subdivided Llanquihue drift into three units on the basis of morphostratigraphic and sedimentologic criteria. Type or reference sections were defined for Llanquihue I (the oldest and outermost), II, and III drifts. Each drift unit was mapped near Lago Llanquihue and Seno Reloncaví. Llanquihue I drift, which in most places comprises the outermost Llanquihue moraine belt, was certainly deposited more than 19,000 ^{14}C yr BP and probably much more than 40,000 ^{14}C yr BP (Porter 1981). The highest Llanquihue outwash plains are graded to the outer moraines of Llanquihue I drift. Llanquihue II drift comprises well-preserved moraines which, between Puerto Octay and Llanquihue, are fronted by outwash that passes around the Llanquihue I moraines. Near Puerto Varas, the Llanquihue II moraines are nested behind the Llanquihue I moraines. The Llanquihue II moraines were dated by Porter (1981) between 20,100±550 ^{14}C yr BP (RL-116) (the age of the reworked peat clast in outwash at Frutillar Alto; Mercer 1972) and 18,900±370 ^{14}C yr BP (UW-418) (the age of basal peat from Canal de la Puntilla). The Llanquihue III sediments in the Lago Llanquihue basin are confined to the lakeside terrace described by Mercer (1976), but in the Seno Reloncaví basin the Llanquihue III drift forms moraines situated only a few kilometers behind those of Llanquihue II age. On the northern shore of Seno Reloncaví, Llanquihue III till overlies laminated glaciolacustrine sediments; near the base of these sediments at Punta Penas is a 20-cm-thick peat bed that yielded dates of 15,220±160 ^{14}C yr BP (UW-422), 15,400±400 ^{14}C yr BP (W-948), and 14,200±135 ^{14}C yr BP (UW-421) (Ives *et al*. 1964; Porter 1981; Heusser 1981).

The organic beds in the Puerto Varas terrace are covered by a thin unit of glaciolacustrine sediments and/or by volcanic breccias that Porter (1981) interpreted as lahars. The volcanic breccias can be traced on the lake-margin terrace from Puerto Varas to near Volcán Calbuco, as well as between Puerto Varas and the Río Maullín outlet at the town of Llanquihue. Porter (1981) argued that the Lago Llanquihue piedmont ice lobe must have reached the western margin of the lake and stood against the terrace when the volcanic breccias were deposited by lahars that originated on Volcán Calbuco. Otherwise, the lahars would have discharged directly into the lake, rather than following the terrace surface along the lake edge to the Río Maullín outlet.

By obtaining new dates of 13,965±235 ^{14}C yr BP (UW-481) (Bella Vista Bluff site) and 13,145±235 ^{14}C yr BP (UW-480) (Northwest Bluff site) from or-

ganic beds in the Puerto Varas terrace, Porter (1981) postulated a more complex history of ice-margin fluctuations during Llanquihue III time than did Mercer (1976). From elevations and ages of the organic beds, Porter (1981) estimated that an ice advance (and associated rise of lake level) began prior to 15,700 ^{14}C yr BP and culminated at 15,000–14,000 ^{14}C yr BP. Following ice recession and lake-level drop, a second advance (and lake-level rise) was underway by 13,965 ^{14}C yr BP and culminated after 13,145 ^{14}C yr BP at the western margin of Lago Llanquihue when laharic breccias were deposited on the terrace.

Laugenie (1982) mapped moraine belts and outwash plains in the entire Chilean Lake District at a scale of 1:250,000. Near Lago Llanquihue, the Llanquihue moraine system of Laugenie (1982) corresponds with the Llanquihue drift of Porter (1981) and the Llanquihue moraine system of Mercer (1976). Laugenie (1982) divided the Llanquihue glaciation into three principal parts, each with subsidiary stades and interstades: Eo-Llanquihue (>40,000 ^{14}C yr BP), Meso-Llanquihue (25,000 to >40,000 ^{14}C yr BP), and Neo-Llanquihue (25,000 to 12,200 ^{14}C yr BP). The outermost Trapen moraine belt near Seno Reloncaví is assigned to the Eo-Llanquihue, along with the main outwash plain graded to this moraine. Most outer moraine belts fringing Lago Llanquihue (including the Puerto Varas moraine and the outer moraines near Bahía Muñzo Gamero) are also Eo-Llanquihue. Largely nested within these outer moraines are those of the Neo-Llanquihue, including the San Antonio moraine near Seno Reloncaví and the Frutillar moraine near Lago Llanquihue. The Neo-Llanquihue limit near Bahía Muñoz Gamero is placed not at the Puerto Chico moraine, as suggested by Mercer (1976), but at the moraines at the head of the two important spillway channels discussed earlier. Only near Bahía Frutillar does the Neo-Llanquihue moraine belt represent the outermost limit of the Llanquihue-age piedmont ice lobe, here dated by Mercer (1972) to shortly after 20,100 ^{14}C yr BP. Following the Puerto Varas interstade at 16,270–13,200 ^{14}C yr BP, the Ensenada readvance, the last of Neo-Llanquihue age, reached the Río Pescado moraine belt south of Lago Llanquihue (Laugenie 1982).

Meso-Llanquihue time was marked by restricted Andean glaciers (Laugenie 1982), and the environment is defined by a pollen diagram from near Laguna Bonita alongside Lago Rupanco (Heusser 1974). The older Moraine de Casma and Moraine de Colegual, each fronted by an extensive outwash plain (Laugenie 1982), correspond with the Casma and Colegual moraines and drift of Mercer (1976). Laugenie (1982) suggested that both moraines date to the Colegual glaciation. The Moraine de Fresia of Laugenie (1982), deposited during the Fresia Glaciation, corresponds with the Río Frío moraine belt of Mercer (1976).

On Isla Grande de Chiloé, Heusser and Flint (1977) mapped three major drifts and associated moraine belts; from oldest to youngest these are Fuerte San Antonio drift, Intermediate drift, and Llanquihue drift. A mire situated on the outermost Llanquihue moraine at Taiquemó afforded a basal age of 42,400±1000 ^{14}C yr BP (QL-1012) (Heusser 1990). Dates of 14,355±700 ^{14}C yr BP (GX-8686), 14,970±210 ^{14}C yr BP (I-12996), and 15,600±560 ^{14}C yr BP (GX-9978) come from a wood layer on the surface of an organic deposit buried by Llanquihue drift at Dalcahue (Mercer 1984). Samples from deeper in the organic deposit are as old as 17,750±560 ^{14}C yr BP (Beta-33820) and 19,630±180 ^{14}C yr BP (QL-4324) (Heusser 1990), affording a minimum age for underlying Llanquihue till. At the Teguaco section, interdrift organic silt yielded dates of 25,500±500 ^{14}C yr BP (QL-1017) to 30,000±300 ^{14}C yr BP (QL-1019) (Heusser 1990). Finally, dates of basal organic samples from mires on the Llanquihue moraine belt on Isla Grande de Chiloé indicate deglaciation prior to 13,000 ^{14}C yr BP (Heusser 1990).

Methods

Five steps were involved in establishing a radiocarbon chronology of Llanquihue drift and landforms. The first was to produce glacial geomorphologic maps of Llanquihue drift west of Lago Puyehue, Lago Rupanco, Lago Llanquihue, Seno Reloncaví, Golfo de Ancud, and northern Golfo Corcovado. Extensive aerial photographic analysis resulted in the production of preliminary maps, which were extensively field checked over six years. After additional aerial photographic analysis, the results were integrated into the maps in Andersen *et al.* (1999) and in Figs 2–6.

The second step was to interpret the sediments exposed in borrow pits, road cuts, and natural sections within each morphologic unit distinguished on the maps. The third step was to describe the key stratigraphic sections. The fourth step was to date multiple radiocarbon samples from stratigraphic sections, particularly where glacial sediments rest

on undisturbed old landscape surfaces. Organic interdrift deposits were subjected to pollen analysis. The fifth step was extensive coring of mires and lakes in closed depressions on Llanquihue moraine belts. A square-rod Wright piston head was used to collect overlapping cores from deep mires for pollen analysis, and a motor-driven piston head was used to obtain 50-cm-long sediment cores from the base of mires.

We did not establish formal rock-stratigraphic units for Llanquihue drifts, each defined by type and reference sections, because we could trace individual lithologic units for only short distances, as sections are not closely spaced. Also, many individual units exposed in stratigraphic sections are laterally discontinuous. In addition, we could not establish morphostratigraphic units because the Llanquihue moraine belts feature discontinuous cross-cutting ridges, in places with palimpsest landforms.

Glacial geomorphology

Figures 2–5 are glacial geomorphologic maps from Andersen *et al.* (1999) of Llanquihue drift belts in the area of the southern Lake District, Seno Reloncaví, and northern Isla Grande de Chiloé. The three main glacial geomorphologic features are outwash plains, moraine belts, and kame terraces.

Outwash plains

Except in a few places, the highest and most prominent Llanquihue outwash plains grade to the outermost Llanquihue moraine belts. Distal ends of the highest outwash plains converge toward the major drainage systems that pass westward through or around the Cordillera de la Costa. For example, the main outwash plains that head at moraines deposited by the northern Lago Llanquihue, the Lago Rupanco, and the southern Lago Puyehue piedmont glaciers all converge into Río Rahue, which is a tributary of a major river that flows westward to the Pacific Ocean. Another example is where the main outwash terraces of the southern Lago Llanquihue lobe and the entire Seno Reloncaví lobe converge into Río Maullín. A third example occurs on Isla Grande de Chiloé. Here the northern sector of the main outwash plain converges on Canal de Chacao, whereas the central sector converges on Río Butalcura, which flows northwestward through the coastal range to the Pacific Ocean.

Subsidiary Llanquihue outwash terraces are situated behind the outermost Llanquihue moraine belts. These terraces are lower and less extensive than the main Llanquihue outwash plains. At their proximal ends they grade to subsidiary Llanquihue moraine belts. At their distal ends they pass through the outermost Llanquihue moraines in channels that then become set within the main outwash plain. They eventually converge into westward-flowing drainage systems, such as Río Maullín in the southern sector of the former Lago Llanquihue lobe and Río Chanchán in the northern sector. In places, the narrow subsidiary terraces progressively merge with the main outwash terrace with increasing distance from the outermost Llanquihue moraine belt.

From Fig. 3 it is evident that several of long channels leading westward from subsidiary moraine belts are incised into the main outwash plain west of Lago Llanquihue. These channels captured meltwater outflow from the Lago Llanquihue piedmont glacier when it stood at the subsidiary moraines. Although these channels were initially occupied by meltwater, some may also have been spillways for small lakes dammed between the moraine belt and the piedmont ice lobe during initial recession. But the Río Maullín channel, incised as much as 40 m into the main Llanquihue terrace, took over as the major outlet as soon as ice cleared the western shore of Lago Llanquihue, stranding the intakes of other channels high in the moraine system. Hence these high channels were active only when the ice margin stood at a subsidiary moraine or at the upper edge of the ice-contact slope above Lago Llanquihue.

Figs 2–6 (see PLATES 1–5 in separate cover)

Fig. 2. Glacial geomorphologic map of the area of Lago Puyehue and Lago Rupanco. Plate 1.

Fig. 3. Glacial geomorphologic map of the Lago Llanquihue area. Plate 2.

Fig. 4. Glacial geomorphologic map of the Seno Reloncaví area. Plate 3.

Fig. 5. Glacial geomorphologic map of the northern sector of eastern Isla Grande de Chiloé. Plate 4.

Fig. 6. Explanation for Figs 2–5. Plate 5.

The two most important of the stranded meltwater channels are Canal de Chanchán and Canal de la Puntilla (Fig. 3). Both pass through the Llanquihue moraine belts and both originate at the crest of the ice-contact slope about 130 m above the present level of Bahía Muñoz Gamero. Both were originally cut and occupied by meltwater outflow from the Lago Llanquihue piedmont glacier when it stood against this ice-contact slope. Now banked against the slope are lacustrine terraces about 70 m above the current lake level. These terraces were formed in a local lake dammed by an ice lobe in Bahía Muñoz Gamero. It is probable that the Chanchán and Puntilla meltwater channels also served as spillways for this ice-marginal lake.

The geometry of the Chanchán and Puntilla channels defines their central role in the chronology of the Llanquihue moraine belt. The dates of 18,900±370 ^{14}C yr BP (UW-418) previously obtained for basal organic material in Canal de la Puntilla and of 18,170±650 ^{14}C yr BP (GX-5274) from Canal de Chanchán (Porter 1981) afford minimum ages for the two Llanquihue moraine systems distal to the lakeside ice-contact slope where the channels originate. The inner system is traced by Laugenie (1982) to the outer Llanquihue moraine at Frutillar Alto, where a reworked organic clast in coeval outwash afforded an age of 20,100 ±500 (RL-116) (Mercer 1976) (site 13 in Table 1 pp. 216–229). As pointed out above, this geomorphologic situation was the basis for placing the maximum of the Lago Llanquihue piedmont ice lobe between 20,100 and 18,900 ^{14}C yr BP (Porter 1981). However, as outlined below, we were not able to replicate this moraine tracing from Frutillar Alto northeastward to the Chanchán and Puntilla channels.

Overall, the main Llanquihue outwash plain is generally graded to the outermost Llanquihue moraine belt and converges to the main fluvial drainages through the coastal mountains to the Pacific Ocean. This plain extends through gaps in pre-Llanquihue moraine ridges. Dissected into this plain are long, narrow meltwater channels that head at subsidiary Llanquihue moraines or at lakeside ice-contact slopes. Some of these channels merge into the main outwash plain with increasing distance from the outermost Llanquihue moraine belt. But most form a fluvial network that drains westward into the Pacific Ocean.

Moraine belts

Numerous individual ridges and hillocks together form broad moraine belts that are continuous for as much as 20 km, particularly where separated from other moraine belts by subsidiary outwash terraces. For example, two (and in places three) complex moraine belts can be traced along the western margin of Seno Reloncaví (Fig. 4). Moraine belts are difficult to discriminate where they are juxtaposed without intervening terraces. In places, moraine belts intersect at a sharp angle and are inferred to be cross-cutting.

Individual hills and ridges within moraine belts range from 2 m to as much as 20 m in relief. They are commonly surrounded by gently undulating morainal topography. Steep ice-contact slopes occur on the proximal sides of moraine belts. Hill-and-ridge elements within each moraine belt show the lobate configuration of former ice margins. For example, such elements reflect small sublobes in embayments along the western margin of Lago Llanquihue (Fig. 3). Prominent ice-contact slopes occur at the head of outwash terraces or on the proximal side of individual moraine elements. They link the complex matrix of ridges and hills to individual ice-marginal positions. The resulting patterns of such slopes, as for example in Fig. 3, show numerous closely spaced ice-marginal positions that are commonly cross-cutting. Mapping of this detailed pattern shows that the outer Llanquihue moraines between Frutillar Alto and Canal de Chanchán do not represent a single contemporaneous ice margin of the Lago Llanquihue piedmont glacier (Fig. 3). Thus, unlike Laugenie (1982), we were not able to trace a distinct Llanquihue moraine belt from Frutillar Alto to the Puntilla and Chanchán meltwater spillway channels. For example, the outermost moraine at Frutillar Alto cross-cuts and is proximal to a slightly older moraine element about 2 km northeast of the key radiocarbon site of Mercer (1976). About 12 km northeast of Frutillar Alto, this moraine element again cross-cuts the outer moraine, and then itself forms the outer Llanquihue moraine element for the next 6 km to the north. Some 4 km southwest of Canal de la Puntilla, the outer moraine is cut in turn by a younger moraine element that forms the outermost ice-margin position near the critical Puntilla and Chanchán channels. The innermost moraine system cut by these channels has a major ice-contact slope on its proximal side where the channels originate. Fig. 3 shows that these innermost moraines

also cannot be matched with the outer moraine at Frutillar Alto. Rather, the outer Llanquihue moraine near the Puntilla meltwater channel is younger than the Frutillar moraine element, and hence the moraines at the head of the Puntilla and Chanchán channels are younger still.

Such cross-cutting relationships carry the implication that the main Llanquihue outwash terrace is graded to a complex of moraines of slightly differing ages, and therefore itself cannot be strictly of one age. A similar example comes from the moraine belts west of Seno Reloncaví, which are spread farther apart than those west of Lago Llanquihue. As a consequence the intermoraine areas are filled with subsidiary outwash terraces that converge on drainage gaps through the outer moraine belt and are incised into the main Llanquihue outwash plain, where they form tributaries to the major Río Maullín drainage channel from Lago Llanquihue. But the outer moraine belt itself is composed of numerous individual elements that are overlapping or occur one behind the other. The detailed map pattern of these elements in Fig. 4 suggests that the outer moraine belt may represent several fluctuations of the Seno Reloncaví piedmont glacier.

The configuration of the Llanquihue moraine belts, along with the trend of surface till flutes, shows the intersection of two former piedmont glaciers northwest of Calbuco (Seno Reloncaví lobe in the north and Golfo de Ancud lobe in the south). In Fig. 4 the outermost moraine in the north appears to be cut by younger moraines at this intersection. The implication is that the younger advance was stronger for the southern than for the northern lobe, with ice from the southern lobe riding far up onto the mainland. These overlapping moraines again point to the probability that the main Llanquihue outwash plain is composite. North of the intersection zone, the main outwash plain is graded to an outer prominent moraine belt west of Seno Reloncaví. South of the intersection zone, this outer belt is dissected and nearly buried by outwash from the inner moraine belt, which here is close to the maximum Llanquihue position. Outwash graded to this inner belt surrounds and passes through the remnants of the outer moraine belt.

Mapping of moraine morphology along the outer Llanquihue drift limit west of Lago Llanquihue is complicated by outwash folded into ridges parallel to the former ice margin (Fig. 3). These folded ridges, described as push moraines (Schlüchter *et al*. 1999), occur in four patches northeast of Frutillar Alto. The southern two patches have single ridges, whereas the northern two patches have multiple ridges. Individual ridges are as much as 15 m in relief and up to 1 km in length.

Kame terraces

The third major morphologic feature depicted in Figs 2–5 involves kame terraces banked against high ice-contact slopes alongside Lago Llanquihue and Bahía Puerto Montt. A prominent terrace, in places up to 1 km broad, fringes much of the western and southern shores of Lago Llanquihue. On promontories north of the Río Maullín outlet, the position of coarse outwash in the terrace requires a buttressing ice lobe. In embayments the terrace is composed largely of lacustrine sediments, again requiring an adjacent ice lobe. All the lakeside terraces are depicted as kame terraces in Fig. 3, with some ice-contact slopes modified by wave action.

Kame terraces alongside Bahía Muñoz Gamero are composed of lacustrine sediments and have surface elevations of as much as 130–145 m. Most are banked against an ice-contact slope about 30–40 m elevation below the intakes for the Chanchán and Puntilla channels. A large terrace, again with a surface elevation of about 130 m, has an ice-contact slope that merges into the long moraine ridge projecting part of the way across the mouth of Bahía Muñoz Gamero as Punta Centinela (Fig. 3). As depicted in Fig. 3, Punta Centinela is on line with a prominent moraine ridge that trends east–west about 1 km inland from the northern lake shore. Laugenie (1982) referred to this ridge as the Puerto Chico moraine. Terraces occur on both the proximal and the distal side of the Puerto Chico moraine. The inner lacustrine terraces probably formed beside an ice lobe that still filled much of Bahía Muñoz Gamero shortly after recession from the bayside ice-contact slope. As mentioned above, this high ice-marginal lake in Bahía Muñoz Gamero probably drained westward through the Chanchán and Puntilla channels. The moraine and terrace near Punta Centinela most likely reflect a separate ice advance. Fig. 3 shows that the shores of Lago Llanquihue east and southwest of Bahía Muñoz Gamero lack significant lake-marginal terraces. Instead, kame terraces along the northern lake shore east of Bahía Muñoz Gamero have moraines on their proximal sides and reflect an ice lobe that extended out of the main lake basin. Likewise, the ice-marginal deposits alongside Bahía Rincones, and as far south as the north shore of Bahía Frutillar, do not feature kame terraces. In fact, extensive terraces extend only from the

north shore of Bahía Frutillar to the Río Maullín outlet at the town of Llanquihue. It is also evident from Fig. 3 that the lakeside terraces at Bahía Frutillar are not continuous with those at Bahía Muñoz Gamero. Therefore, kame terraces cannot be connected as a continuous system from the Río Maullín outlet northward to Bahía Muñoz Gamero.

In Fig. 3 we mapped a continuous kame terrace alongside southern and western Lago Llanquihue for 65 km from Punta Cabras to Bahía Frutillar. From both north and south, the surface of this terrace declines to a common elevation of about 70 m at the Río Maullín outlet. It seems probable that this terrace represents a coherent ice-marginal position of the former Lago Llanquihue piedmont glacier, a situation compatible with the presence of debris-flow volcanic breccia on the terrace surface south of the Río Maullín outlet. There are at least three, and perhaps four, such debris-flow deposits. They are generally sandy, although some have coarse pumice and angular andesite clasts. Most exhibit crude vertical sorting. Some fill erosional channels as much as 2 m deep. Laminated glaciolacustrine sediments occur between some of the debris-flow units. Porter (1981) attributed these sediment flows to lahars from Volcán Calbuco, whereas H. Moreno (pers. comm. 1996) attributes them to debris flows associated with periodic outbursts of a lake dammed on the northern flank of Volcán Calbuco by the former Lago Llanquihue piedmont ice lobe. In either case the distribution of the debris-flow sediments requires that the Lago Llanquihue ice lobe stood against the terrace. Thus our reconstruction is similar to that of Porter (1981), except that we are not able to trace a continuous kame terrace north of Bahía Frutillar.

Prominent kame terraces near Bahía Puerto Montt occur on the distal side of a discontinuous Llanquihue moraine belt along the upper lip of an extensive bayside ice-contact slope (Fig. 4). This moraine belt consists of small ridge fragments that mark the marginal position of the former Seno Reloncaví piedmont glacier when the prominent kame terraces were formed. Other fragmentary ice-contact deposits are on the proximal side of smaller and lower terraces beside Bahía Puerto Montt. Overall, the geometry of the terraces and associated ice-marginal features shows that Rió Coihuín, which now flows from Volcán Calbuco directly into Seno Reloncaví, was deflected along the kame terraces by a blocking Seno Reloncaví piedmont glacier. The resulting ice-marginal river built the prominent kame terraces near Bahía Puerto Montt, and then flowed northeast to Río Maullín, depositing subsidiary outwash terraces. Farther south extensive subsidiary terraces separate Llanquihue moraine belts of the Seno Reloncaví piedmont glacier. The proximal ends of these terraces are graded to the inner moraine belt adjacent to Bahía Puerto Montt. The distal ends converge into narrow channels. One of these tributary channels exits southward from the subsidiary plain and joins the channel of Río Gomez, which cuts through Llanquihue moraine belts and the main Llanquihue outwash plain. The Río Gomez channel also formed the main outflow for a similar subsidiary terrace that heads at the inner moraine system northwest of Calbuco.

Overall, Fig. 4 shows that high kame terraces near Bahía Puerto Montt merge into an extensive system of subsidiary outwash terraces, all of which drain to Río Maullín in narrow channels that cut through both the outermost Llanquihue moraine belts and the main outwash plain. These kame terraces all head at an inner moraine belt at the top of an ice-contact slope beside Seno Reloncaví. Near Bahía Puerto Montt is a complex of small kame terraces banked against the lower portions of this ice-contact slope. These terraces, many of which have small moraine remnants on their ice-contact edges, were deposited by ice-marginal streams as the Seno Reloncaví piedmont glacier lobe downwasted from the top of the gulfside ice-contact slope.

Glacial sediments

Five major types of glacial deposits make up Llanquihue drift; gravelly diamicton, lodgement till, waterlain till, outwash, and laminated glaciolacustrine sediments. In addition, *in-situ* and reworked pyroclastic flows from Andean volcanoes mantle moraine belts and outwash plains; remnants of flow sediments also occur between glacial units in stratigraphic sections. Fig. 7 shows a schematic diagram of how these five major types of deposits fit into a glaciogenic facies model related to morphological units depicted in Figs 2–5.

Gravelly diamicton and lodgement till

Complex glaciogenic sequences dominated by gravelly diamicton form moraine cores. These sequences are as much as 10 m thick and feature massive to faintly bedded gravelly diamicton separated by lenses of sand and sorted gravelly outwash. At their distal ends, they are interlayered with outwash or lacustrine sediments. The enclosed clasts are

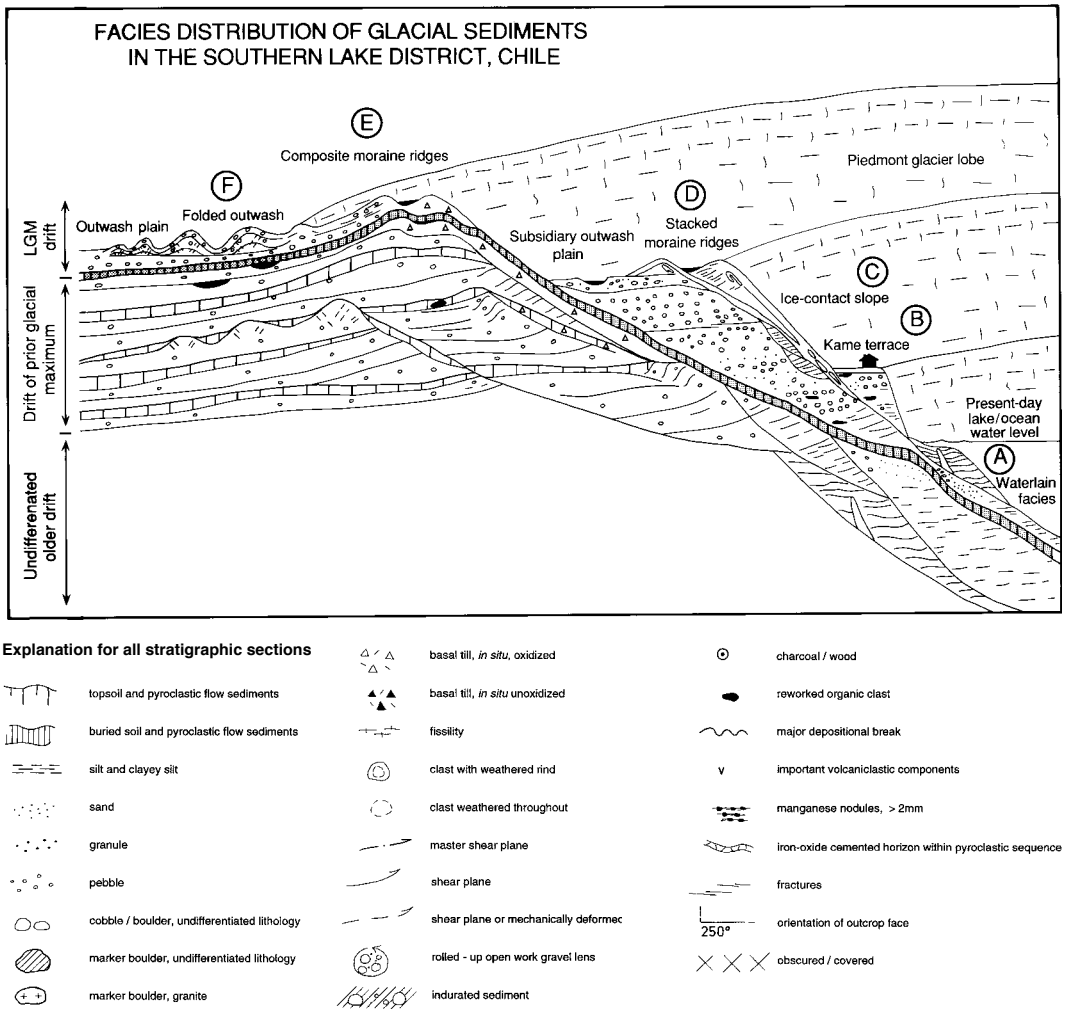

Fig. 7. Facies model of glaciogenic deposits in the southern Lake District. The cross-sections focus on the moraine belts along the western margin of lakes in Valle Central. The relic land surface prior to the LGM is accented to show the facies left during one glacial cycle (above) separated from the complex of facies left during earlier glacial cycles (below). Details for each of the major units are shown in the corresponding diagrams (A–F). (A) Waterlain facies. Sediment supply is from super-, en- and subglacial positions, but in all cases the depositional processes occur primarily in the proglacial lake. Subglacial till is absent, but local low-amplitude folding, faulting, and injection of clastic dikes indicate large-scale fracturing of sediments. Deformation is limited to soft-sediment units that were deposited rapidly. See Turbek and Lowell (1999) for additional details. (B) A kame terrace. Such a terrace may be composite from more than one glacial advance as outlined by the darker lines. Deposition in the lower portions is in a subaqueous environment, but a transition to subaerial deposition commonly occurs within the stratigraphic sequence that makes up the terrace. Debris-flow sediments of volcanic breccia occur on the terrace surface (Porter 1981). (C) An ice-contact slope. Glacial overrunning serves to smooth such slopes by infilling topographic lows and by eroding topographic highs. Injections, clastic dikes, and transported blocks are common in the lower parts of such slopes, and lodgement till is common at the tops of such slopes. See Turbek and Lowell (1999) for additional details. (D) Stacked moraine ridges that represent ice-marginal positions and may occur along the top of ice-contact slopes. The sediments in these ridges vary from lodgement till to gravelly sediment flows, with most material being stratified. Deformation and transport of inclusions are limited to the proximal sides of such ridges. (E) Composite moraine ridges that represent ice margins reoccupying the same place several times. Ridge cores may be deeply weathered, with pyroclastic flow sediments separating internal deposits of different ages. Erosion on the proximal side may result in old sediments being at or near the present land surface. (F) Ridges composed of outwash folded beyond the former ice margin (Schlüchter *et al.* 1999). Such ridges occur in a few restricted areas. A detachment plane probably occurs within the outwash at the base of the folds.

Fig. 7. Continued.

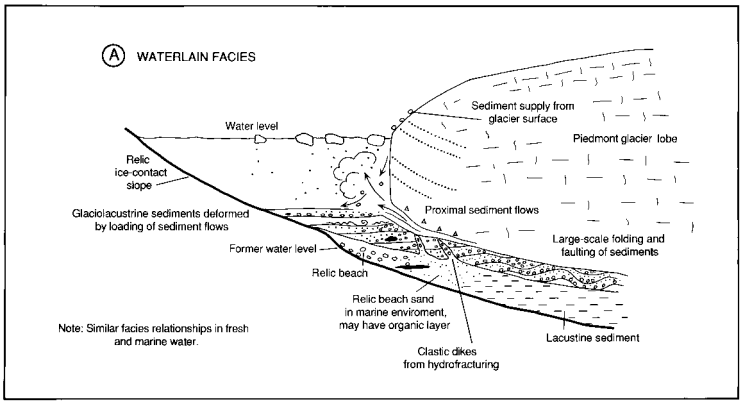

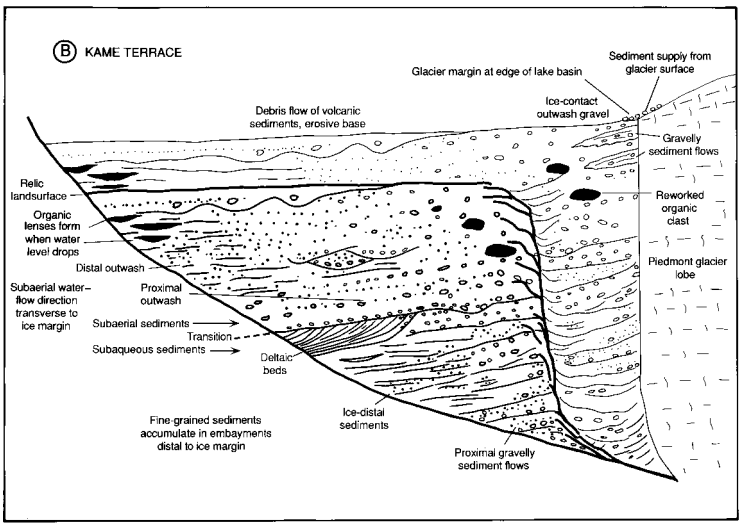

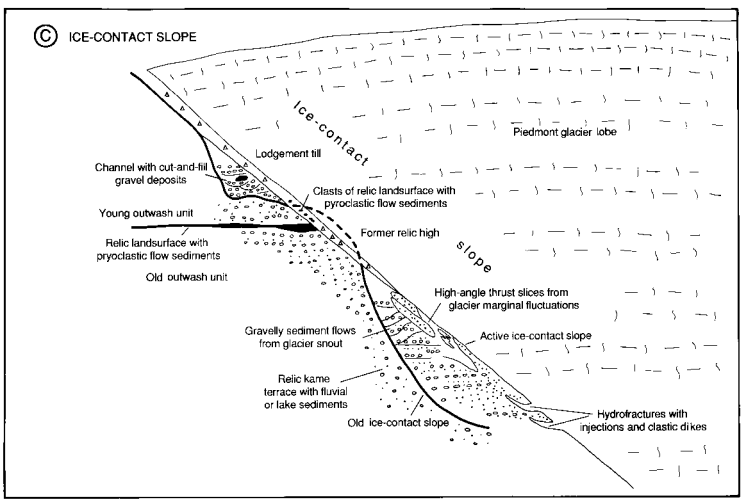

Fig. 7. Continued.

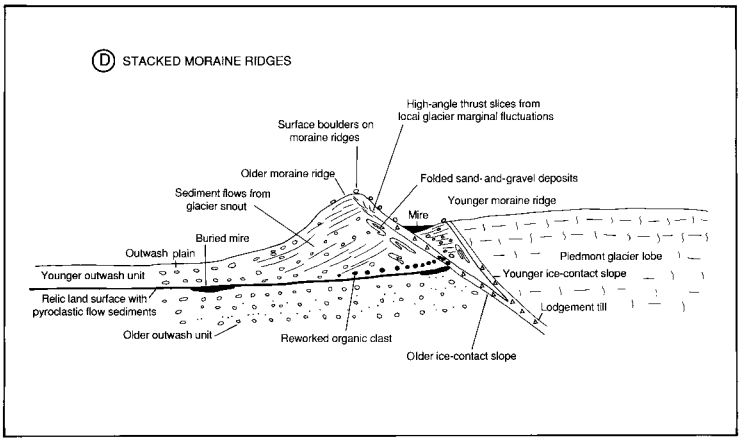

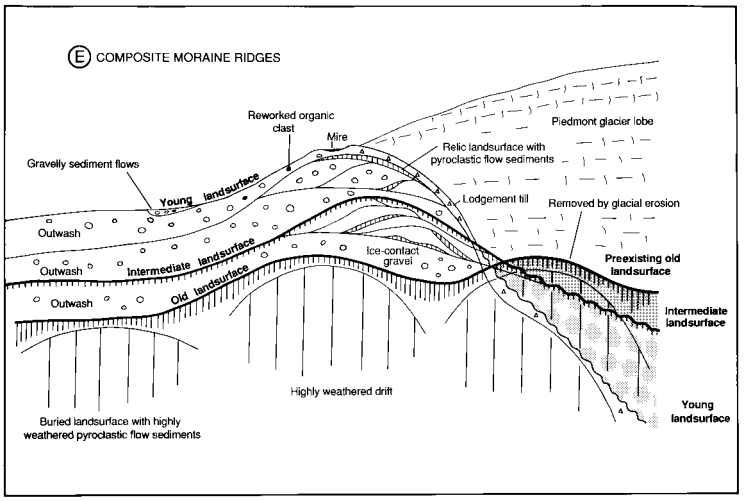

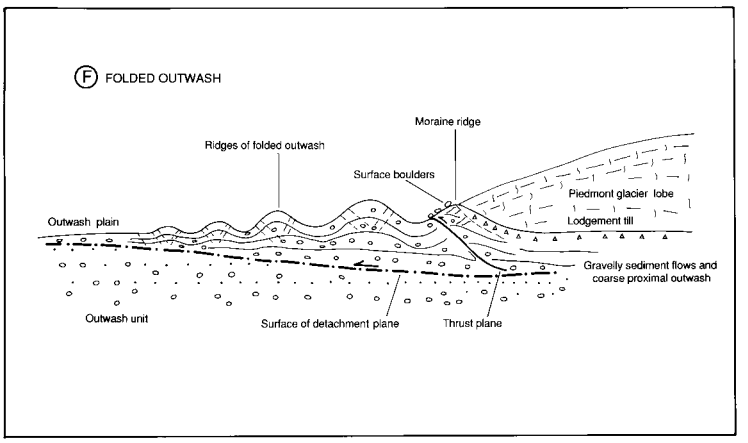

volcanic and crystalline rocks from the Andes. We interpret the faintly bedded diamictons as gravelly sediment flows from former ice margins at the proximal edges of moraine ridges and hillocks. The banded appearance comes from the stacking of several individual sediment flows within each moraine core. Fig. 7D shows a schematic example of such a moraine core. Because most clasts in the gravelly diamictons are round to subround, the flow material was probably derived from outwash terraces and former moraine cores overrun by advancing ice.

Compact diamicton mantles many moraines and ice-contact slopes (Fig. 7). This diamicton commonly achieves a thickness of 0.5–1.5 m, although in places it is as much as 3 m thick. It is light-to-medium gray in color, compact, stony, and non-sorted. Clasts are volcanic and crystalline rocks from the Andes. Most clasts are round to subround and up to cobble size. Some are striated. The diamicton commonly exhibits well-developed fissility, features lenses and boudins, and contains isolated large, oriented boulders. Fissility is associated with severe shear deformation that in places slices large boulders. We interpret this massive, compact diamicton as lodgement till. A separate facies, located beneath the lodgement till, involves faintly bedded diamicton layers formed by gravity flows from adjacent advancing ice.

Both the gravelly glaciogenic sequences and the till units have been deformed in many places, with conspicuous shearing and stacking of lenses. Well-developed shear planes have slickensides and oriented, pushed, and rolled boulders. Compression joints are common.

Waterlain till

Waterlain till is widespread near the present-day water level along the western shore of Lago Rupanco, Lago Llanquihue, and Seno Reloncaví, as well as along the eastern coast of northern Isla Grande de Chiloé. Because it is so indurated, this waterlain till controls the outlet elevations of Lago Rupanco and Lago Llanquihue.

Figure 7A illustrates our view of the origin of waterlain till. It typically consists of laminated glaciolacustrine sediments with lenses and discontinuous beds of coarse material, including cobbles of volcanic and crystalline rocks from the Andes (Figs 8, 9). These coarse sediments represent a flow regimen featuring turbidites at all scales, with highly developed grading distal from the former ice margin. Convolutions and interfingering of fine and crude stratification form irregular contact surfaces. There is occasional compaction faulting. Abrupt facies changes are common. Most cobbles in the turbidites are subangular to subround, and some are striated. Diapirs derived from underlying beds are commonly injected into these coarse lenses and beds. Flame and diapir structures are also present within the lacustrine beds themselves. In addition, the lacustrine sediments show slump structures with consequent folding of individual beds, including one case with a bed rolled around itself. Other structures include clastic dikes of diamicton injected along joint planes within lacustrine sediments. The waterlain units are folded near promontories. Fine bedding in lacustrine beds, turbidites, and loading structures of waterlain till are preserved in detail. Basal lodgement till does not occur near the lake edge below the modern high-water level. Above the high-water mark, the waterlain till passes beneath an organic bed within a kame terrace near the town of Llanquihue, and grades to surface lodgement till along the north shore of Bahía Puerto Montt.

Outwash

Outwash of the main and subsidiary Llanquihue terraces shows coarsening toward the moraines that mark coeval ice margins (Fig. 10), where subround-to-round clasts of Andean origin are as much as 0.3 m in diameter. In places, the outwash contains reworked organic clasts derived from peat and soils developed on pyroclastic flow deposits. The standard glaciofluvial outwash facies consists of horizontally stratified, medium-to-bouldery gravel, with all transitions from sandy diamicton to openwork gravel. Laminar cross-bedding is present, but not dominant. The outwash has extensive sand units. In positions near the former ice margins, it also contains massive, bouldery-to-sandy grain flows that commonly disrupt pre-existing bedding. In places, the advancing ice subjected the outwash to mechanical reworking, faulting, folding (with overturned folds), boudinage, and elongations. Figs 11 and 12 give typical examples of outwash deformed by advancing ice, whereas Fig. 13 shows

Figs 8–10, *see p. 189.*

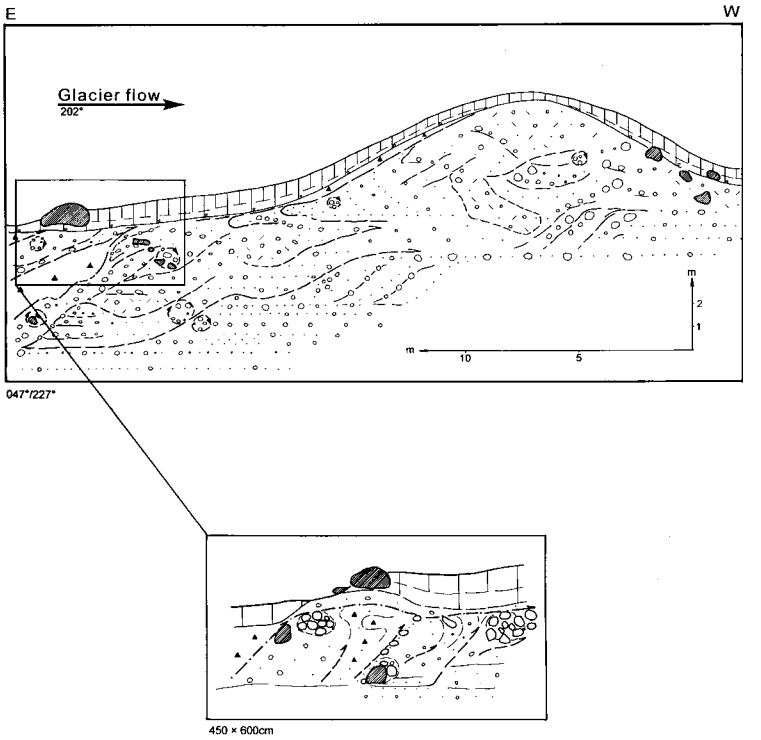

Fig. 11. Site 31 on east side of Route 5 south of Puerto Varas. Location is given in Fig. 15. See legend in Fig. 7 (p. 177) for lithologic details. The lithological section records the features produced by an advancing ice lobe that highly deformed its own ice-contact outwash sediments. The easternmost sector of the outcrop displays mechanically reworked stacks of gravel with rolled-up gravel-lens structures. The glacier margin advanced to the top of the ridge, with continuing deformation of the outwash. Toward the top of the section there was increasing accumulation of flow till. The inset shows stacking of gravelly outwash with intense deformation (rolled-up lenses) and till beds cut by steep shear planes. The radiocarbon samples listed in Table 1 for site 31 do not come from this section, but rather from another nearby borrow pit on the west side of Route 5.

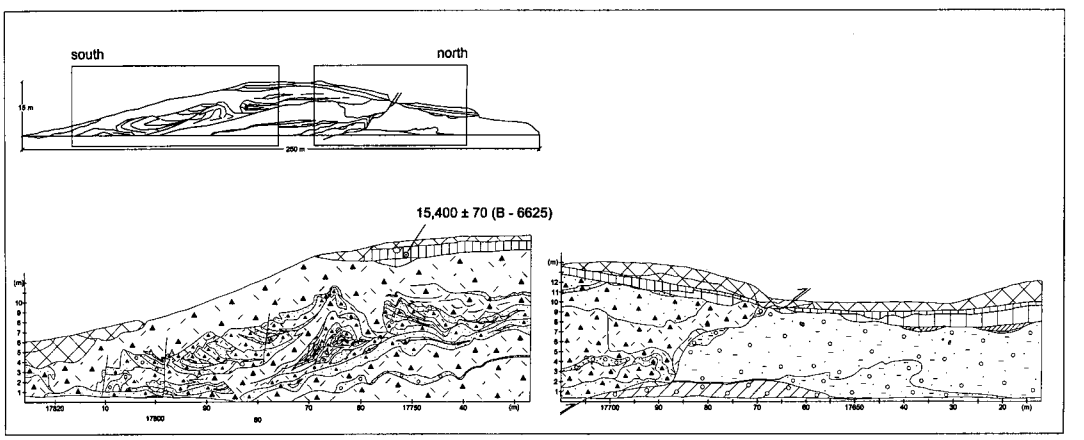

Fig. 12. Road cut showing stratigraphic section through the core of a Llanquihue moraine ridge beside Route 5 at site 33 in Fig. 15. See legend in Fig. 7 (p. 177) for lithologic details. The section shows highly deformed glaciofluvial gravel and till thrust onto a core of older fine-grained diamicton (open hatched signature) and outwash. The main ridge of the deformed sediment (southern sector) can be interpreted as two compressed and thrust folds. The morphological expression of this deformation is a pronounced moraine ridge. The radiocarbon samples listed in Table 1 for the core of the moraine at site 33 are from a borrow pit 150 m west of this road cut.

Table 2. Error-weighted mean of radiocarbon dates of individual organic beds in selected stratigraphic exposures. The locations of these exposures are plotted by site number in Figs 14–17. The individual radiocarbon dates are listed in Table 1. The individual organic beds are described in the text.

Site No.	Description	Total number of dates	Weighted mean of all dates (^{14}C yr BP)	Original test statistic	Number of dates remaining**	Weighted mean of final dates (^{14}C yr BP)	Final test statistic	Samples removed in order indicated
7	Top of Puerto Octay organic bed	5	29,363±178	4.23*	5	29,363±178	4.23	
16	Top of Bahía Frutillar Bajo organic bed (Fig. 25)	17	26,797±65	130.6	10	26,437±84	15.9	AA-13734, A-7656, UGA-6915, UGA-6819, UGA-6817, UGA-6820, UGA-6818
23	Top of Llanquihue organic bed (Fig. 18)	8	14,869±38	16.2	7	14,822±41	7.97	A-8173
26	Lower of two thin peat beds at railroad bridge, Puerto Varas (Fig. 22)	4	14,550±54	5.57*	4	14,550±54	5.57	
26	Top 7 cm of prominent 26-cm-thick organic bed at railroad bridge, Puerto Varas (Fig. 22)	10	14,613±25	60.2	7	14,510±30	10.9	QL-1335, A-8175, A-8553
28	Top of Northwest Bluff organic bed	2	14,882±72	0.47*	2	14,882±72	0.47	
30	Top of Bella Vista Bluff organic bed (Fig. 20)	8	14,540±29	36.4	7	14,610±32	3.97	A-9189
46	Top of upper peat bed at Canal Tenglo (Fig. 29)	2	23,059±87	0.43*	2	23,059±87	0.43	
46	Top of peat bed at Canal Tenglo (Fig. 29)	6	29,385±95	38.2	4	29,414±112	3.7	A-8172, A-8171
47	Top of upper of two thin organic beds at Punta Penas (Fig. 28)	4	14,879±42	7.78*	4	14,879±42	7.78	
47	Top of lower of two thin organic beds at Punta Penas (Fig. 28)	3	15,554±60	11.59	2	15,671±69	0.01	AA-21009
86	Top of organic bed	4	22,570±87	1/61*	4	22,570±87	1.74	
97	Top of Teguaco organic bed	12	22,295±40	69.23	9	22,398±46	14.3	A-7729, AA-13732, A-7710
98	Top of Dalcahue organic bed (Fig. 31)	34	14,805±19	98.3	29	14,793±20	40.9	UGA-6983, AA-13710, A-7716, UGA-6921, AA-13730

* no evidence to reject the null hypothesis that the observations are consistent at 0.05 level.
** Ages making the largest contribution to T were sequentially removed and the average recalculated until the test statistic fell to values where the null hypothesis could not be rejected at the 0.05 level.
Procedures follow Ward and Wilson (1978).

undeformed outwash overlain by a moraine. A special type of feature in deformed outwash involves the reorganization of open-work lenses into rolled-up gravel balls. Most deformation involves high-angle shear planes. Some clasts are broken by loading. Deformation of sand units produced compaction folds with conjugated faults.

Glaciolacustrine sediments

Glaciolacustrine sediments are widespread in kame terraces beside Lago Llanquihue and beneath till alongside northern Seno Reloncaví. These sediments feature sandy silty rhythmites, and were deposited rapidly. In places they have enclosed dropstones.

Fig. 13, *see p. 192.*

Pyroclastic deposits

Fine-to-coarse pyroclastic sediment, ranging from 0.5 m to several meters in thickness, covers moraine belts, outwash plains, and kame terraces. It also makes up interdrift sediments exposed in stratigraphic sections. The glass component of this material is weathered, but feldspar crystals, pumice lithics, and small pieces of charcoal are commonly well preserved. The deposits thicken in depressions and thin on moraine ridges and hills. This volcanic material likely represents the aggregate accumulation from successive pyroclastic flows from Andean volcanoes. Some individual flows crossing the Lake District were hot enough to reduce wood to charcoal, still enclosed in the pyroclastic sediments. It is difficult to determine the thickness of individual flows, because in the field area they are not usually separated by airfall tephras. However, the overall fine grain size suggests that only the thin distal facies of the flows are present west of Lago Llanquihue and Seno Reloncaví, as well as on Isla Grande de Chiloé.

Glaciogenic features and moraine preservation

Two features in Fig. 7 deserve further comment. The first is that some moraines and kame terraces are sheared and stacked. The other is that many ice-contact slopes commonly exhibit complex glacial deposits from several ice advances. The implication is that the individual ice-contact slopes in Figs 2–5 do not necessarily depict a single ice-marginal position, but may have been occupied repeatedly.

Clay minerals produced by rapid weathering of interstitial volcanic glass cement drift in the southern Lake District. The result is a striking preservation of glacial landforms, not only of Llanquihue but also of pre-Llanquihue age. We made use of this preservation of moraine belts and outwash plains, along with the relative weathering differences in till in the moraine belts, to separate Llanquihue from older drifts. Individual moraine belts, commonly separated by outwash plains, can be delineated as in Fig. 3. For example, the main Llanquihue outwash plain depicted in Fig. 3 separates a prominent set of moraines fringing Lago Llanquihue from older moraines and outwash plains farther to the west. Weathering of near-surface till in these successive moraine belts shows consistently sharp differences that correspond with morphologic boundaries. Till in moraine belts near the lakes is virtually unweathered. Porter (1981) reported weathering rinds of as much as 0.5 mm on near-surface volcanic clasts in this till. Oxidation of the matrix is slight and confined to the upper meter. Except where it is very compact, the till in the older end-moraine systems is colored yellowish-brown through its observed thickness from limonite staining along fissures and in clast sockets. On the basis of this weathering difference, then, the moraine belt fringing Lago Llanquihue is composed of Llanquihue drift and the older moraines are composed of Casma/Colegual drift. The two well-preserved moraine belts (each fronted by an outwash plain) that we mapped west of the Llanquihue moraine belts (Fig. 3) are equivalent to the Casma and Colegual moraines of Mercer (1976) and Laugenie (1982).

Radiocarbon dates of Llanquihue drift

Table 1 gives more than 450 new radiocarbon dates of Llanquihue drift deposited by the Lago Rupanco, Lago Llanquihue, Seno Reloncaví, Golfo de Ancud, and northern part of the Golfo Corcovado piedmont glaciers. Table 2 gives weighted mean dates of selected individual organic beds within drift sequences. Site numbers for radiocarbon samples are listed in Table l and plotted in Figs 14–17 and in Fig 1. Additional dates for pollen diagrams are given in Heusser *et al*. (1999) and Moreno *et al*. (1999). We now discuss the most pertinent of the dates from the regions of Lago Rupanco, Lago Llanquihue, Seno Reloncaví, and northern Isla Grande de Chiloé, in

Figs 14–17 (see PLATES 6–9 in separate cover)

Fig. 14. Location of radiocarbon sample sites and stratigraphic sections cited in Table 1 and in text for Lago Puyehue and Lago Rupanco map sheet of Fig. 2. Plate 6.

Fig. 15. Location of radiocarbon sample sites and stratigraphic sections cited in Table 1 and in text for Lago Llanquihue map sheet of Fig. 3. Plate 7.

Fig. 16. Location of radiocarbon sample sites and stratigraphic sections cited in Table 1 and in text for Seno Reloncaví map sheet of Fig. 4. Plate 8.

Fig. 17. Location of radiocarbon sample sites and stratigraphic sections cited in Table 1 and in text for Isla Grande de Chiloé map sheet of Fig. 5. Plate 9.

each case starting with the youngest and progressing to the oldest dates. See Bentley (1997) for additional new radiocarbon dates from near Lago Puyehue.

Lago Rupanco Region

Limiting maximum radiocarbon dates for the outermost late Llanquihue moraine near Lago Rupanco come from the borrow pit at site 1. Mercer (1976) reported an age of 19,450±350 (I-5679) for ashy peat just below till at this site. The specific sample locality has been destroyed as the borrow pit has been expanded. The pit now features a cap of lodgement till over a moraine core of mechanically dislocated glaciofluvial and organic beds. In only one locality, in the southeast corner of the pit, is there an undisturbed transformation from peat sealed with gray silt giving way upward to sand and till. A sample from the peat–silt contact yielded an age of 22,460±135 ^{14}C yr BP (A-9516) (Table 1), which we take to be a close maximum for ice advance because the youngest dates of additional samples from translocated organic beds beneath the till cap are 22,560±495 ^{14}C yr BP (T-9660A) and 22,745±295 ^{14}C yr BP (T-10309A) (Table 1).

Lago Llanquihue Region

Lakeside kame terraces. The prominent kame terrace beside Lago Llanquihue is dated at several localities. An important section occurs on the lakeside edge of the terrace near the town of Llanquihue about 2 km south of the Río Maullín outlet (site 23) (Figs 18 and 19). Situated 3.0 m above the present-day lake level, an organic silt bed near the base of this section contains fossil beetles and wood fragments. Eight dates of wood from near the top of this bed yielded an error-weighted mean of 14,869±38 ^{14}C yr BP (Tables 1 and 2, Fig. 18). A small wood piece from near the base of the organic bed yielded an AMS date of 15,600±120 (AA-21939) (Fig. 18). Thus the organic bed was deposited between 14,869 and 15,600 ^{14}C yr BP.

The Llanquihue organic bed represents an interval when lake level was near or even below its present-day value. Below the organic bed is a compact unit of waterlain till that represents glacier advance across the site. Above the organic bed are glaciofluvial units that make up the kame terrace. Nearby, the terrace is capped by debris-flow sediment composed of silt-to-coarse-sand-sized pyroclastic material. The Lago Llanquihue piedmont glacier must have been at or very close to the current outer edge of the terrace to allow deposition of the glaciofluvial units in this topographic situation on the organic bed. It still must have been in essentially the same position when the debris-flow volcanic sediments were deposited on the terrace surface. Therefore, the Llanquihue site affords evidence for an advance of the Lago Llanquihue ice margin to a position alongside the prominent kame terrace on the western lake shore at 14,869 ^{14}C yr BP, with the ice persisting until deposition of the debris-flow volcanic sediments on the terrace surface.

An organic bed in the kame terrace at Puerto Phillippi (site 19) is sealed by glaciolacustrine sediments. The top of this bed dates to 14,650±75 ^{14}C yr BP (A-9423).

We obtained new dates from three stratigraphic sections in the kame terrace at Puerto Varas. At Bella Vista Bluff (site 30) a recent slip revealed a fresh exposure of the organic bed and lacustrine sediments (Figs 20 and 21) previously reported by Porter (1981). The organic bed, located near the center of the section, is 23 cm thick. Two wood pieces (each about 20 × 8 cm) occur within glaciolacustrine sediments 8 cm above this bed. These pieces, both probably washed into the lake, afforded ages of 14,430±140 ^{14}C yr BP (A-6322) and 14,655±75 ^{14}C yr BP (A-8546) (Table 1). *In-situ* organic litter (with twigs) sealed with glaciolacustrine sediments occurs on the top surface of the bed at 60.97 m elevation (the present lake level varies but is close to 51 m elevation). Samples from this litter yielded ages of 14,715±85 ^{14}C yr BP (A-8549R), 14,560±95 ^{14}C yr BP (T-9656A), 14,595 $^{+80}_{-75}$ ^{14}C yr BP (A-9187), 14,585±80 ^{14}C yr BP (A-9191), 14,600±75 ^{14}C yr BP (A-9185), and 14,135 $^{+80}_{-75}$ ^{14}C yr BP (A-9189) (Table 1). The weighted mean is 14,540±29 ^{14}C yr BP (Table 2). Most basal samples from the organic bed date to 15,200–15,300 ^{14}C yr BP, but the oldest are 15,635±95 ^{14}C yr BP (A-8550) and 15,730±160 ^{14}C yr BP (A-9190). Therefore, the Bella Vista Bluff organic bed was deposited between about 15,700 and 14,532 ^{14}C yr BP, very

Fig. 19, *see p. 192*.
Fig. 21, *see p. 192*.

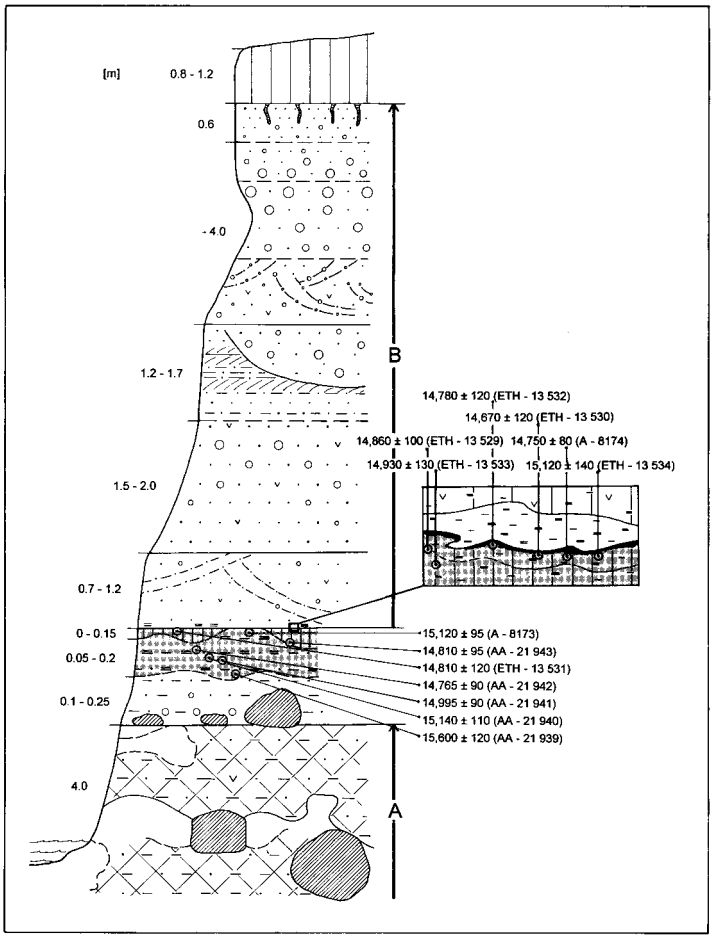

Fig. 18. Composite lithostratigraphy of lakeside cliff section near the town of Llanquihue at site 23 in Fig. 15. See legend in Fig. 7 (p. 177) for lithologic details. Radiocarbon dates are described in Table 1. Unit A is waterlain till at the base of the section, indicative of glacier advance. It consists of strongly deformed silty sand and sand, interbedded with laminated clayey silt and with flows of massive-to-bedded diamicton that includes boulders and cobbles. Unit A is overlain by a nonglacial complex with numerous radiocarbon samples. It consists of a fining-upward sequence, with basal boulders and silty to sandy gravel grading upward into massive clayey sandy silt with beetle and wood fragments, which is overlain first by clayey silt and clayey peat with wood fragments and then by clayey silt with wood fragments. The non-glacial beds are only preserved at this locality; they are missing a few meters to the south and approximately 10 m to the north. Unit B is a coarsening-upward sequence grading from bedded-to-cross-bedded, medium-to-coarse sand, with pumice clasts and rip-up fragments from lower units, into sandy gravel and sand with well-developed climbing ripples and then to massive and cross-bedded gravel. A high amount of volcaniclastic sand occurs throughout the upper part of the section. This sequence represents the ice advance responsible for the kame terrace. Unit B is overlain by topsoil developed in pyroclastic flow sediments.

close to the age range of the organic bed near the town of Llanquihue. The Bella Vista bed is a lateral continuation of the one that previously yielded an age of 13,965±235 ^{14}C yr BP (UW-481) (Porter 1981); the reason for the difference is not known (Table 1, Fig. 20).

Below the Bella Vista organic bed are gray, horizontally bedded glaciolacustrine sediments, without dropstones, that give way upward to beach sand. Above the organic bed is laminated glaciolacustrine silt, overlain sharply along a bedding plane by at least three units of debris-flow volcanic breccia (3–4 m thick). Glaciolacustrine sediments separate the lowest two volcanic flow deposits. The highly erosive flows that deposited the lowest breccia unit peeled away lacustrine sediments along a bedding plane and overturned them into a fold. The orientation of this fold indicates that the debris flow passed from south to north across the top of the terrace.

At Northwest Bluff (site 28) an organic bed at 63 m elevation rests on a coarse gravel deposit in the lakeside terrace (Porter 1981). The top of the organic bed is sealed by glaciolacustrine silt and fine sand, which in turn is overlain by several units of the same debris-flow volcanic breccia found at Bella Vista Bluff. Two samples from the sealed top of the organic bed yielded ages of 14,825±110 ^{14}C yr BP (A-9523) and 14,925±95 ^{14}C yr BP (A-9524) (Table 1); the weighted mean is 14,882±72 ^{14}C yr BP (Table 2). This is the same organic bed that previously yielded an age of 13,145±235 ^{14}C yr BP (UW-480) (Porter 1981), an unexplained discrepancy.

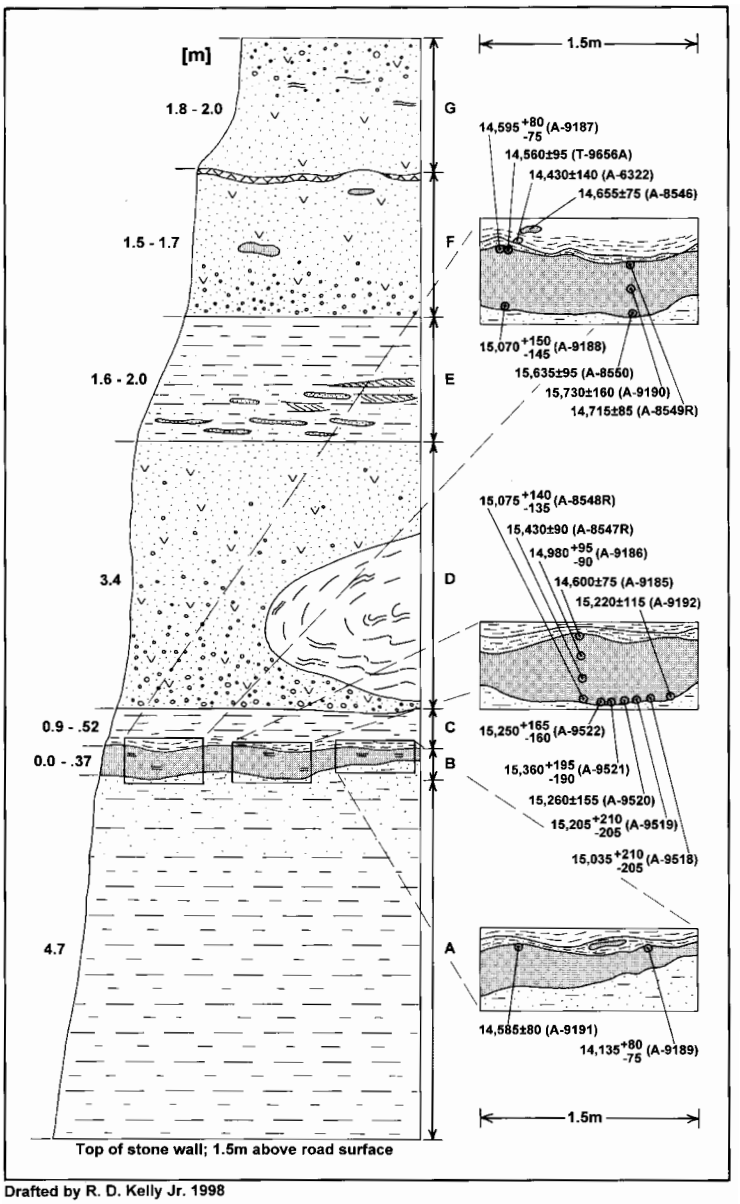

Fig. 20. Schematic composite lithostratigraphy of stratigraphic section at Bella Vista Bluff (site 30 in Fig. 15), Puerto Varas. See legend in Fig. 7 (p. 177)for lithologic details. Unit A is laminated glaciolacustrine clay and silt coarsening upward to silt at the top of the unit. Unit B is an organic bed (up to 26 cm thick) capped by lacustrine silts and clays that make up unit C; wood fragments (up to 15 cm long and 7 cm in diameter) occur in the organic bed and again in lacustrine silts and clays 3 to 10 cm above the organic bed. Unit D is composed of debris-flow deposits of volcanic breccia that fine upward from granules and gravel at the base to coarse sand at the top; folded beds of lacustrine sediment occur within unit D, either as rip-up clasts or as rotated lacustrine beds partially entrained in debris-flow sediments. Unit E is a fining-upward sequence of lacustrine sand and silt. The coarse fraction (medium-grained sand) is composed of volcanic pumice; numerous climbing ripples and diapirs occur near the base of unit E. Unit F is a debris-flow deposit that fines upward and includes some organic rip-up clasts. This unit shows a sharp planar contact with the underlying lacustrine sediments. Unit G is the uppermost debris-flow unit of volcanic breccia that forms the terrace surface. The topmost 40 cm feature large (1–2 cm diameter) pumice fragments; the base of this unit is cemented with iron oxides, forming an indurated layer 5 cm thick on top of the intermediate debris-flow unit. Insets give details of organic bed and of radiocarbon sample localities.

We obtained new dates from the railroad bridge site (26) of Heusser (1974), Mercer (1976), Porter (1981), and Hoganson and Ashworth (1992) in western Puerto Varas. Heusser (1974) previously described the section as exposing, from top to bottom, laharic sediments as reinterpreted by Porter (1981) (470 cm), peat (10 cm), gyttja (70 cm), peat (5 cm), gyttja (165 cm), and gravel (75 cm). A piece of wood from 15 cm above the base of the lower gyttja dated to 16,270±360 ^{14}C yr BP (RL-113) (Mercer 1972, 1976; Heusser 1974). The base of the upper, 10-cm-thick peat bed yielded an age of 14,250±400 ^{14}C yr BP (GX-2948), and the top of this peat bed gave an age of 13,300±550 ^{14}C yr BP (GX-2947) (Heusser 1974). Additional ages given by Mercer (1976) of this upper organic bed are 13,200±320 ^{14}C yr BP (GX-4169) for the uppermost 0.5 cm of peat and 13,750±295

^{14}C yr BP (GX-4170) for wood at 2 cm depth. Hoganson and Ashworth (1992) reported an age of 14,060±450 ^{14}C yr BP (GX - 5507) for the top of the peat bed.

It proved difficult for us to piece together the stratigraphic section, because a concrete retaining wall and two abutments have been built since the site was first described. We therefore received permission from town officials to re-excavate key portions of the section including the part now behind the retaining wall. Fig. 22 gives our interpretation of the section on the south side of Route V-50 near the railroad bridge, based on the new hand-dug excavations, as well as on notes from S.C. Porter and A. Ashworth (written comm. 1996). The lowermost unit consists of horizontally laminated glaciolacustrine silt with dropstones, 48 cm thick, exposed 14 m east of the railroad abutment. Poorly sorted, coarse gravel with a sandy matrix, 92 cm thick, rests on the glaciolacustrine unit. The upper surface of the gravel unit dips downward toward the west. The crystalline and volcanic erratics within this deposit were derived from the Andes. One granite boulder is 50 cm long. About 9 m east of the railroad abutment, organic silt, 26 cm thick with a faint gyttja layer, occurs between the gravel unit below and the debris flow of volcanic breccia above. The organic silt is exposed laterally for at least 5 m. It comfortably overlies the gravel unit, and has a highly eroded contact with the overlying volcanic debris-flow sediments. Several diapirs of organic silt rise into the overlying debris-flow sediments.

In the re-excavated portion of the section behind the retaining wall described by Heusser (1974) and Hoganson and Ashworth (1992), organic silt, 1.68 m thick with wood pieces (one in vertical growth position) and diffuse brown bands, rests on sand and gravel. This silt is capped by a 26-cm-thick organic layer with peat and wood. The top of the organic layer, in turn, is sealed by a 29-cm-thick massive, coarsening-upward volcanic sand unit. This volcanic sand is overlain, in turn, by a silt unit with two 1-cm-thick peat beds that include small wood fragments. The upper 4.2 m of the exposed section feature several compact, massive units of volcanic breccia emplaced by debris flows across the site, just as at Bella Vista Bluff and Northwest Bluff. Pyroclastic flow deposits cap the sequence where it is undisturbed.

We think that the gravel unit exposed 14 m east of the abutment corresponds with the gravel unit described by Heusser (1974) and Mercer (1976) at the base of the section behind the retaining wall. This gravel unit, in turn, probably corresponds with gravel exposed on the laminated glaciolacustrine silt unit west of the concrete abutment for the road overpass. The organic silt resting on the gravel east of the railroad bridge abutment almost surely matches the thick lower organic silt unit between the abutments. The same debris-flow volcanic breccias extend across the entire section. The upper peat beds are missing east of the railroad abutment, probably due to erosion by debris flows. The sudden loading from the emplacement of the debris-flow volcanic sediments produced diapirs of organic silt. Our correlations suggest that both the coarse gravel unit and the laminated lacustrine sediment with dropstones, both exposed 7–14 m east of the railroad abutment, project stratigraphically below the organic silt and peat beds between the abutments.

We undertook extensive dating of the two thin peat layers encased in the silt that overlies the 29-cm-thick massive volcanic sand unit above the prominent organic bed. Our first attempt yielded unsatisfactory results, because we had not yet received permission to reopen the excavation and hence were forced to sample in an area with potential rootlet and groundwater contamination. When subjected to standard acid–base–acid pretreatment, fibrous peat from the upper of the two thin layers yielded an age of 12,840±90 ^{14}C yr BP (AA-7459); a redating of the same sample after strong acid–base–acid pretreatment afforded an age of 13,940±85 ^{14}C yr BP (AA-7459B). This discordance suggests contamination by humates. An age of 14,175±110 ^{14}C yr BP (AA-7460) was obtained for a fibrous peat sample from the lower of the two thin layers. But this date may also be too young, as a small wood piece from the same horizon gave an age of 14,600±110 ^{14}C yr BP (AA-7465) with standard acid–base–acid pretreatment and of 14,350± 90 ^{14}C yr BP (AA-7465C) with acid–base–acid pretreatment and then extraction of cellulose. Another small wood sample from the lower of the two thin peat layers yielded ages of 14,290±100 ^{14}C yr BP and 14,460±85 ^{14}C yr BP (ETH-13528) for the same graphite target. But a complete redating with separate pretreatment yielded an anomalously

Fig. 22, *see p. 190.*

young age of 12,950±100 ^{14}C yr BP (ETH-13528), again suggesting contamination. Therefore we consider this initial set of dates from the two thin peat beds to be unreliable.

Following re-excavation, we collected four uncontaminated samples from the lower of the two thin peat layers that yielded concordant ages of 14,600±100 ^{14}C yr BP (AA-21011), 14,360±100 ^{14}C yr BP (AA-21012), 14,570±150 ^{14}C yr BP (AA-21013), and 14,680±100 ^{14}C yr BP (AA-21014) (Table 1); the weighted mean is 14,550±54 ^{14}C yr BP (Table 2).

The prominent 26-cm-thick organic bed has pockets of wood in the upper 7 cm. We subdivided three individual wood samples in order to obtain replicate ages for each. Replicates of one sample were 14,415±70 ^{14}C yr BP (A-9193) and 14,475 $^{+75}_{-70}$ ^{14}C yr BP (A-8551). Replicates of another wood sample were 14,620±90 ^{14}C yr BP (A-9194) and 14,735±75 ^{14}C yr BP (A-8553). The third replicate set gave ages of 14,570 $^{+80}_{-75}$ ^{14}C yr BP (A-8554) and 14,520 $^{+80}_{-75}$ ^{14}C yr BP (A-9195). Individual dates of other wood samples from this same horizon are 14,625±75 ^{14}C yr BP (A-8552), 14,930 ±80 ^{14}C yr BP (A-8175), and 14,285 $^{+110}_{-105}$ ^{14}C yr BP (A-8775) (Table 1). Porter (1981; written comm., 1996) reported a date of 15,050±100 ^{14}C yr BP (QL-1335) for wood from this horizon (Table 1). Overall, the weighted mean age for wood samples from the upper 7 cm of the organic bed is 14,613± 25 ^{14}C yr BP (Table 2). It was samples from this 26-cm-thick organic layer that previously yielded ages of 13,200 to 14,200 ^{14}C yr BP (Heusser 1974; Mercer 1976; Hoganson and Ashworth 1992). Again, the reason for the discrepancies of these earlier ages with our new dates is not known.

We obtained 11 new dates of wood pieces from varying depths in the organic silt and sand unit that underlies the 26-cm-thick organic bed (Table 1, Fig. 22). These dates range from 17,320±140 ^{14}C yr BP (AA-23726) to 17,880±140 ^{14}C yr BP (AA-23732), implying rapid deposition of the silt and sand unit. Three dates of a small tree in growth position 116–126 cm below the top of the silt and sand unit are: 17,505±150 ^{14}C yr BP (A-9526.l), 17,520 ±140 ^{14}C yr BP (AA-23729), and 17,790±140 ^{14}C yr BP (AA-23731). All the new dates are considerably older than the age of 16,270±360 ^{14}C yr BP reported earlier for wood from near the base of the silt unit (Mercer 1972, 1976; Heusser 1974). Again, the reason for the discrepancy is not known.

At the Calle Santa Rosa site (site 27) in Puerto Varas, situated about halfway between the railroad bridge and Bella Vista Bluff, Mercer (1976) described an organic bed between units of horizontally laminated glaciolacustrine sediment. Here the kame terrace is also capped by the debris flows of volcanic breccia present at Bella Vista Bluff, Northwest Bluff and the railroad bridge site. Organic matter sealed at the surface of the organic bed at 62 m elevation (Porter 1981) at the Calle Santa Rosa site yielded an age of 14,820±230 ^{14}C yr BP (I-5033) (Mercer 1976).

From this revised chronology, we subdivide the sediments in the kame terrace at Puerto Varas into a threefold sequence; the units above the organic beds, the organic beds themselves, and the units below the organic beds. Exposed below the organic beds is horizontally laminated lacustrine silt without dropstones at the Bella Vista Bluff (Fig. 20), Bella Vista Park (Porter 1981), and Calle Santa Rosa (Mercer 1972, 1976) sites. At the Northwest Bluff site, gravel underlies the organic bed (Porter 1981). At the railroad bridge site, a thin gravel unit and laminated glaciolacustrine silt with dropstones underlie the organic beds. Above the organic beds are glaciolacustrine sediments at all sites except the railroad bridge; at least three units of debris-flow sediments of volcanic breccia cover the terrace at all sites.

The organic beds in the Puerto Varas terrace lie within an elevation range of 60–67 m. We surveyed the top of the newly exposed Bella Vista Bluff organic bed at 60.97 m elevation, and Porter (1981) placed the top of this bed at 60.8 m in an adjacent exposure now covered. We surveyed the top of the prominent 26-cm-thick organic layer at the railroad bridge site at 67.12 m elevation, compared with Porter's (1981) value of 66.2 m. Porter (1981) placed the top of the organic beds at 60.1 m elevation at Bella Vista Park, at 62.0 m at Calle Santa Rosa, and at 63.0 m at Northwest Bluff.

The dates of peat and wood in these organic layers originally had a significant scatter between 15,715 ^{14}C yr BP and 13,200 ^{14}C yr BP (Mercer 1972; Heusser 1974; Porter 1981; Hoganson and Ashworth 1992). But the top of the Bella Vista Bluff bed is now dated to 14,540 ^{14}C yr BP (Table 2), and the base of the organic layer is 15,700 ^{14}C yr BP (A-9190) (Table 1). These results are in reasonable agreement with the single age of 15,715±440 ^{14}C yr BP (GX-5275) from within the organic bed at the nearby Bella Vista Park site (Porter 1981). The top of the Northwest Bluff organic bed now dates to 14,882 ^{14}C yr BP (Table 2) rather than 13,145 ^{14}C yr BP (Porter 1981). The upper portion of the 26-cm-

Fig. 8. Waterlain till on a promontory alongside Lago Llanquihue near Bella Vista Bluff (site 30) in Puerto Varas.

Fig. 9. Waterlain till on a promontory alongside Lago Llanquihue near Bella Vista Bluff (site 30) in Puerto Varas.

Fig. 10. Outwash at site 11 at Frutillar Alto. The surface of this outwash unit, shown in fig. 7 of Andersen *et al*. (1999), is graded to the outermost Llanquihue moraine. The borrow pit at site 11 yielded numerous dates of reworked organic clasts (Table 1) that are maximum values for the outwash and hence for the outer Llanquihue moraine to which the outwash is graded.

thick organic layer at the railroad bridge site now dates to 14,613 ^{14}C yr BP (Table 2) rather than to 13,200–14,060 ^{14}C yr BP. The original age of the Calle Santa Rosa organic bed (14,820±230 ^{14}C yr BP, I-5033; Mercer 1972) is compatible with the new dates. The lower of the two 1-cm-thick peat layers at the railroad bridge site is now placed at 14,550 ^{14}C yr BP (Table 2). Near-basal wood in the organic silt and sand at the railroad bridge site dates to about 17,800 ^{14}C yr BP (Table 1) rather than 16,270 ^{14}C yr BP (Mercer 1976). Thus the tops of the organic beds within the Puerto Varas embayment now yield nearly identical dates. However, basal organic sediments at the inland railroad bridge site are

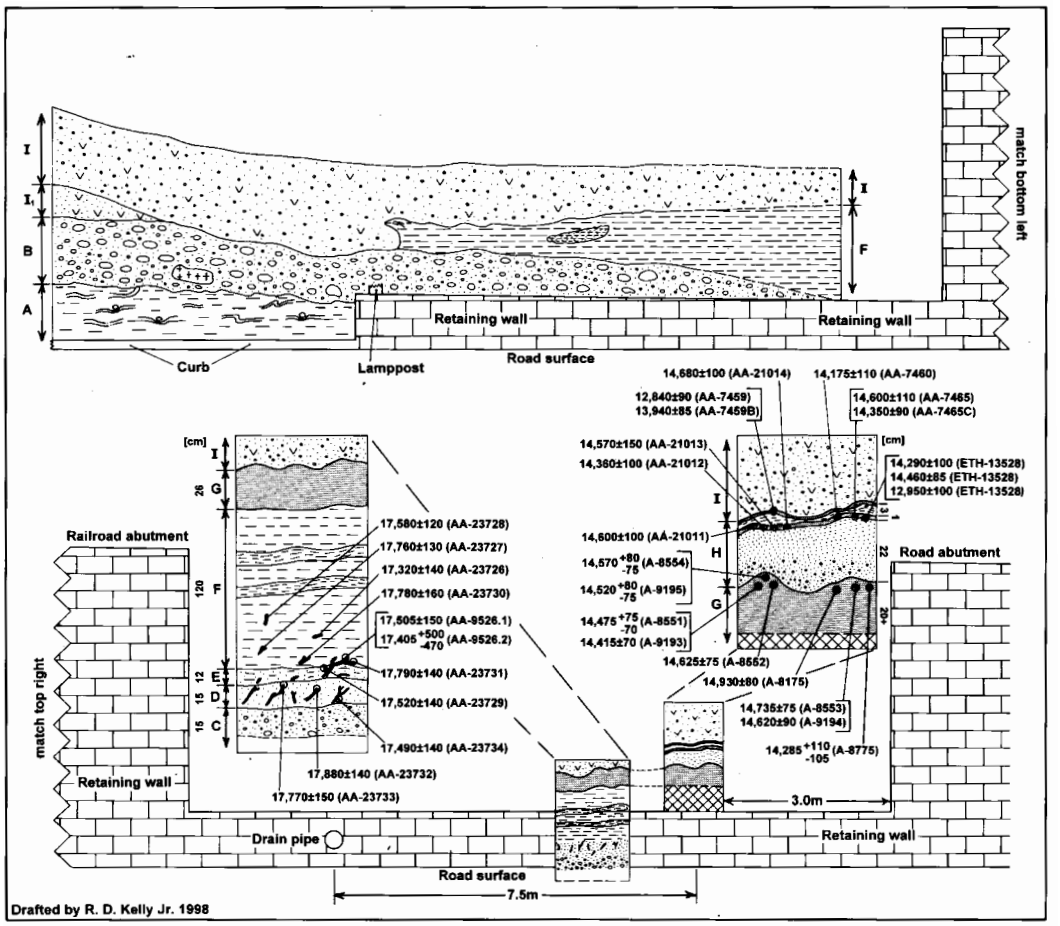

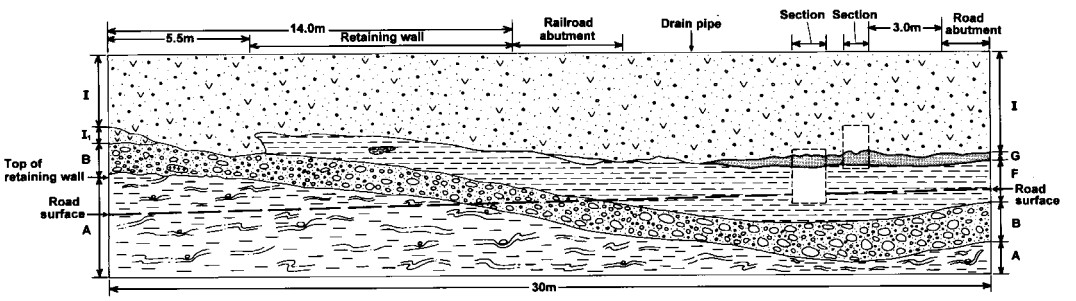

about 2000 ^{14}C yr older than basal organic sediments at the lakeside Bella Vista Bluff site. In turn, the base of the organic layer at the Llanquihue site is the same age as at Bella Vista Bluff.

The Lago Llanquihue piedmont glacier stood against the kame terrace during deposition of sediments overlying the organic deposits. Deposition of glaciofluvial sediments on the organic bed in the kame terrace near the town of Llanquihue (site 23) requires an adjacent buttressing ice margin. Deposition of the debris-flow sediments of volcanic material on the terrace also requires that ice stood at the terrace edge between the Río Maullín outlet and Punta Cabras, so that flows of volcanic sediment were directed along the terrace surface from Río Pescado to Río Maullín. That deposition of the glaciofluvial sediments and the volcanic flow sediments in the terrace near the town of Llanquihue was nearly simultaneous is shown by dates at the top of the organic beds at the Llanquihue and Puerto Varas stratigraphic sites.

The position of glaciolacustrine sediments on the top of the Bella Vista Bluff organic unit is best explained by a buttressing ice lobe that dammed a local, ice-marginal lake in the Puerto Varas embayment. This conclusion is supported by the similarity in ages of the top of the Bella Vista Bluff and Llanquihue organic beds. This local ice-dammed lake did not flood the railroad bridge site, where volcanic flow breccias afford the only evidence of a buttressing ice margin younger than the organic beds.

At the Northwest Bluff site the position of the poorly sorted gravel below the organic bed probably requires an adjacent ice margin. The glaciolacustrine units beneath the organic beds at the railroad bridge and Bella Vista Bluff sites both probably reflect an ice lobe in the Puerto Varas embayment. The simplest explanation is that the glaciolacustrine units beneath organic beds at the railroad bridge and Bella Vista Bluff sites are the same age and hence reflect the same adjacent ice margin. But there are two serious problems with this explanation. First, numerous dropstones are present in the glaciolacustrine units below the organic beds at the railroad bridge but not at the Bella Vista Bluff site. Also, the close minimum ages for the glaciolacustrine units are substantially different, about 17,800 ^{14}C yr BP at the railroad bridge site and 15,730 ^{14}C yr BP at Bella Vista Bluff. Thus it is more likely that the two glaciolacustrine units represent separate events. The glaciolacustrine unit at the railroad bridge site probably represents a buttressing ice margin deep in the Puerto Varas embayment at shortly before 17,800 ^{14}C yr BP. The lower glaciolacustrine unit at Bella Vista Bluff probably represents an adjacent ice margin shortly before 15,730 ^{14}C yr BP. Glaciolacustrine sediments deposited in the youngest of these ice-marginal lakes would make up the core of what is now the eastern part of the overall Puerto Varas terrace, but would not have been deposited on the organic beds at the railroad bridge site.

This interpretation of the terrace sequence at Puerto Varas is in accord with our reconstruction of lake-level fluctuations. The rim of indurated waterlain till exposed along the western shore of Lago Llanquihue now controls the Río Maullín outlet. We postulate that this outlet would always quickly

Fig. 22. Stratigraphic section at the railroad bridge site (26), Puerto Varas. Location given in Fig. 15. See legend in Fig. 7 (p. 177) for lithologic details. The upper panel gives the position of hand-dug and road-cut sections at the railroad bridge site. The lower panel gives our interpretation of the stratigraphic data presented in (a); the location of the road surface, railroad abutment and road abutment are all indicated on the diagrams. Top panel shows Unit A, the lowermost unit exposed at the railroad bridge site, west of the railroad abutment. Unit A is a glaciolacustrine deposit formed of silt and clay with numerous dropstones. This glaciolacustrine deposit is unconformably overlain by coarse-grained gravel (unit B) with individual crystalline clasts (granite) up to 50 cm in diameter. At the eastern end of the railroad bridge site, the gravel is, in turn, overlain unconformably by medium-grained and coarse-grained debris-flow breccia units (I_1 and I) that show fining-upward sequences. Just east of the retaining wall, the gravel is overlain by massive organic silts (unit F). The organic silts form well-defined diapirs and flame structures that penetrate the overlying debris-flow sediments. Bottom panel gives the location and stratigraphy of two hand-dug sections between the railroad and road abutments. Coarse-grained debris-flow sediments again form the uppermost unit (unit I). The western hand-dug section has two thin peat layers separated by fine- to medium-grained volcanic sands (unit H) from a lower, prominent organic bed. The organic layer (unit G) in this western section is as much as 26 cm thick, and in the upper 7 cm contains numerous pieces of wood 5–8 cm in length. The inset on the left of the upper panel shows the detailed stratigraphy revealed in the eastern hand-dug reexcavation behind the retaining wall. This re-excavation shows the following stratigraphy. Unit I is composed of debris-flow volcanic sediments. Unit H and the upper two thin organic beds (both of which occur in the excavation 1.5 m to the east) are not exposed at this site (emplacement of the overlying debris-flow sediments probably removed these deposits). Unit G is a thick (up to 26 cm) organic bed with numerous wood fragments. Unit F is organic silt (120 cm thick) with two diffuse horizons of increased organic content. Wood fragments, many in growth position, occur through this unit. Unit E is fine-grained organic sand and silt with large fragments of wood. Unit D is an admixture of fine- and medium-grained organic sand, with abundant wood fragments, many in growth position. Unit C is gray, coarse-grained sand with small pebbles.

Fig. 13. Stratigraphic section through a moraine ridge located a kilometer south of site 33 on west side of Route 5. Location given in Fig.15. The photograph shows a moraine ridge resting on an intact outwash unit. The two units have an erosional contact. Weathered pyroclastic deposits rest on the moraine surface. Nearby moraines overlie the same outwash unit, without any glacial deposits on the outwash in areas between the moraines.

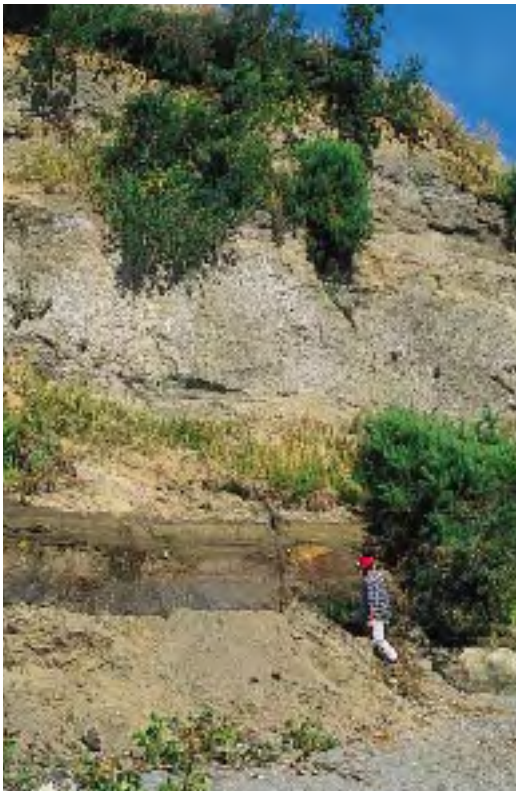

Fig. 19. Stratigraphic section at site 23 near the town of Llanquihue. See Fig. 18 for details. The organic beds are near the bottom of the photograph. Overlying the organic bed are the glaciofluvial sediments that make up the kame terrace at this locality. Underlying the organic bed is waterlain till that crops out along the shore of Lago Llanquihue.

Fig. 21. Overview of the Bella Vista Bluff section (site 30 in Fig. 15). The organic bed is in the center of the photograph at the top of the pickax handle. See Fig. 20 for description of units.

Fig. 24. Photographs of interdrift pyroclastic flow sediments at the crossroad section B at site 25 in Fig. 15. The location of these pyroclastic flow sediments, as well as the character of the drift units above and below, is shown in Fig. 23b. (a) Taken from the center of the section, looking south. (b) Taken from the same place, looking north.

cut through terrace sediments and moraines, both composed largely of unconsolidated glaciofluvial gravels or gravelly sediment flows, and stabilize at the level of the indurated compact waterlain till. The highest outcrop of waterlain till yet located is at 53 m elevation (about 2 m above the present-day lake level) at the Llanquihue site 23, about 2 km south of the Río Maullín outlet. Thus we think that ice advance over the eastern Río Petrohué outlet would not by itself cause a lake-level rise, because indurated waterlain till would still control the Río Maullín outlet. If this is correct, then higher-than-present lake levels recorded in the Puerto Varas terrace sections represent local glacial lakes impounded by an adjacent piedmont ice lobe. Conversely, a fall in lake level signifies recession of a piedmont lobe from the Puerto Varas embayment. Thus we infer that lake-level lowerings leading to deposition of organic silt and sand at the railroad bridge site by 17,800 ^{14}C yr BP and at the Bella Vista Bluff site by 15,730 ^{14}C yr BP (A-9190) were caused by ice recession from the Puerto Varas embayment. Flooding of the organic bed at Bella Vista Bluff at 14,540 ^{14}C yr BP (Table 2) was caused by a readvance of the piedmont glacier to the proximal edge of the kame terrace.

An important remaining question concerns the extent of ice recession when the organic beds were deposited in the Puerto Varas embayment. Mercer (1976) suggested deglaciation of the eastern Río Petrohué outlet. Overflow through Río Petrohué also would have required glacier recession from

both Seno Reloncaví and Estero Reloncaví. By our reconstruction, however, a lowered lake level merely requires that the ice margin pull back from the western lake shore. Near the town of Llanquihue (site 23), the base of the organic-rich silt bed is only 3 m above present-day lake level. Hence lake level dropped to or below 54.0 m elevation during deposition of the organic beds at both the Puerto Varas and Llanquihue sites, because of their nearly identical ages. Therefore, it is just possible that the Llanquihue (and hence the Bella Vista Bluff) organic bed formed while Lago Llanquihue drained through the Río Maullín outlet. But it is equally possible that Lago Llanquihue drained through the Río Petrohué outlet when the organic beds were deposited at Llanquihue and in the Puerto Varas embayment. We merely point out that such easterly drainage is not a necessity.

Llanquihue moraine belt. The Llanquihue moraines between the lakeside kame terraces and the main Llanquihue outwash plain farther west have bracketing dates from several key localities. Minimum limiting ages come from organic material on or within the moraines. New basal dates from mires are 20,160±180 ^{14}C yr BP (AA-9296) for Canal de la Puntilla (site 6), along with 20,580±170 ^{14}C yr BP (AA-9303) and 20,380±170 ^{14}C yr BP (AA-9298) for Canal de Chanchán (site 5). The basal age for Canal de la Puntilla is the end member of a consistent sequence of dates through the thickness of the mire (Moreno *et al*. 1999). These basal ages are minimum values for this entire sector of the Llanquihue moraine belt, which is traversed by the two meltwater channels. Moreover, the channels have not been scoured by meltwater or lake spillover since organic deposition began on the channel floors implying that readvances of the Lago Llanquihue piedmont glacier have not been extensive enough to dam a lake that spilled over into the channels, let alone reach the bayside ice-contact slope. Such a situation is consistent with that at Puerto Varas, where the railroad bridge site has not been overrun by ice since at least 17,800 ^{14}C yr BP.

Similar basal ages come from sediment cores in depressions elsewhere on the Llanquihue moraine belt. At Fundo Liña Pantanosa (site 8), situated just within the two outermost Llanquihue moraines, a 3.50-m-deep mire yielded near-basal ages of 19,768±397 ^{14}C yr BP (AA-14774) and 19,993±257 ^{14}C yr BP (AA-15900) (Table 1) (Heusser *et al*. 1999). A 7.07-m-deep mire just within the outermost Llanquihue moraine at Fundo Llanquihue (site 18) afforded ages within the basal meter of 20,645±220 ^{14}C yr BP (UGA-6907), 20,890±185 ^{14}C yr BP (UGA-6908), 20,455±180 ^{14}C yr BP (UGA-6909), 20,650±175 ^{14}C yr BP (UGA-6910), 20,680±175 (UGA-6912), and 20,585±170 ^{14}C yr BP (UGA-6913) (Table 1) (Heusser *et al*. 1999). A basal date of 19,760$^{+250}_{-240}$ ^{14}C yr BP (A-8534R) comes from a 2.7-m-thick mire in a small depression on the proximal side of the two outer Llanquihue moraines near Frutillar Alto (site 14) (Table 1).

Maximum limiting ages for the Llanquihue moraine belt are derived from organic clasts reworked into outwash of the main Llanquihue plain. The youngest ages are 23,020±280 ^{14}C yr BP (QL-4539) from north of Bahía Muñoz Gamero (site 3); 20,840±400 ^{14}C yr BP (QL-4527) from near Canal de la Puntilla (site 4); 22,700$^{+180}_{-175}$ ^{14}C yr BP (A-9514), 22,790±410 ^{14}C yr BP (A-6197), 21,120±180 ^{14}C yr BP (AA-25374) and 21,840±700 ^{14}C yr BP (QL-4548) from near Frutillar Alto (site 11); and 22,250±220 ^{14}C yr BP (Wk-2536) and 22,985±235 ^{14}C yr BP (TUa-470A) from southwest of Puerto Varas (site 32). As mentioned above, Mercer (1972) reported an age of 20,100±500 ^{14}C yr BP (RL-116) for a peat clast reworked into Llanquihue outwash at Frutillar Alto (site 13) about 1.5 km south of site 11 where we obtained many samples. Also, a clast dated to 22,870±310 ^{14}C yr BP (A-6196) is reworked into ice-contact drift south of Bahía Frutillar at site 17.

The map pattern of Llanquihue moraines, along with the geometric relations of Canal de Chanchán and Canal de la Puntilla to these moraines, are key to interpretation of these dates. The minimum ages of 20,580±170 ^{14}C yr BP (AA-9303) for Canal de Chanchán (site 5) and of 20,160±180 ^{14}C yr BP (AA-9296) for Canal de la Puntilla (site 6) apply to all of the Llanquihue moraines distal to the lakeside terraces that fringe Bahía Muñoz Gamero. They are consistent with ages for basal organic material at Fundo Llanquihue of as much as 20,890±185 ^{14}C yr BP (UGA-6908). Hence the outer Llanquihue moraines at these sites antedate 20,580–20,890 ^{14}C yr BP. From moraine geometry it is difficult to argue that the outermost Llanquihue moraine at Frutillar Alto is younger than these ages. Indeed, Fig. 3 implies that the Frutillar Alto frontal moraine is older, not younger, than the frontal Llanquihue moraine cut by Canal de Chanchán and Canal de la Puntilla. Also, the outermost Llanquihue moraine near Frutillar Alto is probably equivalent to the outermost moraine near the Fundo Llanquihue site. The overall implication is that the maximum age of

20,100±500 ^{14}C yr BP (RL-116) for the outermost Llanquihue moraine at Frutillar Alto (Mercer 1972) is too young by more than 790 ^{14}C yr. A further implication is that the age of 20,840±400 ^{14}C yr BP (QL-4527) for an organic clast in outwash (site 4) near Canal de la Puntilla may be too young, because basal dates from the Puntilla and Chanchán channels suggest that this outwash antedates 20,120–20,580 ^{14}C yr BP. There is strong paleoenvironmental and chronologic evidence from Canal de la Puntilla (Moreno *et al*. 1999) and Canal de Chanchán (Table 1) that the Lago Llanquihue ice lobe did not advance into this moraine system after 20,580 ^{14}C yr BP. Hence, most new chronologic data show that the entire Llanquihue moraine belt west of Lago Llanquihue has a minimum age of 20,580–20,890 ^{14}C yr BP and a maximum age of 23,020–22,250 ^{14}C yr BP (see below for alternate interpretation).

The revised chronology indicates that the Llanquihue moraine belt west of Lago Llanquihue cannot be subdivided into two units that relate to two episodes of glacier expansion. The outermost moraines were formerly called Llanquihue I and taken to antedate the LGM (Porter 1981). Likewise, most of the main Llanquihue outwash terrace graded to these moraines was also thought to antedate the LGM (Mercer 1976; Porter 1981). Moraines of Llanquihue II age, with a mapped outer limit well within the Llanquihue moraine belt except near Frutillar Alto, were believed to represent the LGM, and were placed between 18,900 and 20,100 ^{14}C yr BP (Mercer 1976; Porter 1981). Part of the reason for this original subdivision involved old dates of intertill wood samples from exposures within the moraine belt west of Puerto Varas (Mercer 1976), which we now discuss.

The morainal landforms near the crossroad site (25) at the intersection of Routes 5 and V-50 west of Puerto Varas reflect old drift overrun by ice that deposited the outermost Llanquihue drift farther west at the LGM. The section beside Route V-50 near the southwest corner of the crossroad site was originally described by Mercer (1972). Called crossroad south in Fig. 23, this section shows intense mechanical deformation of the upper glacial unit that makes up the moraine surface. The crossroad north section in Fig. 23 also shows complex shear deformation of the uppermost glacial unit, as well as of the weathered interdrift pyroclastic flow units (Fig. 24).

At the crossroad south section in Fig. 23, wood has been sheared off the surface of the interdrift pyroclastic flow sediments into the overlying glacial unit. The location of dated wood and charcoal samples is shown in Fig. 23. Because they fall at the outer age limit of reliable radiocarbon dating, these ages are all regarded as minimum values. From wood and peat in the interdrift pyroclastic flow deposits of the crossroad south section, Mercer (1976) previously reported dates of > 39,900 ^{14}C yr BP (I-4170) and > 39,900 ^{14}C yr BP (I-5032) and Porter (1981) gave a date of 57,800 $^{+2300}_{-3200}$ ^{14}C yr BP (QL-1336). Again, these ages are minimum values.

The mechanical deformation of drift above the pyroclastic flow sediments could have been imparted during glacier overriding of the crossroad sections. Hence, the stratigraphic sequences at the crossroad site cannot be used to assign an age to the outer Llanquihue moraines farther west. Instead, the pertinent dates come from a stratigraphic exposure (site 24) on the north side of Route V-50 where it passes through the outer Llanquihue moraines 500 m west of the crossroad site. The exposure reveals organic pyroclastic flow sediments (remobilized by glacier overriding) that separate a lower, little-weathered outwash (>30 m thick) from upper thin till with morainal topography of moderate relief. Dates of 25,020±290 ^{14}C yr BP (UGA-6939), 26,150±220 ^{14}C yr BP (UGA-6821), 29,350 $^{+325}_{-310}$ ^{14}C yr BP (A-7712), and 29,360 $^{+215}_{-210}$ ^{14}C yr BP (A-7715) pertain to the remobilized organic pyroclastic sediments beneath the till. The outermost Llanquihue moraine adjacent to the Fundo Llanquihue site 18, with its minimum dates of 20,680–20,890 ^{14}C yr BP, can be traced directly to the outermost Llanquihue moraine both west and south of Puerto Varas (Fig. 3). In turn, outwash graded to this same moraine south of Puerto Varas is younger than 22,250 ±220 ^{14}C yr BP (Wk-2536) (site 32), as described above. Hence, we conclude that the outermost Llanquihue moraine was deposited during the LGM, despite the presence of only older deposits at the crossroad site.

An organic silt clast reworked into the outwash beneath the remobilized pyroclastic sediments at site 24 yields a date of >44,400 ^{14}C yr BP (UGA-6938). The outwash has a flattish terrace surface

Fig. 23, *see pp. 197–198.*
Fig. 24, *see p. 193.*

Fig. 26. Frutillar Bajo stratigraphic section at the top of the ice-contact slope at site 16 in Fig. 15 alongside southern Bahía Frutillar Bajo. The organic bed, composed largely of pyroclastic flow sediments, is near the base of the photograph, and is being sampled for pollen and radiocarbon samples. Overlying the organic bed is the lodgement till of unit E in Fig. 25.

Fig. 27. The Puerto Octay stratigraphic section (site 7 in Fig. 15) on the south side of Route V-55-U, about 1 km southwest of Puerto Octay near the top of the ice-contact slope that rises above Bahía Muñoz Gamero.

Fig. 31. Photograph of the Dalcahue stratigraphic section at site 98 in Fig. 15. See text for details. The two human figures are beside an excavation dug into the organic bed. The stratigraphy of the drift units above and below this organic bed is described in the text. A and B are the locations of the radiocarbon dates described in the text and in Table 1. Location B is the site of the pollen diagram described in Heusser *et al.* (1999).

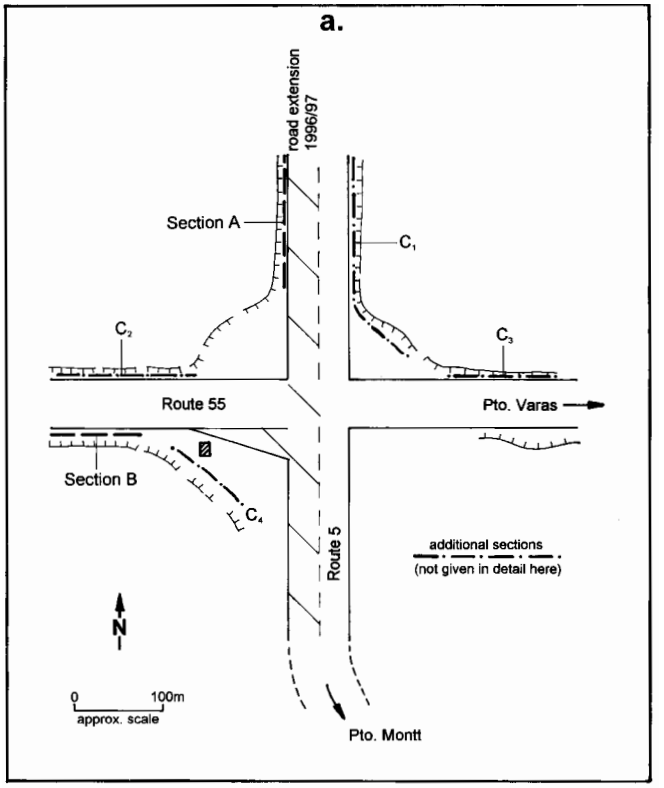

Fig. 23. Stratigraphic sections at the crossroad site (25) at the intersection of Routes 5 and V-50 in the Llanquihue moraine belt west of Puerto Varas. See legend in Fig. 7 (p. 177) for lithologic details. Panel *a* gives location of individual sections. Sections A and B are selected for detailed descriptions because of new road construction in 1996/97. Panel *b* shows section A along the west side of Route 5 north of the intersection. This exposure shows highly deformed Llanquihue drift that rests conformably on older drift and gravel units (southern half of section). MSP is a master shear plane with well-developed slickensides at the base of the Llanquihue sediment complex. Insets (a), (b), and (c) give details of the degree of syndepositional and post-depositional shear deformation. Panel *c* shows section B along Route V-50, west of the intersection with Route 5. Here highly deformed Llanquihue drift is stacked on beds of weathered pyroclastic flow sediments. The base of the outcrop (eastern and central part of section) shows older drift and gravel. Inset (a) of Panel *c* shows details of weathered pyroclastic flows, with three distinct depositional units resting on indurated older drift. The top unit has abundant wood and charcoal fragments. Inset (b) shows an example of mechanical stacking of weathered pyroclastic flows at the base of Llanquihue drift, with a complex cross-cutting pattern of shear planes. Panel *d* displays a schematic composite lithostratigraphic section for the crossroad site. Included are the composite lithostratigraphy with average thickness, which varies considerably from site to site, radiocarbon dates on wood and charcoal (Table 1), lithologic descriptions, and stratigraphic interpretations.

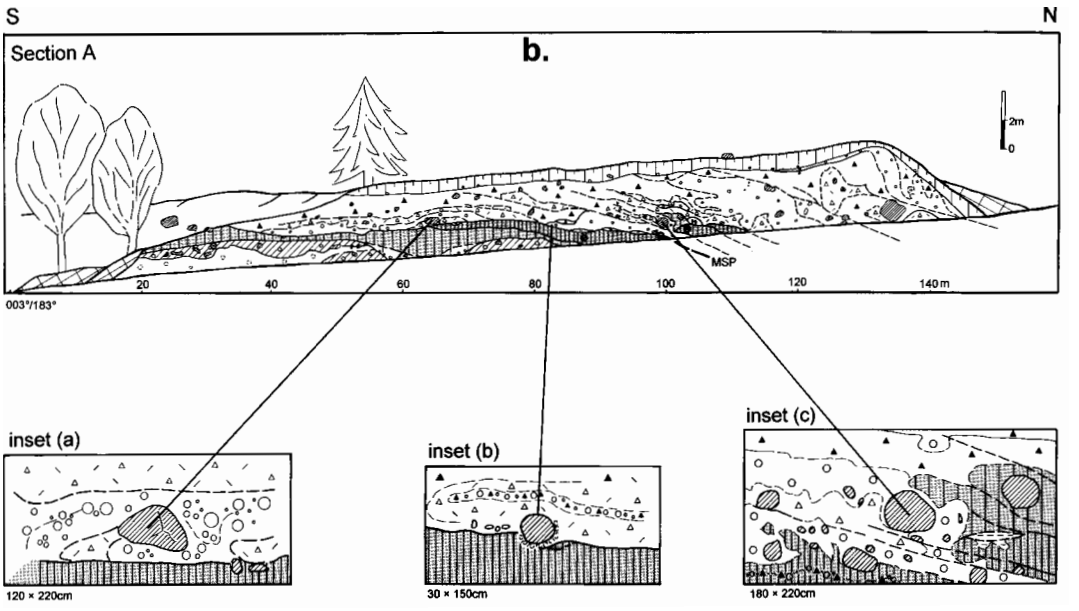

Fig. 23. Continued.

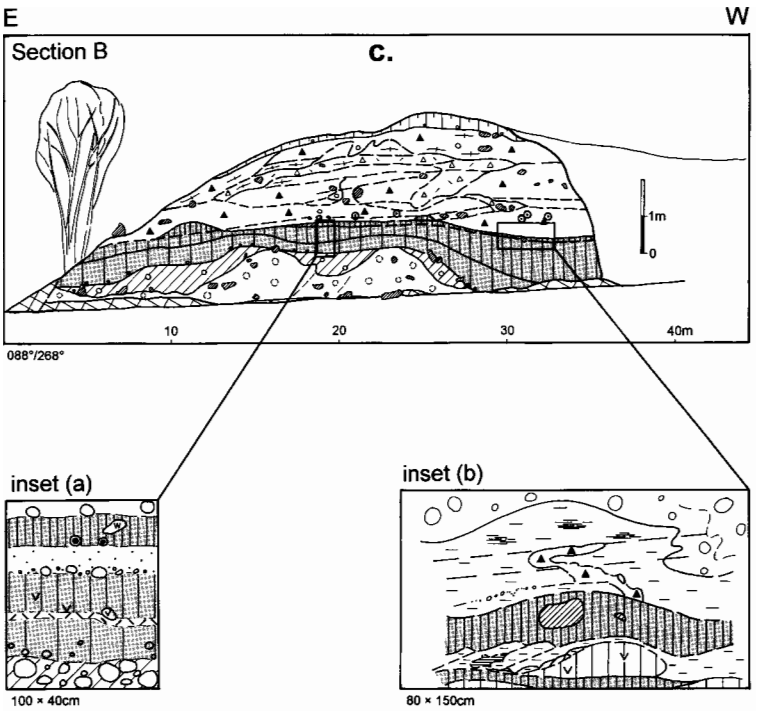

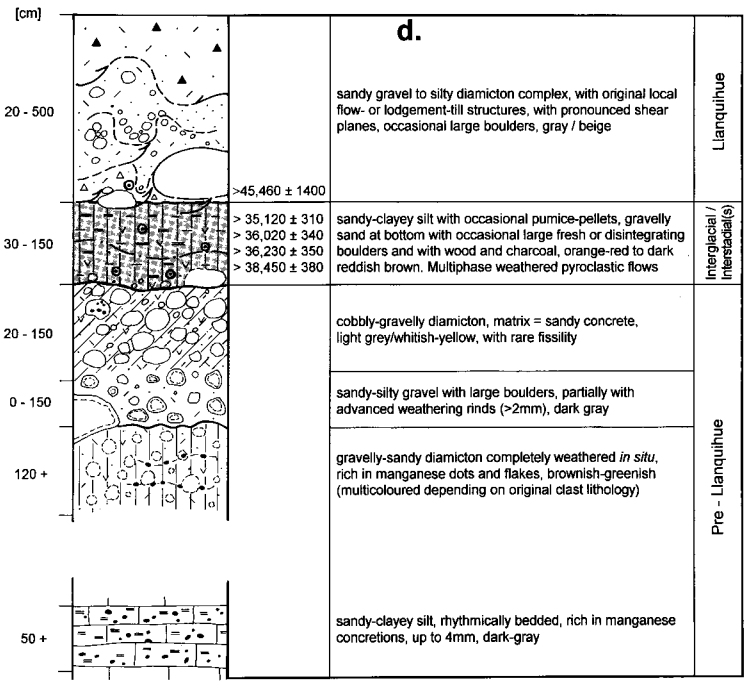

that, by projection, forms the main Llanquihue plain. The terrace surface can be traced eastward for 300 m beneath the late Llanquihue morainal topography of moderate relief, where it grades to a large buried moraine ridge. Hence the ice front associated with the terrace was situated only a few hundred meters behind the position reached by the late Llanquihue piedmont lobe. The outwash of the terrace is far less weathered than any deposits exposed in the crossroad sections below the pyroclastic flow sediments and lying beyond the range of radiocarbon dating. Hence, it is probably of middle or early Llanquihue age.

Additional evidence for middle or early Llanquihue glacial drift comes from two important exposures in the Llanquihue moraine belt at the top of the ice-contact slope above the lakeside kame terraces. One is alongside Bahía Frutillar Bajo (site 16) and the other is alongside Bahía Muñoz Gamero near Puerto Octay (site 7).

Figure 25 depicts the Bahía Frutillar Bajo section (site 16), where a lens of organic pyroclastic flow sediments separates two till units (Fig. 26), both of which are compact, little weathered, medium-gray in color, and characterized by boudinage structures and numerous shear planes. Both are taken to be lodgement tills. Where they are not separated by organic pyroclastic sediments, the two tills could be mistaken for a single unit. The intertill organic pyroclastic sediments are as much as 95 cm thick and have an exposed lateral extent back into the face of about 15 m. A shear plane constitutes the contact between the organic bed and the upper till for 7.5 m of lateral extent on the lakeside portion of the exposed section. In the inland portion of the exposure, a wedge-shaped unit of silt and gravelly diamicton with crude layering separates the organic bed from the overlying till. The basal shear plane of the upper till passes inland from the top of the organic bed to the top of this diamicton wedge. Beneath the shear plane, the top of the lakeside end of the organic bed has been removed. But beneath the inland diamicton wedge, the vegetation litter of the old land surface of the organic bed is preserved intact. We attribute the sealing diamicton to sediment flows off an advancing ice margin, and the subsequent shearing to subglacially imparted stresses beneath the glacier ice that deposited the upper till. Hence dates of the sealed land surface pinpoint an advance of the Lago Llanquihue piedmont lobe across the lakeside ice-contact slope at the inner edge of the Llanquihue-age moraine belt. Seventeen such dates of organic pyroclastic sediment, wood, and fibrous organic matter from different localities along the exposed sealed land surface yielded a weighted mean of 26,797±65 ^{14}C yr BP (Tables 1 and 2).

Dates from the base of the Frutillar Bajo organic bed at three localities are 34,765±840 ^{14}C yr BP (UGA-6945), 34,985±440 ^{14}C yr BP (UGA-6919), and 36,960±550 ^{14}C yr BP (UGA-6724) (Table 1, Fig. 25). Other dates of the organic bed are given in Table 1. Thus the ice-free interval separating deposition of the two till units lasted at least 10,000 ^{14}C yr, from prior to 36,960 ^{14}C yr BP (Table 1) to 26,797 ^{14}C yr BP (Table 2). The lack of significant weathering of the till below the organic bed suggests a Llanquihue age. Such a conclusion is in accord with the pollen record from the organic bed of continued Subantarctic Parkland cold and wet conditions (Heusser *et al.* 1999). There is not any suggestion of an interglacial evergreen forest or a lowland deciduous forest. The implication of this pollen record is that the till below the organic silt bed was deposited subsequent to the last interglaciation and hence is middle or early Llanquihue in age.

It is worth pointing out that an exposure 200 m to the east, but in the same topographic position on the ice-contact slope as the Frutillar Bajo site, reveals coarse stratified drift with an enclosed organic clast dated to 22,870±310 ^{14}C yr BP (A-6196) (site 17). Evidently this same ice-contact slope was occupied at least twice, once during the advance at 26,797 ^{14}C yr BP and again during the young advance that reached the outer Llanquihue moraines west of Frutillar Bajo.

A road cut through the ice-contact slope above the lakeside terraces west of Bahía Muñoz Gamero at the Puerto Octay site (7) exposes two superimposed outwash units separated by a 90-cm-thick layer of organic pyroclastic flow sediment (Fig. 27). Dates of the uppermost organic sediment from five separate localities along the lateral extent (150 m) of the organic bed (Table 1) give a weighted mean of 29,363±178 ^{14}C yr BP (Table 2). Both outwash units head at the ice-contact slope, where poorly sorted stratified drift with enclosed boulders is exposed. Thus both were deposited in an ice-proximal position when a former piedmont glacier stood at the top of the slope, which is within 2.2 km

Figs 26–27, *see p. 196.*

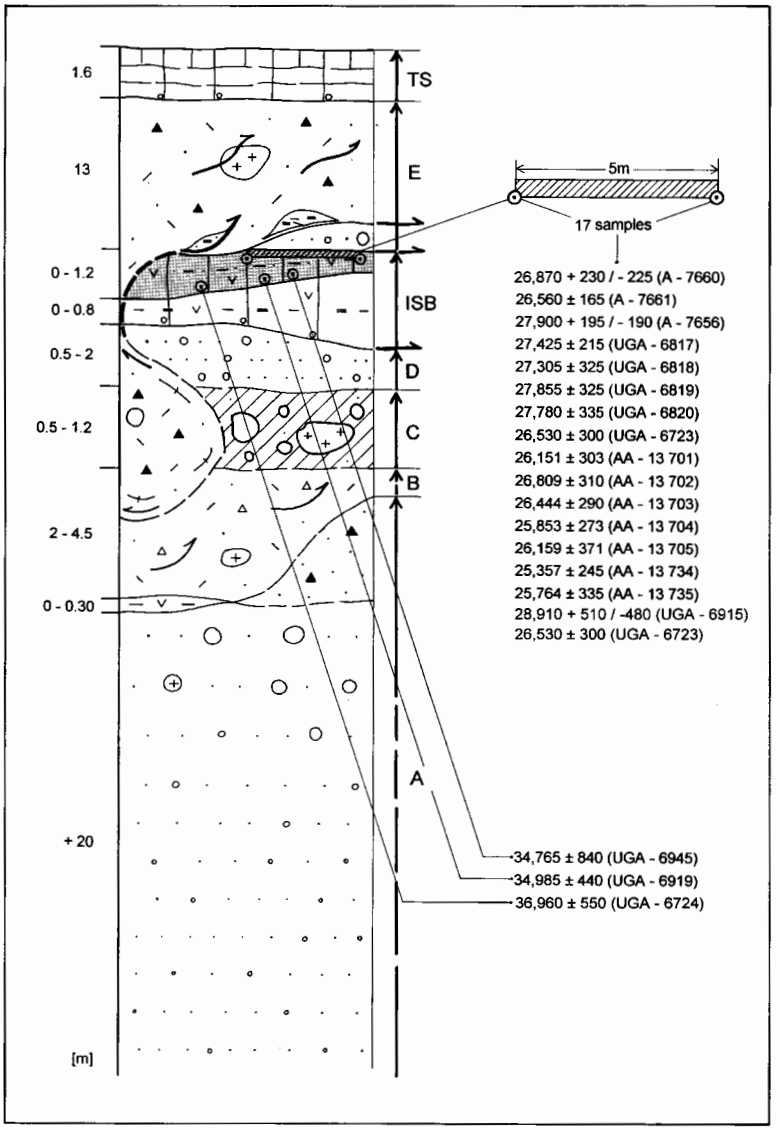

Fig. 25. Schematic composite lithostratigraphy of the Frutillar Bajo section at site 16 in Fig. 15. See legend in Fig. 7 (p. 177) for lithologic details. Unit A is gravelly sand to sandy gravel, with well-rounded components, a polymictic gravel fraction, and abundant volcaniclastic sediment. The upper 5 m of unit A exhibit lenses of volcaniclastic clayey silt in a coarsening-upward sequence, which is overlain by massive basal till. Unit B is matrix-supported sandy-silty gravel, with some boulders and with mechanically emplaced clasts of bedded silty sand; the unit is sheared and is probably a lodgement till. Unit C is a matrix-supported, sandy-silty, bouldery gravel that is highly cemented, with yellowish-whitish fissility infillings; it is probably a basal till. Unit D is a bedded sandy gravel, interpreted to be glaciofluvial outwash. ISB consists of non-glacial beds; the lower unit is massive clayey silt with charcoal and with a basal orange-brown gravel layer composed dominantly of pyroclastic flow sediments. The upper unit is massive weathered sandy silt with charcoal, interpreted to be a tuffaceous pyroclastic flow sediment. Top (inset) shows a preserved grass layer covered by glacial silt (inset shows location of radiocarbon samples in Table 1). The lower part of unit E is matrix-supported sandy-silty gravel, with subrounded clasts, and faint bedding, interpreted to be till flows. The upper part of unit E is matrix-supported silty-sandy gravel with some boulders and mechanically emplaced clasts of silty-sandy rhythmites; this upper part is lightly sheared and probably represents lodgement till. TS is the topsoil, which is largely composed of pyroclastic flow sediments. Units A–D are interpreted as sediments of a single glacier advance, with unit B and unit C being formed during oscillations of the ice margin. ISB represents a non-glacial interval. Unit E represents a glacier advance during which sediment flows from an ice margin sealed intact part of the top of unit B.

of the outer Llanquihue moraine belt. The upper surface of the organic bed between the outwash units lacks a preserved land surface and hence may not be original. In fact, in a locality not sampled at the head of the ice-contact slope, the upper surface of the organic bed has been sheared by overriding ice. However, the consistency of the dates suggests, but does not prove, that little material has been eroded off the top of the organic bed. The argument for this inference is that the ages given in Table 1 increase markedly with depth within the organic bed, and hence that the upper surface would have yielded highly disparate ages if even a few centimeters had been eroded. Therefore, we suggest that the age of about 29,363 ^{14}C yr BP probably affords a close limiting value for deposition of the upper outwash and hence for glacier advance to the top of the ice-contact slope. However, given the lack of a preserved land surface, we cannot be sure that the advance was not younger than 29,363 ^{14}C yr BP.

Four basal samples from the inter-outwash organic pyroclastic bed at differing localities along the exposure yield limiting minimum dates for the lower outwash unit of 33,900–39,340 ^{14}C yr BP (Table 1). Overall, the Puerto Octay exposure reveals an organic bed composed largely of pyroclastic flow sediments that range from ≥ 39,340 to 29,363 ^{14}C yr BP in age and that separate two ice-proximal outwash units. The lower outwash unit shows little weathering and, in the absence of the intervening organic bed, could not have been distinguished from the upper outwash unit. The pollen record from the organic bed shows the continuous presence of a Subantarctic Parkland, with cold and wet conditions, similar to the situation at the Frutillar Bajo site (Heusser *et al*. 1999). Notably missing is an indication of the numerous thermophilic tree species of an interglacial evergreen forest or deciduous lowland forest. Just as at the Frutillar Bajo site, the implication is that the lower outwash unit was deposited subsequent to the penultimate interglaciation and is therefore probably of middle or early Llanquihue age.

Seno Reloncaví Region

An extensive system of Llanquihue moraines fringes Seno Reloncaví (Fig. 4). The main Llanquihue outwash plain is graded to the outermost of these moraines. Subsidiary Llanquihue outwash plains are nested within the outer moraine system and are graded to inner moraine belts. A high ice-contact slope occurs alongside Bahía Puerto Montt, where prominent kame terraces, together with small moraine fragments, occur on the proximal side of this ice-contact slope. We recognize several glacier advances into these moraine belts and the gulfside ice-contact slope. We now discuss the evidence for these advances, starting with the youngest.

Dates at three sites document a glacier advance that culminated shortly after 15,000 ^{14}C yr BP. At Punta Penas on the north shore of Seno Reloncaví (site 47), lodgement till unconformably overlies a glaciolacustrine unit (Fig. 28). Any lake in this position would have been proglacial. The thickness of the glaciolacustrine unit is variable, reflecting the amount of lacustrine material removed by overriding ice. Near the base of the glaciolacustrine unit is a 20-cm-thick organic layer about 7.2 m above high-tide mark. Dates of this organic bed are 15,940±315 ^{14}C yr BP (T-10296A) at the top, 16,275±440 ^{14}C yr BP (T-10297A) in the middle, and 16,000±275 ^{14}C yr BP (T-10298A) at the base. This 20-cm-thick organic layer is overlain first by lacustrine sediments with several thin organic layers, and then by glaciolacustrine sediments without organic layers. Two of the thin organic layers are particularly prominent, with organic macrofossils and wood on the upper surfaces. The dates of surface organic matter from the lowest of these two thin layers are 15,675±90 ^{14}C yr BP (A-9019), 15,665 $^{+110}_{-105}$ ^{14}C yr BP (A-9020), and 15,200±120 ^{14}C yr BP (AA-21009) (Table 1), giving a weighted mean of 15,554±60 ^{14}C yr BP (Table 2). The dates of surface organic litter from the highest of these two thin beds are 15,020±120 ^{14}C yr BP (AA-21010), 15,000±75 ^{14}C yr BP (A-9017), 14,735 $^{+80}_{-75}$ ^{14}C yr BP (A-9018), and 14,835±80 ^{14}C yr BP (A-9506) (Table 1), giving a weighted mean of 14,879±42 ^{14}C yr BP (Table 2).

These organic beds point to a time of low lake level that requires the former piedmont ice lobe to be pulled back from the western shore of the Seno Reloncaví embayment enough to allow drainage through Canal de Chacao at a time when sea level was more than 100 m below the present-day value (Fairbanks 1989). Subsequent flooding of the peat beds by a proglacial lake, accompanied by rapid accumulation of glaciolacustrine sediments beginning about 14,879 ^{14}C yr BP, reflects an advance of the Seno Reloncaví piedmont lobe that culminated inland of the Punta Penas site when the surface till was deposited.

A small, subsidiary Llanquihue outwash plain graded to the ice-contact slope west of Bahía Puer-

to Montt (sites 44, 45) yielded reworked organic clasts with dates of 16,900±120 ^{14}C yr BP (A-6491), 15,640±100 ^{14}C yr BP (A-6492), 16,060±120 ^{14}C yr BP (UGA-6942), and 15,040±100 ^{14}C yr BP (A-6493) (Table 1). Each date affords a maximum limiting value for advance of the Seno Reloncaví piedmont ice lobe to the upper edge of the ice-contact slope at this locality.

At site 73 on Isla Maillen in Seno Reloncaví, a compact peat mat is sealed by laminated glaciolacustrine sediments that are overlain by lodgement till. The date of 15,220±80 ^{14}C yr BP (A-9507) (Table 1) for the top of the peat registers an advance of the Seno Reloncaví piedmont glacier over Isla Maillen.

Farther south near Calbuco (site 94), lodgement till 1.5 m thick covers a delta built into a proglacial lake within the limits of a Llanquihue moraine belt about 6 km west of Seno Reloncaví. Organic clasts reworked into the foreset beds of the delta yielded dates of 15,285 $^{+150}_{-145}$ ^{14}C yr BP (A-7702), 15,500±85 ^{14}C yr BP (A-7698), 15,535±85 ^{14}C yr BP (A-7697), 16,160±80 ^{14}C yr BP (A-8776), 15,730±70 ^{14}C yr BP (A-8777), 15,365±85 ^{14}C yr BP (A-8778), 15,390 $^{+85}_{-80}$ ^{14}C yr BP (A-8779), 15,110±100 ^{14}C yr BP (A-9427), 15,130±125 ^{14}C yr BP (A-9425), 15,250±175 ^{14}C yr BP (AA-25373), and 14,900 $^{+160}_{-155}$ ^{14}C yr BP (A-9426) (Table 1). These dates afford maximum limiting values for the advance of the Golfo de Ancud piedmont ice lobe registered by the lodgement till on the delta.

The data from sites 44, 45, 47, and 94 thus document a major advance that culminated shortly after 15,000 ^{14}C yr BP. Fig. 4 shows that the northern three sites reflect advance of the Seno Reloncaví lobe only to the ice-contact slope near Bahía Puerto Montt; in one place (sites 44, 45) the lobe reached the top of this slope, allowing meltwater to deposit a small tongue of outwash within the Llanquihue moraine system. Farther south, however, the cor-

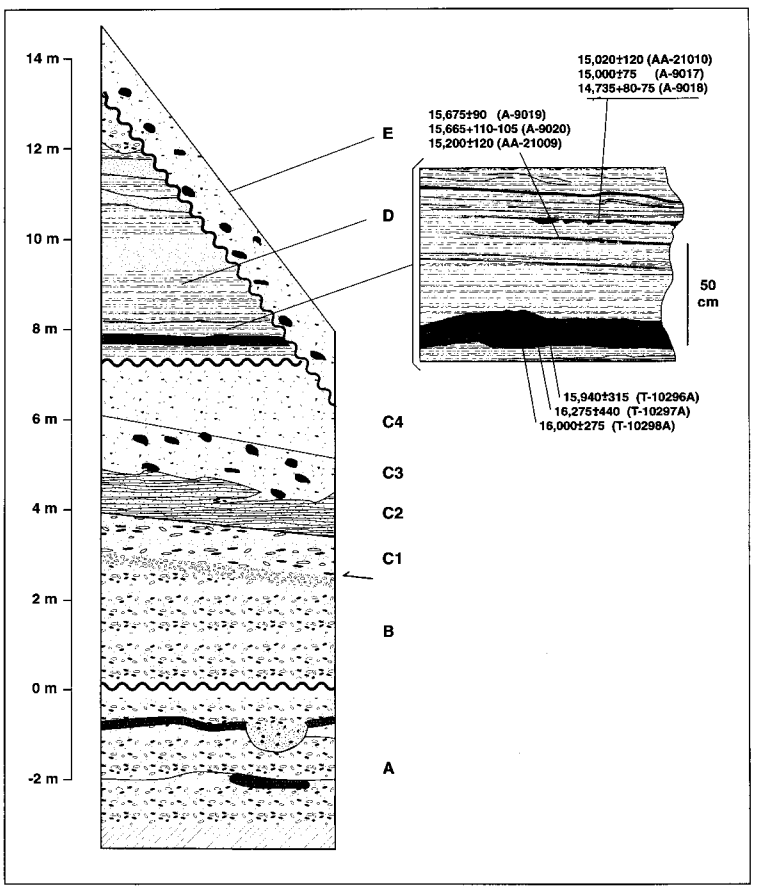

relative advance of the Golfo de Ancud lobe passed inland over the Calbuco site 95. To confirm the reality of this difference, we undertook a coring program to determine how far the last advance extended into the Llanquihue moraines west of Seno Reloncaví. We noted earlier that the complicated moraine belts fringing Seno Reloncaví could be subdivided into two, and perhaps three, groups on the basis of morphologic relationships. The resulting basal ages of mires in depressions on these Llanquihue moraine belts are listed in Table 1. Each of these dates affords a minimum age for the underlying morainal topography. It is not possible to determine how close these minimum ages are to the time of deposition of the moraine, unless closely bracketing maximum ages are also available.

There are now 21 basal dates from mires on the inner and intermediate moraine belts fringing Seno Reloncaví (Table 1). Eight dates fall between 13,000 and 14,000 ^{14}C yr BP, three fall between 14,000 and 15,000 ^{14}C yr BP, and one falls between 15,000 and 16,000 ^{14}C yr BP. The key site is the Huelmo mire (site 81), on the proximal side of a continuous moraine belt that trends north–south just inland of the ice-contact slope beside Seno Reloncaví (Moreno 1998). The basal date for the Huelmo mire is 16,410±110 ^{14}C yr BP (AA-23244), a value consistent with dates of samples from higher in the core. The implication is that the readvance of the Seno Reloncaví piedmont lobe about 14,900 ^{14}C yr BP did not reach these moraines, but must have terminated instead on the ice-contact slope alongside Seno Reloncaví. This is entirely consistent with the situation farther north near Bahía Puerto Montt where the piedmont ice lobe barely reached the top of this ice-contact slope. Thus the relatively limited extent of the Seno Reloncaví piedmont lobe during this advance is similar in magnitude to the extent of the Lago Llanquihue lobe.

To check the conclusion from the coring program that the inner prominent moraine belt beside Seno Reloncaví antedated the advance at shortly after 15,000 ^{14}C yr BP, we also dated organic clasts reworked into the associated subsidiary outwash terrace (Table 1). With one exception, all the dates are 25,300±300 ^{14}C yr BP (Wk-2541) (site 71) or older. The single exception is a reworked organic clast dated to 19,820±185 ^{14}C yr BP (TUa-468A) (site 53). These dates show that the inner moraine

Fig. 28. Composite stratigraphic section at Punta Penas at site 47 in Fig. 16. See legend in Fig. 7 (p. 177) for lithologic details. The site consists of two exposures; the first is a sea cliff in the tidal zone and the second is a road cut just inland and northwest of the sea cliff. Datum for this site is the high-tide level. There are five basic stratigraphic units at Punta Penas. Unit A includes interbedded horizontal sand, ash, and gravel layers exposed within the present tidal zone. There are some reworked organic clasts. Unit A also contains organic silt beds with wood and large tree remains rooted in place. Porter (1981) reported an age of 42,400±500 (QL-1337) from an *in situ* stump. The beds of unit A have been eroded and infilled several times, with channels cutting the organic beds and, in turn, infilled with partly consolidated pebble gravels. The horizontally laminated stratified deposits of unit A represent former littoral zones, with accompanying changes in base level resulting from submergence during tectonic events. Unit B is outwash made up of horizontally bedded gravel with sand layers. The maximum thickness of this outwash unit is 2.7 m. Locally this gravel is matrix-supported and bedding is not well defined. All enclosed clasts of pebbles and cobbles are well rounded. There are rare boulders up to 30 cm in diameter, as well as a reworked inclusion of organic silt. The most probable source for this inclusion is an organic bed in unit A, suggesting that erosion and reworking occurred subsequent to deposition of unit A. The lower contact of the outwash unit was not observed. Unit C is basal till with subglacial thrust planes. Unit C makes up most of the exposure and forms the core of the sea cliff. There are four lithologic subunits. At the top, subunit C4 is a diamicton with a silty matrix with a clast concentration of less than 10%. Fracture lines are common in this subunit. Observed thickness is 2.8 m, but vegetation and reworking make this a minimum value. A pervasive shear plane marks the contact with subunit C3, which has a granular matrix and a clast concentration of over 20%. An irregular contact separates the diamicton of unit C3 from the underlying laminated silt unit C2. The silt laminations are 3–8 mm thick and are disturbed. There are high-angle faults through the thickness of the silt bed. A 2-m-long clastic dike penetrates the silt near its upper contact with the overlying diamicton. Clastic dikes also occur in several other parts of the section. The silt bed has a thickness of 1 m, and is not in an original depositional orientation. It appears to have been a distal glaciolacustrine package prior to translocation. Subunit C1, the lowest part of unit C, consists of translocated gravels approximately 1 m thick and rising 13° toward the northwest. Beds within this gravel unit have a vertical offset of at least 1 m. At the base of this unit is a sheared zone containing numerous angular clasts; at several locations the individual fragments of the clasts are adjacent to each other, indicating that the clasts were broken and transported less than 2 cm. This sedimentary package is interpreted as subglacial thrust slices at the base, with reworking of these sediments into subglacial till at the top. Unit D is a proglacial lacustrine sequence, best exposed in a road cut 38 m northwest of the limit of the sea cliff. The base lies 3.6 m above datum. Sediments in this sequence extend to at least 10 m above the datum, where they lie below the top of a terrace. The basal 2 m are composed of finely laminated silt with a few organic beds. At 5.2 m above the datum is a 20-cm-thick organic bed with localized disruptions of the bedding. Above this 20-cm-thick organic bed, there are individual thin (~1 cm thick) organic beds, of which two are prominent. The dates reported in Table 1 come from these three organic horizons, as shown on the diagram. Bedded coarse sand lies 2–3 m above the 20-cm-thick organic silt bed. Here the entire sequence coarsens upward, with a small gravel unit near the upper contact. The thickness of unit D is variable because it is cut by unit E, a basal till with a silty matrix. Clast concentrations in the till range from 10 to 20%. Fracture planes are parallel to the base of the till and reflect subglacial deposition.

belt is late Llanquihue in age. But none of the samples is in the age range of the reworked organic clasts at the Calbuco site or from the young outwash plain near Bahía Puerto Montt. Hence these results are consistent with the basal age of Huelmo mire in indicating that the inner moraine belt alongside Seno Reloncaví was not deposited during the advance shortly after 15,000 ^{14}C yr BP.

The mapping program, however, showed quite a different situation near the Calbuco site (94), as already suggested by the chronologic results. Here a fluted surface drift suggests a strong advance from the southeast that overran the site and probably reached close to the outer Llanquihue moraines limit (Fig. 4). This advance was of a piedmont glacier lobe from Golfo de Ancud, not from Seno Reloncaví. Again, the implication is that the advance shortly after 15,000 ^{14}C yr BP was stronger for the southern than for the northern lobe. As discussed below, such a strong advance is also characteristic of the northern part of the Golfo Corcovado lobe, which achieved its maximum on Isla Grande de Chiloé during an expansion that culminated close to 14,805 ^{14}C yr BP (Table 2). Thus there is a major increase in the strength of the advance shortly after 15,000 ^{14}C yr BP between the Lago Llanquihue and Seno Reloncaví piedmont lobes to the north, and the Golfo de Ancud and the northern Golfo Corcovado lobes to the south.

Numerous new dates afford maximum limiting values for the outermost Llanquihue moraine belt deposited by the Seno Reloncaví piedmont glacier. This belt forms a continuous arc from the interlobate intersection north of the Calbuco site (94) to the east of the town of Alerce (Fig. 5). Organic clasts reworked into the moraine core, or into outwash graded to the moraine, afford the following ages: 26,230±340 ^{14}C yr BP (A-6487); 28,970±410 ^{14}C yr BP (A-6488); 28,060 $^{+160}_{-155}$ ^{14}C yr BP (A-8780); 27,405 $^{+350}_{-335}$ ^{14}C yr BP (A-8781); 27,510±530 ^{14}C yr BP (UGA-6984) and 29,410 $^{+325}_{-300}$ ^{14}C yr BP (A-8783) from the core of a moraine north of Bahía Puerto Montt (site 33); 29,080±360 ^{14}C yr BP (A-6777) from outwash that passes beneath the outer Llanquihue-age moraine (site 40); 32,780 $^{+390}_{-385}$ ^{14}C yr BP (A-8785) and 26,475 $^{+265}_{-255}$ ^{14}C yr BP (A-8787) from outwash at site 60; 32,235 $^{+315}_{-300}$ ^{14}C yr BP (A-8789) from outwash at site 61; 26,560 $^{+240}_{-235}$ ^{14}C yr BP (A-8790) from outwash at site 62; and 29,605 $^{+285}_{-275}$ ^{14}C yr BP (A-8791) from outwash at site 63 (Table 1).

Fourteen samples of basal organic material from mires in topographic depressions afford minimum limiting ages for the outer moraine belt (Table 1). It is certain that this outer moraine belt antedates 18,000 ^{14}C yr BP, as four basal dates fall between 18,000 and 19,000 ^{14}C yr BP. There is also a high likelihood that the moraine is older than 20,480 $^{+325}_{-315}$ ^{14}C yr BP (A-8525), 21,230±169 ^{14}C yr BP (AA-16244), and 22,680 $^{+415}_{-395}$ ^{14}C yr BP (A-8526), the near-basal dates of mires at sites 56, 66, and 55, respectively.

The pre-late Llanquihue stratigraphic record is revealed in sections exposed during building construction on the gulfside ice-contact slope near Bahía Puerto Montt on the western bank of Canal Tenglo (site 46) (Fig. 29), as well as on the gulfside road at Punta Pelluco (site 48) (Fig. 30). The lower part of the Canal Tenglo section reveals debris-flow sediments and fluvial units, both composed of pyroclastic materials, interbedded with lacustrine sediments and peat beds. None of these lower units contains crystalline clasts from the Andes. Numerous dates show that the lower peat beds range in age from about 29,385 ^{14}C yr BP (Table 2) to 39,660 $^{+640}_{-595}$ ^{14}C yr BP (A-7699) (Table 1). These dates document a long interval when the Seno Reloncaví piedmont glacier lobe had withdrawn from the ice-contact slope near Puerto Montt alongside Seno Reloncaví. As discussed in Heusser *et al*. (1999), pollen analysis of all the dated peat beds shows Subantarctic Parkland environmental conditions.

During this ice-free interval Canal Tenglo was probably the channel of a river draining Volcán Calbuco. The fluvial units were deposited rapidly in the channel, as shown by climbing ripple structures that in some cases are deformed because of sediment loading. The debris-flow units of volcanic material, one of which encloses a tree in growth position dated to 31,905 $^{+265}_{-260}$ ^{14}C yr BP (A-7721), are probably the distal facies of lahars that radiated outward in drainage channels from Volcán Calbuco. Therefore, it is likely that each package of volcanic sediment between peat beds represents rapid deposition associated with a discrete volcanic event.

The upper part of the Canal Tenglo section is distinctly different from the lower part, in that it contains two thick ice-proximal outwash units, each with crystalline cobbles and boulders of Andean origin. Dates of associated peat beds afford close maximum ages for these outwash units. Sand that coarsens rapidly upward into coarse gravel of the lower outwash unit rests on the youngest of the lower peat beds mentioned above. The undisturbed top of the peat bed yielded six consistent ages with an error-weighted mean of 29,385±95 ^{14}C yr BP

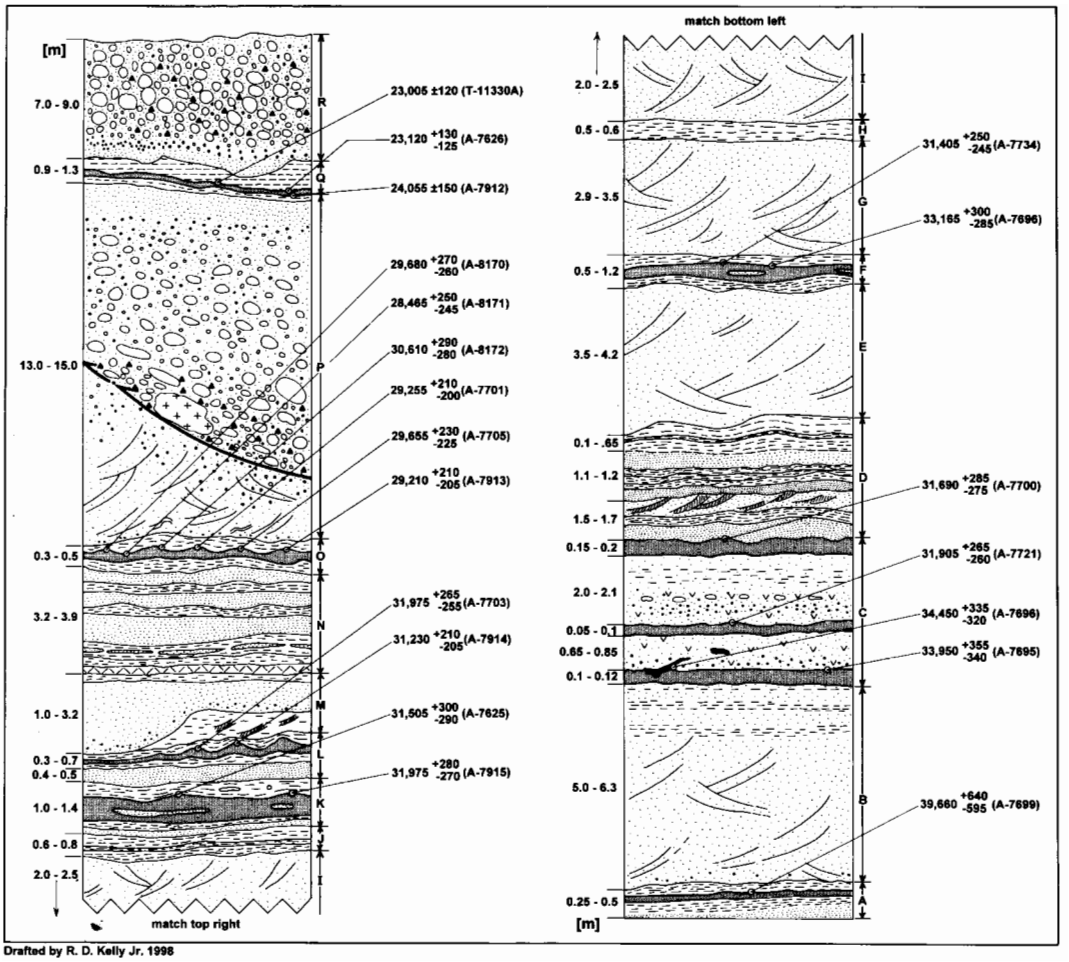

Fig. 29. Schematic composite lithostratigraphy of a sequence of glaciofluvial, fluvial volcanic, and peat units stacked in an ice-contact slope that rises 130 m above Canal Tenglo. See legend in Fig. 7 (p. 177) for lithologic details. Unit A features fibrous, organic-rich silt sealed with fine-grained lacustrine sediments. Unit B consists of coarse-grained volcanic sand with large-scale, cross-bedded stratification; this unit fines upward from small granules to fine-grained silt and sand. Unit C is fibrous peat with wood (some pieces in growth position) interbedded with coarse-grained volcanic debris-flow sediments; some reworked wood fragments occur within the volcanic sand. Unit D consists of thin beds (about 10 cm thick) of peat interbedded with coarse-grained volcanic sand. Units E and G feature large, cross-bedded volcanic sand that fines upward to fine-sand and silt. Unit F is fibrous peat with numerous wood fragments. Some wood fragments are sealed beneath laminated silt and clay. Unit H is peat with a low organic content. Unit I features cross-bedded volcanic sand; this unit fines upward from coarse-grained sand to fine sand and silt. Unit J is peat with a low organic content. Unit K is fibrous peat with numerous wood fragments (up to 10 cm in length) some sealed by silt and clay. Unit L is fibrous peat sealed by laminated silt and clay. Unit M is stratified silt and sand (with flame structures and well-developed diapirs). Unit N features well-defined horizons of peat (with low organic content) interbedded with well-stratified medium- to fine-grained sand. Unit O is fibrous peat with wood fragments sealed by laminated silts. Unit P is a coarsening-upward sequence of massive and stratified sand, gravel, cobbles, and boulders of Andean origin. It is interpreted to be glaciofluvial in origin. A major shear plane occurs a third of the way up this unit from the base. Unit Q is fibrous peat capped with laminated silts. Unit R features coarse gravel and fine-grained cobbles of Andean origin resting unconformably on unit Q; it is interpreted to be glaciofluvial in origin.

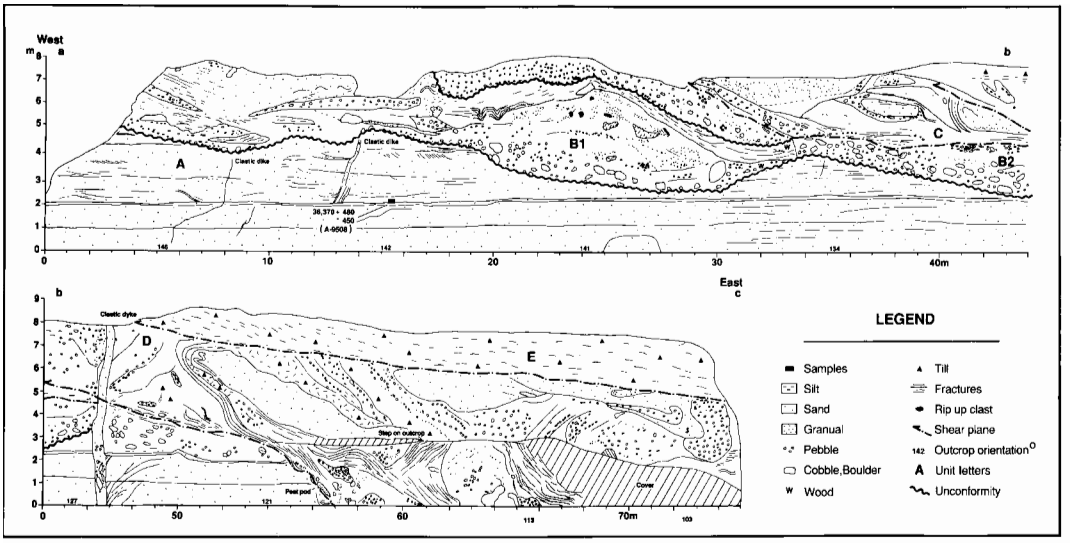

Fig. 30. Stratigraphic section at Punta Pelluco (site 48 in Fig. 15). Unit A is an intertidal delta sequence with horizontal beds of coarse volcanic sand, locally cross-bedded. Thin silt beds are concentrated in zones that are 1–2 m apart. Unit A extends upward from the present intertidal zone, with a maximum observed thickness of 11 m. Clastic dikes penetrate the unit from below. See Table 1 for a description of the radiocarbon sample from unit A. Unit B is a chaotic mixture of boulder gravel to coarse silt, deposited in a high-energy environment associated with proglacial drainage. Basal gravel and reworked organic clasts indicate a major unconformity. The unit is finer-grained on the western side of the outcrop than on the eastern side. Unit B2 is a proglacial channel gravel deposited in a high-energy environment associated with proglacial drainage. Coarse gravel is eroded on Unit B. Unit C features basal glacial thrust planes with imbricated slices of volcanic sand separated by gravel and diamicton. The lower contact is a major thrust slice. Unit D includes basal glacial thrusts with included blocks of sand and gravel. The unit has an erosive basal contact, with reworked organic clasts. All beds are reoriented, and several thrust planes occur within individual beds. Unit E is basal till with a sandy silt matrix and with fissility.

(Tables 1 and 2). A similar situation occurs higher in the section, where proximal outwash with Andean crystalline clasts overlies another peat bed. The lowest peat in this bed yielded a date of 24,055 ±150 ^{14}C yr BP (A-7912) (Table 1); the top of the peat bed afforded two consistent dates with a weighted mean of 23,059±87 ^{14}C yr BP (A-7626 and T-11330A) (Table 2). This date is a close maximum value for the ice advance represented by the upper outwash unit.

At site 86 about 3.8 km south of Huelmo in Fig. 5, an organic bed 500 m long separates glaciofluvial units exposed in a seaside cliff alongside Seno Reloncaví. The upper glaciofluvial unit underlies Llanquihue moraines. The upper surface of the organic bed is sealed intact with a thin silt layer that gives way to a coarsening-upward outwash sequence. Four dates of the upper surface of the peat bed yielded a weighted mean of 22,570±87 ^{14}C yr BP (Table 2) for an advance of the Seno Reloncaví piedmont lobe into the Llanquihue moraine belt.

Shells dated to 20,925±115 ^{14}C yr BP (A-7627) are embedded in marine silt and mud at the present shoreline of Seno Reloncaví at site 95. The shell-bearing sediments have been glacially displaced, and thus record ice-free conditions at or slightly seaward of the site.

Overall, the stratigraphic sections alongside Seno Reloncaví record a long ice-free interval in the outer moraine belt that began prior to 39,660 ^{14}C yr BP and ended with the deposition of proximal outwash about 29,385 ^{14}C yr BP (Table 2) at Canal Tenglo. Another major readvance is recorded at the Canal Tenglo section by renewed deposition of proximal outwash and probable glacier overriding shortly after 23,059 ^{14}C yr BP. The same advance is most likely recorded south of Huelmo (site 86) at 22,570 ^{14}C yr BP (Table 2). We estimate that this advance probably culminated with the deposition of the outer Llanquihue moraine belt fringing Seno Reloncaví, which has maximum dates of 26,230–26,475 ^{14}C yr BP and minimum dates of 21,230–22,680 ^{14}C yr BP. Recession was under way from the outer moraine belt by 21,230–22,680 ^{14}C yr BP. The coast was ice-free at 20,925 ^{14}C yr BP. A younger readvance culminated shortly after 15,000

^{14}C yr BP. To the north, the relatively small Seno Reloncaví piedmont lobe reached only to the western edge of the marine embayment. To the south, the large Golfo de Ancud piedmont lobe advanced beyond the coast well into the Llanquihue-age moraine belt. Although the intermediate moraine belts of the Seno Reloncaví ice lobes are undated, they must represent additional advances.

Northern Isla Grande de Chiloé

Figure 5 depicts Llanquihue moraine belts in the northern sector of eastern Isla Grande de Chiloé. The main Llanquihue outwash plain is graded to the outermost Llanquihue moraine belt, and subsidiary outwash terraces are graded to moraines nested behind the outermost belt. We have not yet carried out extensive field work on Isla Grande de Chiloé, but we report here new radiocarbon dates from several sites described previously.

The Taiquemó mire (site 96) is in a depression within the outermost Llanquihue moraine belt (Fig. 5). Thirty dates were obtained from a core through the 6.55 m of peat and lacustrine sediments in this mire (Heusser *et al*. 1999). These dates are progressively older with increasing depth in the core. The youngest is 10,355±75 ^{14}C yr BP (AA-17974) at 90 cm depth, and the oldest is > 49,892 ^{14}C yr BP (AA-14770) at 600 cm depth (Heusser *et al*. 1999). The results show that the outermost Llanquihue moraine in the eastern sector of northern Isla Grande de Chiloé antedates the LGM. The dates show continuous, or nearly continuous, accumulation of peat and lacustrine sediment. The pollen record documents the existence of a Subantarctic Parkland environment during cold stadials, from at least 15,000 ^{14}C yr BP back to > 49,892 ^{14}C yr BP. In middle Llanquihue time, Subantarctic Forest characterizes interstadials. Conspicuously absent from the entire record prior to 15,000 ^{14}C yr BP is an indication of the present-day interglacial rain forests of Isla Grande de Chiloé. The implication of these data is that the outer Llanquihue moraine at Taiquemó is considerably older than 49,892 ^{14}C yr BP and yet postdates the penultimate interglaciation. The most likely situation is that this outer moraine is middle or early Llanquihue in age.

There is evidence for at least two advances into the Llanquihue moraine belt on Isla Grande de Chiloé during the LGM. The youngest of these advances is documented at the Dalcahue site (98) (Fig. 31), previously described by Laugenie (1982) and Mercer (1984), where an organic bed of pyroclastic sand and silt accumulated in a small basin on compact, medium-gray lodgement till with Andean volcanic and crystalline erratics. In turn, the organic bed is overlain by a moraine with a core of glaciofluvial sand and gravel capped by thin (0.20–1.5 m) lodgement till with several large (up to 1.5 m long), striated crystalline erratics derived from the Andes. The basal part of the glaciofluvial sequence in the moraine core consists of fine- to medium-bedded sand that seals intact the upper surface of the organic bed. Thus the Dalcahue organic bed occurs between two glacial drift units, both representing advances of an Andean piedmont glacier lobe onto Isla Grande de Chiloé. A pollen profile constructed at centimeter intervals for the thickest portion (152 cm) of the organic bed (location B in Fig. 31) shows the continuous existence of a Subantarctic Parkland environment from shortly after 25,176 ^{14}C yr BP until about 14,720 ^{14}C yr BP (Heusser *et al*. 1999). Dates of the uppermost organic sediment at the location of the pollen profile are 14,720±100 ^{14}C yr BP (A-6189) and 14,770±110 ^{14}C yr BP (A-6190). Dates for the base of the organic bed are 28,558±366 ^{14}C yr BP (AA-19438) at 151 cm depth; 30,070 $^{+225}_{-215}$ ^{14}C yr BP (A-7685), also at 151 cm depth; and 27,910±315 ^{14}C yr BP (AA-19439) at 152 cm depth (Table 1). Table l shows numerous additional dates from within the organic bed at the pollen site. About 10 m south of the location of the pollen profile, the upper surface of the organic bed, here only 90 cm thick, reveals a wood layer buried intact by the stratified sand at the base of the glaciofluvial sequence. An additional 33 dates both of wood and of organic silt and sand range from 15,260±115 ^{14}C yr BP (UGA-6983) to 14,480±180 ^{14}C yr BP (UGA-6918) (Table l). Overall, the total of 35 dates of wood and organic sediment from the intact original surface of the organic bed at the two sampling localities yields a mean of 14,805±18 ^{14}C yr BP (Table 2), which should accurately record the last ice advance over the Dalcahue site. The progressively increasing ages with depth within the Dalcahue organic bed indicate that this advance was the most extensive in at least the last 30,070 ^{14}C yr BP, and therefore the most extensive of the LGM.

Fig. 31, *see p. 196.*

The advance of the northern part of the Golfo Corcovado piedmont lobe that passed over the Dalcahue organic bed reached at least to the Llanquihue moraine at the upper edge of the high ice-contact slope (site 99) 1.5 km north of the Dalcahue site. An exposure at the top of this slope shows ice-contact gravels unconformably cut into till and outwash. The till occurs along much of the ice-contact slope of this moraine, and probably corresponds to the basal till beneath the nearby Dalcahue organic bed. These relationships suggest that the slope marked an ice-marginal position on at least two occasions. The first probably corresponds with the advance dated at more than 30,070 ^{14}C yr BP at the Dalcahue site. The second corresponds with the advance over the Dalcahue organic bed, as shown by ages of organic clasts reworked into the ice-contact gravel at the top of the slope. The youngest of these clasts dates to 14,820±450 ^{14}C yr BP (QL-4532) and affords a maximum limiting age for the last advance to the head of the ice-contact slope. This clast must have been derived from the upper surface of the Dalcahue (or equivalent) organic bed. Other reworked clasts in the ice-contact gravel yielded ages of 20,030±160 ^{14}C yr BP (UGA-6972) and 19,840±180 ^{14}C yr B.P (UGA-6979). These clasts must have been derived from deeper in the Dalcahue organic bed (or from an equivalent organic bed), because the advance over the Dalcahue organic bed is the only one that could have been responsible for reworking such young organic clasts.

We obtained preliminary limiting dates for glacier recession by coring mires in morainal topography south of Dalcahue. Our mapping program shows that the outer Llanquihue moraines bend sharply southwestward near Dalcahue, and that the Llanquihue glacial limit trends toward the coast and out to sea near the middle of Isla Grande de Chiloé. Thus the sites we cored south of Dalcahue, as well as those cored by Villagrán (1988) in southeastern Isla Grande de Chiloé, all lie well within the limit reached by Andean ice during the youngest Llanquihue advance recorded at the Dalcahue site. The Mayol mire (site 100) yielded a sequence of consistently older dates with increasing depth that culminates in a basal age of 14,941±97 ^{14}C yr BP (AA-20370) (Heusser *et al*. 1999). Near-basal ages from the Estero Huitanque mire (site 101) are 13,345±105 ^{14}C yr BP (TUa-258A) and 14,350±240 ^{14}C yr BP (Beta-62029) (Heusser *et al*. 1996). Farther south at site 102, basal gyttja from a mire on Llanquihue drift dates to 13,560±95 ^{14}C yr BP (T-10307A). Villagrán (1988) reported near-basal dates of 13,040±210 ^{14}C yr BP (Beta-10481) from Puerto Carmen (site 103), and 13,100±260 ^{14}C yr BP (Beta-10485) from Laguna Chaiguata (site 104).

The final site that we examined is at Teguaco (site 97), previously described by Heusser (1990). Here a road cut exposes a 28-cm-thick organic silt and gyttja bed sealed by laminated, light-gray glaciolacustrine sediments that are overlain first by sand and then by ice-proximal glaciofluvial deposits. Twelve samples of gyttja with macrofossils from the upper surface of the organic bed and of wood pieces encased within the glaciolacustrine sediments yielded an error-weighted mean of 22,295±40 ^{14}C yr BP (Table 2). Dates from near the base of the organic silt and gyttja bed are 27,345 $^{+190}_{-185}$ ^{14}C yr BP (A-7693) and 26,630±175 ^{14}C yr BP (A-7692) (Table l). Organic sand from the base of the underlying 30-cm-thick organic sand unit afforded a date of 29,240±600 ^{14} C yr BP (QL-4546).

The Teguaco section is located within a deep, southeast-trending river valley. We interpret the stratigraphic sequence as representing an incursion of an Andean piedmont glacier lobe onto Isla Grande de Chiloé, damming a glacial lake that flooded the organic silt bed. The laminated glaciolacustrine sediments sealed the top of the organic bed. The wood in the glaciolacustrine silts was either floated off the land surface, or else was washed into the lake. The advancing piedmont ice lobe then deposited the coarsening upward sequence that culminated in ice-proximal outwash.

As currently understood, the moraines and stratigraphic sections on Isla Grande de Chiloé record three major advances of Andean piedmont glaciers into the Llanquihue moraine belt. The oldest advance, represented by the outermost moraine belt and by the main Llanquihue outwash plain, occurred prior to 49,892 ^{14}C yr BP. The youngest advance culminated at close to 14,805 ^{14}C yr BP at a moraine located 1.5 km northwest of the Dalcahue site (98). In Fig. 5 this moraine, which represents the maximum position achieved by Andean piedmont ice during the LGM, can be traced northward at least 30 km from the vicinity of the Dalcahue site, where it lies within 4 km east of the maximum Llanquihue moraine dated to > 49,892 ^{14}C yr BP at Taiquemó (site 96). Recession from the ice limit reached during the youngest advance was underway south of the Dalcahue site at Mayol (site 100) by 14,941 ^{14}C yr BP. The overall chronology of the Dalcahue site indicates that this youngest advance was the most extensive of the LGM. At least one additional advance during the LGM, dated to

22,295 ^{14}C yr BP at Teguaco (site 97), culminated behind the position reached during the youngest advance that overrode the Dalcahue site.

Discussion

Ice-front dynamics

The Llanquihue-age piedmont glacier lobes in the southern Lake District had flattish surface slopes. For example, the moraine belts mapped in Fig. 3 indicate that the surface slope of the Lago Llanquihue piedmont lobe rose inland toward the Andes at about 3.0 m/1000 m during the LGM. Similar values apply to the former Rupanco and Puyehue ice lobes (Fig. 2). When it stood at the edge of the lakeside kame terrace at the culmination of the readvance about 14,550–14,869 ^{14}C yr BP, the Lago Llanquihue lobe again had an upper surface that rose inland at only about 2.2 m/1000 m. These flattish lobes deposited only waterlain till, not meltout or basal lodgement tills, at the edge of lake and marine basins, in sharp contrast to the situation within the moraine belts, where only meltout, flow, and lodgement tills are present. The waterlain tills at the periphery of the basins were soft at the time of glacial deposition and overriding, as shown by the clastic dikes of diamicton injected into the laminated glaciolacustrine sediments and by the diapir structures caused by loading of the lacustrine sediments with gravelly debris-flow material from adjacent ice. And yet the fine laminations in the glaciolacustrine sediments that make up much of the waterlain till do not show deformation by pervasive shear from overriding glacier ice.

We suggest that waterlain till is the characteristic deposit recording the passage of piedmont ice lobes through the lake and marine basins. The flatness of the ice lobes probably occurred because the glacier ice was supported by high pore-water pressure in the waterlain till. Most of the basal ice flow probably occurred at the ice–sediment interface rather than by pervasive shearing of the underlying waterlain till. Once the ice flowed out of the basin into the fringing moraine system with its widespread porous outwash and gravelly diamicton, water flowed away from the glacier base, and the predominant basal deposit was lodgement till. Thus we postulate that the major facies deposited within the lake basins involved settling from silt plumes associated with meltwater discharge, along with sediment flows of gravelly diamicton from the ice margin. Basal sliding took place at the sediment–ice interface and till was not lodged on the lake floor. In contrast, the major facies deposited when ice lobes advanced out of the lake basins into the moraine belts were outwash, gravelly sediment flows, and lodgement till.

Accuracy of radiocarbon chronology

The validity of the reconstructions of glacier fluctuations depends on the accuracy of the radiocarbon chronology. Overall, the dates are remarkably consistent, but there are some problems. Because critical organic horizons are commonly isolated in stratigraphic sections, many individual results cannot be judged within the context of a consistent sequence of dates. In these cases, we obtained numerous dates of individual horizons, from various organic materials where possible, in order to establish the age from weighted mean values. The results of such exercises at the Dalcahue (98) and Frutillar Bajo (16) sites yielded two additional insights. First, individual dates of wood and organic sediment were indistinguishable. Second, the dates of the upper surface of the Dalcahue (site 98) organic bed have a range of about 780 ^{14}C yr (15,260±115 ^{14}C yr BP, UGA-6983, to 14,480±180 ^{14}C yr BP, UGA-6918) that is not dependent on the type of material analysed or on the dating laboratory (Table 1). Thus an individual date can be as much as 350–400 ^{14}C years different from the mean age of an organic horizon. Similar examples come from individual dates within the series obtained for the upper surface of organic beds at the Puerto Varas railroad bridge (site 26) and Bella Vista Bluff (site 29) sections (Table 1). Third, many dates reported by Mercer (1976) and Porter (1981) for organic beds in the Puerto Varas embayment are too young, compared with the new dates, by as much as 1600 ^{14}C yr. Such discrepancies suggest caution in interpreting the age of glacial events at other sites from individual dates. Hence, we emphasize replicate dating wherever possible in order to obtain the accuracy and precision necessary to establish the chronology of glacier fluctuations.

The most reliable results occur where a sequence of dates is integrated with multiple analyses of various materials from a critical horizon. Examples are the ages of the upper surface of the organic beds at the Dalcahue (site 98) and Frutillar Bajo (site 16) sites. The next most reliable results come from individual organic horizons with numerous analyses; an example is the organic bed at the Llanquihue site (23). Equally reliable are the results of the basal dates from cores and mires that have a sequence of

consistent ages. Examples are the cores from Fundo Llanquihue (site 18) (Heusser *et al*. 1996, 1999) and Canal de la Puntilla (site 6) (Moreno 1997; Moreno *et al*. 1999). The least reliable results are single dates of soil, gyttja, or peat clasts reworked into outwash. These clasts were eroded either from a pre-existing land surface or from organic beds exposed in stratigraphic sections. In such cases we attempted to date multiple reworked clasts from individual outwash units to achieve consistency in the results. We note that different parts of large clasts can obviously have widely varying ages (Table 1). Single dates of organic material from the base of cores through mires on Llanquihue moraine belts also may not be reliable. Again, where possible, we obtained radiocarbon dates from multiple cores to achieve consistency in the results.

Preferred chronology for Llanquihue glacial advances

A fundamental question is whether the low-sloping piedmont glacier lobes in the southern Chilean Lake District and Isla Grande de Chiloé reacted in unison to climate forcing or whether they exhibited the out-of-phase pulsing behavior suggested for low-sloping southern lobes of the Laurentide Ice Sheet and for low-sloping ice streams of the West Antarctic Ice Sheet (Alley and Whillans 1991; Clark 1994). To discriminate between these two possibilities, we obtained numerous dates of the youngest major advance of the Lago Llanquihue, Seno Reloncaví, Golfo de Ancud, and northern Golfo Corcovado piedmont lobes. The details of each site are given above and the dates are listed in Table l. The maximum extent of the Lago Llanquihue lobe during this advance is dated to 14,869 ^{14}C yr BP at the Llanquihue site (23; Table 2); 14,540 ^{14}C yr BP at the Bella Vista Bluff site (30) in Puerto Varas (Table 2); 14,550–14,613 ^{14}C yr BP at the railroad bridge site (26) in Puerto Varas; 14,820 ^{14}C yr BP at the Calle Santa Rosa site (27) in Puerto Varas (Mercer 1976); 14,882 ^{14}C yr BP at the Northwest Bluff site (28) in Puerto Varas (Table 2); and 14,650 ^{14}C yr BP at the Puerto Phillippi site (19) (Table 1). For the Seno Reloncaví lobe this advance is dated to 14,879 ^{14}C yr BP at Punta Penas (47) (Table 2); 15,220 ^{14}C yr BP at the Isla Maillen site (73) (Table 1); and shortly after 15,040 ^{14}C yr BP at the top of the ice-contact slope on the western side of Bahía Puerto Montt (45) (Table 1). For the Golfo de Ancud lobe, this readvance is dated to shortly after 14,900 ^{14}C yr BP west of Calbuco (94) (Table 1). Numerous dates from the Dalcahue site (98) place the last maximum of the northern part of the Golfo Corcovado lobe at close to 14,805 ^{14}C yr BP (Table 2); general recession was underway at the Mayol site (100) by 14,941 ^{14}C yr BP (Table 1). Therefore, we conclude that these four piedmont glacier lobes fluctuated in near synchrony (within the limits of radiocarbon dating) during the youngest major pulse of the LGM.

To test whether such synchronous behavior was characteristic of other ice-marginal fluctuations, we examined the chronology of the outer Llanquihue moraine belts of the northern three piedmont lobes, and of the early LGM advance onto Isla Grande de Chiloé. Here, interpretation of the situation is more complicated than with the youngest readvance. Therefore we established a preferred and an alternate chronology. Our preferred chronology starts with dates of *in-situ* samples in three stratigraphic sections. The first is from site l at the outer limit of Llanquihue moraines fringing Lago Rupanco. Here peat sealed by silt below the till cap of this moraine is 22,460 ^{14}C yr old, thus affording a close maximum date for this moraine (Table 1). On the western coast of Seno Reloncaví at site 86, a major readvance into the Llanquihue moraine belt is dated to 22,570 ^{14}C yr BP (Table 2). The available bracketing ages suggest that the outermost Llanquihue-age moraine belt west and north of Seno Reloncaví was deposited during this advance. Farther south at Teguaco on Isla Grande de Chiloé, a major glacial advance documented by numerous dates at 22,295 ^{14}C yr BP (Table 2) terminated behind the position reached at 14,805 ^{14}C yr BP. Finally, we consider the chronology of the outermost Llanquihue-age moraine belt fringing Lago Llanquihue. Most of the bracketing dates imply that this moraine belt is older than 20,890–20,580 and younger than 23,020–22,250 ^{14}C yr BP. It is thus possible that this moraine belt also was deposited during the major readvance dated elsewhere to about 22,295–22,570 ^{14}C yr BP.

Older advances are recorded for individual lobes. The most firmly established of these earlier advances is recorded at the Frutillar Bajo section (site 16) (Fig. 25), where a landscape surface was buried intact by glacial deposits at 26,797 ^{14}C yr BP. A less certain situation (because of the lack of a landscape buried intact) involves the advance at 29,363 ^{14}C yr BP recorded at the Puerto Octay site (7) and 29,385 ^{14}C yr BP Canal Tenglo site (46).

From the sections at Canal Tenglo and Puerto Octay, it appears that late Llanquihue glacial conditions began at about 29,400 ^{14}C yr BP. From the

chronology of the last major advance and from the minimum ages of deglaciation on Isla Grande de Chiloé, we conclude that the LGM ended shortly after 14,550–14,869 ^{14}C yr BP. The glacial record given here and the pollen records presented in Heusser *et al*. (1999) and in Moreno *et al*. (1999) together suggest that full-glacial or near-full-glacial conditions persisted for most of this 15,000 ^{14}C yr interval. The only discrepancy between these records occurs near the beginning of this interval, where a glacial maximum apparently occurred about 29,400 ^{14}C yr BP, but Subantarctic Forest lingered until a few thousand years later at Dalcahue and Taiquemó. During this long interval, glacier piedmont lobes probably achieved maxima at 14,550–14,869 ^{14}C yr BP; 22,295–22,570 ^{14}C yr BP; 26,797 ^{14}C yr BP; and 29,363–29,385 ^{14}C yr BP. There is a suggestion from the Puerto Varas embayment of additional maxima shortly before 17,800 ^{14}C yr BP and again shortly before 15,700 ^{14}C yr BP. The amount of recession between these maxima cannot yet be determined from direct evidence. But the pollen records from Dalcahue (site 98) and Taiquemó (site 96) on Isla Grande de Chiloé, along with those from Fundo Llanquihue, Canal de la Puntilla, and Alerce in the southern Lake District, suggest persistent cold, wet conditions throughout late Llanquihue time, with mean summer temperature as much as 6–8°C below the present-day value and precipitation about double that of today. Therefore, it is likely that glaciers remained relatively large throughout this long interval of cold, wet climate. However, two times of minor glacier recession deserve mention. The first is the Varas interstade of Mercer (1976). From the Llanquihue (23) and Bella Vista Bluff (30) sites, we now place this recession between 15,700 ^{14}C yr BP and 14,869 ^{14}C yr BP. From the pollen analysis of the Bella Vista Bluff and Llanquihue sites given in Heusser *et al*. (1996, 1999), as well as of the Fundo Llanquihue (18) and Canal de la Puntilla (6) sites (Heusser *et al*. 1999; Moreno *et al*. 1999), we conclude that open Subantarctic Parkland with cold and wet conditions persisted through this interval. Pollen of thermophilic trees is rare or lacking. The Lago Llanquihue piedmont glacier lobe receded from the western lakeshore during this interval, but from the available lake-level history we cannot determine if the lobe evacuated the lake basin. The second minor interval involved ice recession from the outermost Llanquihue moraine system west of Lago Llanquihue prior to 20,890 ^{14}C yr BP at Fundo Llanquihue (site 18); 20,100 ^{14}C yr BP at Canal de la Puntilla (site 6); and 20,580 ^{14}C yr BP at Canal de Chanchán (site 5). Similar recession had occurred from the western edge of the Seno Reloncaví marine embayment by 20,925 ^{14}C yr BP. The pollen records from the Fundo Llanquihue and Canal de la Puntilla cores again show persistence of Subantarctic Parkland under cold and wet conditions during this recession.

Massive glacier recession marked the end of full-glacial climate immediately after the culmination of the last major glacier advance at 14,550–14,869 ^{14}C yr BP, and ice had receded deep into the Andes, within 10 km of modern glaciers, by 12,310 ±360 ^{14}C yr BP (RL-1892) (Heusser 1990) (site 105) (Table 1). This last advance reached the western shore of Lago Llanquihue and Seno Reloncaví. On Isla Grande de Chiloé it was the maximum advance of the LGM. Pollen records from Canal de la Puntilla (Moreno *et al*. 1999) and Fundo Llanquihue (Heusser *et al*. 1999) show cold, wet environmental conditions during this advance. The pollen record places emphasis on the importance of the climate warming that accompanied this glacier recession. A marked rise of *Nothofagus* within a Subantarctic Parkland environment is taken to be evidence of the initial warming at 14,600 ^{14}C yr BP (Moreno 1998; Moreno *et al*. 1999). The pollen records from Canal de la Puntilla (Moreno 1994, 1997; Moreno *et al*. 1999), Fundo Llanquihue, and Alerce (Heusser *et al*. 1996, 1999) all highlight the invasion of the Lago Llanquihue and Seno Reloncaví lowlands by thermophilic tree species of the North Patagonian Evergreen Forest beginning at close to 14,000 ^{14}C yr BP. The Taiquemó pollen record (Heusser *et al*. 1999) shows this to be the most important vegetation change since prior to 49,842 ^{14}C yr BP. A closed-canopy North Patagonian Evergreen Forest then came into existence at 12,700–13,000 ^{14}C yr BP, and reached its fullest development at about 12,200–12,500 ^{14}C yr BP.

The paleoenvironment changes inferred from pollen are similar to those previously interpreted from the beetle record in the Chilean Lake District (Hoganson and Ashworth 1992; Ashworth and Hoganson 1993). However, new dates (Table 1) from the Puerto Varas railroad bridge site (26) now show that 10 of the 12 beetle samples from the organic silt unit refer only to 17,350–17,880 ^{14}C yr BP, and not to a continuous record through the last several thousand years prior to the end of the LGM. The remaining two beetle samples come from the prominent organic bed on the silt unit; it is unclear whether these two samples should be assigned to

17,350–17,880 ^{14}C yr BP or to 14,613^{14} C yr BP. In view of this revised chronology, the available fossil beetle data show cold, wet conditions at the following times within the LGM: 16,000–18,170 ^{14}C yr BP (Canal de Chanchán, site 5); 17,350–17,880 ^{14}C yr BP (railroad bridge, site 26); and 15,715 ^{14}C yr BP (Bella Vista Park, site 29).

Dates of interdrift organic sediments at the Puerto Octay (7), Frutillar Bajo (16), and Canal Tenglo (46) sites indicate an interval of ice-free conditions along the western shores of Lago Llanquihue and Seno Reloncaví, beginning about 36,960–39,660 ^{14}C yr BP and ending about 26,940–29,400 ^{14}C yr BP. We have not found evidence of Andean glacier advance into the outer Llanquihue-age moraine system during this interval. By necessity, then, the extensive outwash plains graded to Llanquihue moraine belts must have been inactive throughout this middle Llanquihue non-glacial interval. We cannot yet determine from direct evidence the magnitude of middle Llanquihue recession of Andean piedmont and mountain glaciers. But the pollen records from the Puerto Octay, Frutillar Bajo, and Canal Tenglo sites are consistent in showing the persistence of a cool, wet Subantarctic Parkland environment through the later part of middle Llanquihue time in the Lago Llanquihue and Seno Reloncaví areas.

Llanquihue drift units that are little weathered occur beneath dated middle Llanquihue interdrift organic deposits near Lago Llanquihue. At the Puerto Octay site (7), outwash dated to >39,340 ^{14}C yr BP represents a glacier advance at least to the top of the adjacent ice-contact slope. At Frutillar Bajo (site 16) a coarsening-upward sequence of glaciofluvial deposits is capped by till, all older than 36,960 ^{14}C yr BP. The associated glacier advance was beyond the top of the ice-contact slope and into the Llanquihue moraine belt. West of Puerto Varas at the outer edge of the Llanquihue moraine belt at site 24, thin late Llanquihue drift overlies thick outwash with an intervening organic layer. The terrace morphology of the outwash can be traced eastward beneath the thin late Llanquihue drift to a massive overridden moraine located about 500 m behind the outermost late Llanquihue ice-marginal position. At the nearby crossroad site 25, the upper portion of the weathered interdrift pyroclastic sediments was sheared into overlying drift during a glacial advance over the site. The likely situation is that this advance culminated at the massive overridden moraine to which the pre-late Llanquihue outwash terrace is graded.

The outermost moraine depicted in Fig. 5 for Isla Grande de Chiloé is also middle or early Llanquihue in age, as shown by the basal date of >49,892 ^{14}C yr BP for the mire at Taiquemó (site 96). For two reasons it seems probable that the Llanquihue moraine at Taiquemó was deposited during marine isotope stage (MIS) 4. First, the moraine is beyond the range of accurate dating. Second, close-interval pollen analysis of the Taiquemó core shows Subantarctic Parkland and Subantarctic Evergreen Forest persisting back to the time of deposition of the moraine (Heusser *et al*. 1999). If this Llanquihue moraine antedated the penultimate interglaciation, then pollen of thermophilic trees of the North Patagonian and Valdivian Evergreen Forests would be expected in the older part of the Taiquemó record (such trees invaded the lowlands of the Lake District and Isla Grande de Chiloé early in the present interglaciation). Hence, the absence of such pollen strongly suggests that the moraine postdates the last interglaciation. An old Llanquihue advance that antedates 49,892 ^{14}C yr BP and postdates the penultimate interglaciation is most likely to be equivalent in age to MIS 4. Old Llanquihue drift in the moraine belt near Lago Llanquihue also is probably equivalent in age to MIS 4; however, it is more difficult to rule out a younger age because, unlike the situation at Taiquemó, the chronology and pollen records of the interdrift organic deposits extend back only to about 40,000 ^{14}C yr BP. In any case, the implication is that the snowline in this sector of the Chilean Andes was depressed as much during the old Llanquihue advance(s) as during the LGM.

Alternate late Llanquihue chronology

We do not wish to leave the impression that our preferred chronology for glacial maxima during the LGM is without problems. For example, only limiting dates bracket the outer Llanquihue moraine belts west of Lago Llanquihue and Seno Reloncaví. Hence the proposed linkage of these outer moraines with the stratigraphic evidence of an advance at 22,295–22,570 ^{14}C yr BP could be questioned. In fact, there are now four dates that do not support this linkage. Three are of reworked organic clasts in outwash graded to the outer Llanquihue moraines. The first of these clasts, from site 4 west of Bahía Muñoz Gamero, dates to 20,840 ^{14}C yr BP. As described above, the geomorphologic relationships depicted in Fig. 2 suggest that this date may be too young. The dated clast is reworked into out-

wash graded to the outermost Llanquihue moraine, situated on the upper edge of a high ice-contact slope. Proximal to this outer ice-contact slope are several subsidiary Llanquihue outwash terraces that, in turn, grade to a moraine belt and ice-contact slope alongside Bahía Muñoz Gamero. The meltwater channels of Canal de Chanchán and Canal de la Puntilla head at this lakeside ice-contact slope, and hence the minimum ages for these two channels (20,580±170 ^{14}C yr BP, AA-9303; and 20,160 ±180 ^{14}C yr BP, AA-9296) apply to all the Llanquihue moraines and ice-contact slopes west of Bahiá Muñoz Gamero. Thus it is difficult, although not impossible, to argue that the outermost Llanquihue moraine and outwash plain are younger than 20,840 ^{14}C yr BP.

The situation is more problematic with regard to the date of 20,100 ^{14}C yr BP from the second of these organic clasts, reworked into outwash that passes beneath the outer Llanquihue moraine at site 13 near Frutillar Alto (Mercer 1976). As outlined above, the geomorphologic tracing of this outer moraine at Frutillar Alto to the northeast shows that it is older than the outer (and hence oldest) Llanquihue moraine cut by Canal de Chanchán and Canal de la Puntilla. Therefore, the same argument concerning the age and geomorphologic position of these channels implies that the date from Frutillar Alto is too young. This conclusion is augmented by the fact that the outer Llanquihue moraine belt at Fundo Llanquihue (site 18) can be traced northward to the outer Llanquihue moraine at Frutillar Alto. But at Fundo Llanquihue this outer moraine belt has minimum ages that extend back to 20,890 ^{14}C yr BP (UGA-6908), again suggesting that the maximum age of 20,100 ^{14}C yr BP derived from the reworked clast in outwash at Frutillar Alto is too young.

The third of these reworked clasts occurs in outwash graded to the outermost Llanquihue moraine at site 11 near Frutillar Alto. This clast dates to 21,120±180 ^{14}C yr BP (AA-25374) (Table 1). Taken at face value, this result could be used to argue that the age of the outer Llanquihue-age moraine system west of Lago Llanquihue is close to 21,000 ^{14}C yr BP. Such an age comes from taking the available maximum (23,020 ^{14}C yr BP at site 3; 22,790 ^{14}C yr BP, 22,700 ^{14}C yr BP, and 21,120 ^{14}C yr BP at site 11 at Frutillar Alto; and 22,250 ^{14}C yr BP and 22,985 ^{14}C yr BP at site 32) and minimum (20,580 ^{14}C yr BP at Canal de Chanchàn, site 5; 20,160 ^{14}C yr BP at Canal de la Puntilla, site 6; 20,890 ^{14}C yr BP at Fundo Llanquihue, site 18) bracketing dates of the outer moraine belt at face value. But we prefer to reserve judgment on this important issue until additional maximum limiting dates are available.

A date of 19,450 ^{14}C yr BP (I-5679) of ashy peat from below till at site 1 in the outer moraine near Lago Rupanco previously reported by Mercer (1976) also does not fit our preferred chronology for the outer Llanquihue moraine system in the southern Lake District. We have been unable to replicate this age, despite dating several samples from a similar stratigraphic position in the same borrow pit (Table l), and hence we have not included it in our preferred chronology.

These potential problems with the preferred chronology leave open the distinct possibility that there were several advances (rather than one advance) into the outer moraine belt between 20,000 and 23,000 ^{14}C yr BP. The earliest would have been that dated at 22,295–22,570 ^{14}C yr BP from stratigraphic sections. It would have represented the Llanquihue maximum for the former Lago Rupanco and Seno Reloncaví piedmont glacier lobes. Farther south on Isla Grande de Chiloé, as well as near Lago Llanquihue, this advance would have culminated short of the outer late Llanquihue moraines. A subsequent advance at close to 21,000 ^{14}C yr BP would have formed the outermost Llanquihue-age moraines west of Lago Llanquihue, and elsewhere would have culminated short of the outermost Llanquihue-age moraines.

Conclusions

- The glacial chronology presented here suggests that the LGM in the region of the southern Lake District, Seno Reloncaví, and Isla Grande de Chiloé began at 29,400 ^{14}C yr BP and ended shortly after 14,550–14,805 ^{14}C yr BP. Within this interval of nearly 15,000 ^{14}C yr, glacial advances into the outer Llanquihue moraine belts culminated at about 29,400 ^{14}C yr BP, 26,797 ^{14}C yr BP, 22,295–22,570 ^{14}C yr BP, and 14,550–14,869 ^{14}C yr BP. Additional glacial advances into the outer moraine belt may have occurred at close to 21,000 ^{14}C yr BP, shortly before 17,800 ^{14}C BP, and shortly before 15,730 ^{14}C yr BP. Snowline depression during these advances was about 1000 m (Porter 1981; Hubbard 1997). Pollen records given in Heusser *et al.* (1999) and in Moreno *et al.* (1999) show that the LGM environment in the southern Lake District remained a Subantarctic Parkland under cold (6–8°C depression of mean summer temperature

below the current value) and wet conditions. However, at Dalcahue on Isla Grande de Chiloé, Subantarctic Forest was present until about 25,176 ^{14}C yr BP, then to be replaced by Subantarctic Parkland (Heusser *et al*. 1999). At Taiquemó, Subantarctic Forest dominated until about 26,019 ^{14}C yr BP (Heusser *et al*. 1999). These results may mean that the estimated beginning of the LGM from the glacier record is several thousand years too old.

- Andean piedmont glacier lobes did not advance into the outer Llanquihue moraine belts during the portion of middle Llanquihue time between 29,400 ^{14}C yr BP and >39,660 ^{14}C yr BP.
- Early or middle Llanquihue glacier expansion to near the outer limit of Llanquihue-age moraines occurred more than about 40,000 ^{14}C yr BP for the Lago Llanquihue piedmont lobe. The Golfo de Ancud and northern Golfo Corcovado piedmont lobes reached their maximum at the outermost Llanquihue moraine on Isla Grande de Chiloé prior to 49,892 ^{14}C yr BP. Pollen analysis of the Taiquemó mire suggests that this moraine probably dates to the time of MIS 4. The implication is that the Andean snowline was then depressed as much as during the LGM.

Acknowledgements

This research was supported by the Office of Climate Dynamics of the National Science Foundation, the Lamont-Scripps Consortium for Climate Research of the National Oceanic and Atmospheric Administration, the National Geographic Society, the Norwegian Research Council, and the Swiss National Science Fund. P.I. Moreno was supported by the EPSCoR Program of the National Science Foundation. W. S. Broecker invited G. Denton, C. Heusser, and L. Heusser on the field trip (funded by Exxon) to southern South America in 1989 that initiated this work; we thank him for his continued support and for numerous discussions about the significance of our Southern Hemisphere paleoclimate data. The field work was carried out in co-operation with the Servicio Nacional de Geología y Minería, Chile. Arturo Hauser Y. and Jorge Muñoz B. helped greatly with logistics and geological advice. Hugo Moreno R. afforded enormous aid in identifying and interpreting the pyroclastic flow sediments on all the glacial landforms, as well as the debris-flow deposits of volcanic breccia on the kame terrace near Puerto Varas. Richard Kelly drafted many of the maps and figures. Dr Seymour typed the manuscript. M. Dubois, D. King, C. Latorre, A. Moreira, S. Moreira, and A. Silva assisted in the field. C. Porter built field equipment and aided in the field work. M. Boegel and Y. Hechenleitner were very helpful in making local arrangements. We thank W. Beck, G.Bonani, C. Eastoe, S. Gulliksen, I. Hajdas, A. Hogg, T. Jull, R. Kalin, R. Nydal, and M. Stuiver for providing radiocarbon dates. We are grateful to A. Ashworth and S. Porter both for discussions and for information about stratigraphic sections in the southern Lake District. We thank R. Rutford for energetic help in the field. This paper is funded in part by a grants/cooperative agreement from the National Oceanic and Atmospheric Administration. The views expressed herein are those of the author(s) and do not necessarily reflect the views of NOAA or any of its sub-agencies.

George H. Denton, Department of Geological Sciences and Institute for Quaternary Studies, Bryand Global Sciences Center, University of Maine, Orono, Maine 04469, USA.

Calvin J. Heusser, 100 Clinton Road, Tuxedo, New York 10987, USA.

Thomas V. Lowell, Department of Geology, University of Cincinnati, Cincinnati, Ohio 45221, USA.

Christian Schlüchter, Institute of Geology, University of Bern, 3012 Bern, Switzerland.

Bjørn G. Andersen, Institute for Geology, University of Oslo, NO-0316, Blindern, Oslo 3, Norway.

Linda E. Heusser, Lamont-Doherty Earth Observatory, Palisades, New York 10964, USA.

Patricio I. Moreno, Institute for Quaternary Studies, Bryand Global Sciences Center, University of Maine, Orono, Maine 04469, USA.

David R. Marchant, Department of Geology, Boston University, 675 Commonwealth Avenue, Boston, Massachusetts 02215, USA.

References

Alley, R.B. and Whillans, I.M., 1991: Changes in the West Antarctic Ice Sheet. *Science*, 254:959–963.

Andersen, B.G., Denton, G.H. and Lowell, T.V., 1999: Glacial geomorphologic maps of Llanquihue drift in the area of the southern Lake District, Chile. *Geografiska Annaler*, 81A: 155–166.

Ashworth, A.C. and Hoganson, J.W., 1993: The magnitude and rapidity of the climatic change marking the end of the Pleistocene in the mid-latitudes of South America. *Palaeogeography, Palaeoclimatology, Palaeoecology,* 101:263–270.

Bentley, M.J., 1997: Relative and radiocarbon chronology of two former glaciers in the Chilean Lake District. *Jorunal of Quaternary Science* 12:25–33.

Blunier, T., Chappellaz, J., Schwander, J., Dällenbach, A., Stauffer, B., Stocker, T.F., Raynaud, D., Jouzel, J., Clausen, H.B., Hammer, C.V. and Johnsen, S.J., 1998: Asynchrony of Antarctic and Greenland climate change during the last glacial period. *Nature,* 394:739–743.

Bond., G.C. and Lotti, R., 1995: Iceberg discharges into the North Atlantic on millennial time scales during the last glaciation. *Science,* 267:1005–1010.

Brüggen, J., 1950: Fundamentos de la geología de Chile. Instituto Geográfico Militar. Santiago.

Clark, P.U., 1994: Unstable behavior of the Laurentide Ice Sheet over deforming sediment and its implications for climatic change. *Quaternary Research,* 41:19–25.

Denton, G.H., Heusser, C.J., Lowell, T.V., Moreno, P.I., Andersen, B.G., Heusser, L.E., Schlüchter, C. and Marchant, D.R., 1999 : Interhemispheric linkage of paleoclimate during the last glaciation. *Geografiska Annaler*, 81 A:107–153.

Fairbanks, R.G., 1989: A 17,000 year glacio-eustatic sea level record: Influence of glacial melting rates on the Younger Dryas event and deep-ocean circulation: *Nature,* 342:637–642.

Hajek, E.R. and di Castri, F., 1975: Bioclimatografia de Chile. Imprenta editorial de la Universidad Católica de Chile. Santiago.

Heusser, C.J., 1974: Vegetation and climate of the southern Chilean Lake District during and since the last interglaciation. *Quaternary Research,* 4:290–315.

— 1981: Palynology of the last interglacial–glacial cycle in mid-latitudes of southern Chile. *Quaternary Research,* 16:293–321.

— 1990: Chilotan piedmont glacier in the southern Andes during the last glacial maximum. *Revista Geológica de Chile,* 17:3–18.

Heusser, C.J. and Flint, R.F., 1977: Quaternary glaciations and environments of northern Isla Chiloé. *Geology,* 5:305–308.

Heusser, C.J., Heusser, L.E. and Lowell, T.V., 1999: Paleoecology of the southern Chilean Lake District–Isla Grande de Chiloé during middle-late Llanquihue glaciation and deglaciation. *Geografiska Annaler*, 81 A:231–284.

Heusser, C.J., Denton, G.H., Hauser, A., Andersen, B.G. and Lowell, T.V., 1995: Quaternary pollen records from the Archipiélago de Chiloé in the context of glaciation and climate. *Revista Geológica de Chile,* 22:25–46.

Heusser, C.J., Lowell, T.V., Heusser, L.E., Hauser, A., Andersen, B.G. and Denton, G.H., 1996: Full-glacial–late-glacial paleoclimate of the southern Andes: Evidence from pollen, beetles and glacial records. *Journal of Quaternary Science,* 11:173–184.

Hoganson, J.W. and Ashworth, A.C., 1992: Fossil beetle evidence for climatic change 18,000–10,000 years BP in south-central Chile. *Quaternary Research,* 37:101–116.

Hubbard, A.L., 1997: Modelling climate, topography and paleoglacier fluctuations in the Chilean Andes. *Earth Surface Processes and Landforms,* 22:79–92.

Ives, P.C., Levin, B., Robinson, R.D. and Rubin, M., 1964: U.S. Geological Survey radiocarbon dates VIII. *Radiocarbon,* 6:37–76.

Laugenie, C., 1982: La Région des Lacs, Chili Meridional. Unpublished PhD thesis. Universit de Bordeaux, Bordeaux, France. Volume 1, 1–332, Volume 2, 335–822.

Laugenie, C.A. and Mercer, J.H., 1973: Southern Chile: A chronology of the last glaciation. *In*: IX INQUA Congress Abstracts. Christchurch, N.Z. 202–203.

Lowell, T.V., Heusser, C.J., Andersen, B.G., Moreno, P.I., Hauser, A., Heusser, L.E., Schlüchter, C., Marchant, D.R. and Denton, G.H., 1995: Interhemispheric correlation of late Pleistocene glacial events. *Science,* 269:1541–1549.

Mercer, J.H., 1972: Chilean glacial chronology 20,000 to 11,000 Carbon -14 years ago: Some global comparisons. *Science,* 176:1118–1120.

— 1976: Glacial history of southernmost South America. *Quaternary Research,* 6:125–166.

— 1984: Late Cainozoic glacial variations in South America south of the equator. *In*: Vogel, J.C.D. (ed.): Late Cainozoic Paleoclimate of the Southern Hemisphere. A.A. Balkema. Rotterdam. 45–58.

Moreno, P.I., 1994: Vegetation and climate near Lago Llanquihue in the Chilean Lake District between 20,200 and 9500 ^{14}C yr BP. MS thesis. University of Maine. Orono, Maine. 50 p.

— 1997: Vegetation and climate near Lago Llanquihue in the Chilean Lake District between 20,200 and 9500 ^{14}C yr BP. *Journal of Quaternary Science*, 12:485–500.

— 1998: Termination of the last ice age in mid-latitudes of South America. PhD thesis. University of Maine. Orono, Maine. 187 p.

Moreno, P.I., Lowell, T.V., Jacobson, G.L. Jr and Denton, G.H., 1999: Abrupt vegetation and climate changes during the last glacial maximum and last termination in the Chilean Lake District: A case study from Canal de la Puntilla (41°S). *Geografiska Annaler*, 81 A:285–311.

Olivares, R.B., 1967: Los glaciones cuaternarias al oeste de Lago Llanquihue en el sur de Chile. *Revista Geográfica,* 67:100–108.

Porter, S.C., 1981: Pleistocene glaciation in the southern Lake District of Chile. *Quaternary Research,*16:263–291.

Schlüchter, C., Gander, P., Lowell, T.V. and Denton, G.H., 1999: Glacially folded outwash near Lago Llanquihue, southern Lake District, Chile. *Geografiska Annaler*, 81 A:347–358.

Sowers, T. and Bender, M., 1995: Climate records covering the last deglaciation. *Science,* 269:210–214.

Steig, E.J., Brook, E.J., White, J.W.C., Sucher, C.M., Bender, M.L., Lehman, S.J., Waddington, E.D., Morse, D.L. and Clow, G.D., 1998: Synchronous climate changes in Antarctica and the North Atlantic. *Science* 282:92–95.

Turbek, S.E. and Lowell, T.V., 1999: Glacial deposition along an ice-contact slope: An example from the southern Lake District, Chile. *Geografiska Annaler*, 81 A:325–346.

Villagrán, C., 1988: Late Quaternary vegetation of southern Isla Grande de Chiloé, Chile. *Quaternary Research,* 29:294–306.

Ward, G.K. and Wilson, S.R., 1978: Procedures for comparing and combining radiocarbon age determinations: A critique. *Archaeometry,* 20:19–31.

Weischet, W., 1958: Studien über den glazial bedingten Formenchatz der südchilenischen Längssenke im West-Ost Profil beiderseits Osorno. *Petermanns Geographische Mitteilungen,* 102:161–172.

— 1964: Geomorfología glacial de la región de los lagos. Communicaciones de la Escuela de Geología No. 4. Universidad de Chile, Santiago. 36 p.

Manuscript received Febr. 1998, revised and accepted Nov. 1998.

Table 1. Radiocarbon dates associated with glacial deposits in the region of the southern Lake District, Seno Reloncaví and Isla Grande de Chiloé from the University of Arizona Laboratory of Isotope Geochemistry (A), the NSF-Arizona Accelerator Mass Spectrometry (AMS) Facility (AA), the University of Georgia Radiocarbon Laboratory (UGA), the Trondheim Laboratoriet for Radiologisk Datering (T and TUa), the University of Washington Quaternary Isotope Laboratory (QL), the University of Waikato Radiocarbon Laboratory (Wk), ETH-Hönggerberg AMS Facility (ETH), and Beta Analytic (Beta). See original references for dating laboratories of dates reported by previous investigators. The locations of the sample sites are given in Figures 1 and 7-10. Asterisks indicate samples used in Table 2.

Site No.	Lab. No.	Age ^{14}C yr BP	δ^{13}C (‰)	Description
1	A-9516	22,460±135	-26.6	Rupanco borrow pit. Sample from top 1 cm of fibrous peat. Top of peat is sealed by a thin layer of silt overlain by sand (20 cm) and then till (50 cm). Date is close maximum for the glacier advance represented by till.
	A-9517	23,060±160	-26.3	Sample from top 1 cm of fibrous peat beside sample A-9516.
	T-9660 A	22,560±495	-24.9	Ashy peat layer mechanically displaced into moraine core. Maximum age for moraine.
	T-9659 A	20,605±880	-27.7	Ashy peat layer mechanically displaced into moraine core. Maximum age for moraine.
	T-10309 A	22,745±295	-26.7	Top of peat layer folded and mechanically displaced in moraine core. Maximum age for moraine.
	T-11326 A	25,280±240	-27.1	Base of peat layer (same layer as sample) T-10309A folded and mechanically displaced in moraine core. Maximum age for moraine.
	A-7704	25,175±150	-27.7	Ditto, except different sample.
	UGA-7092	25,680±330	-25.0	Ditto, except different sample.
	T-11212 A	24,865±205	-26.6	Ditto, except different sample.
	A-6553	$43{,}130^{+2850}_{-2100}$	-28.6	Wood from bed mechanically displaced into moraine core. Maximum age for moraine.
	A-6554	$34{,}030^{+1710}_{-1410}$	-27.5	Ashy peat mechanically displaced into moraine core beneath till. Maximum age for moraine.
	AA-13706	43,742±2169	-28.9	Peat mechanically displaced into moraine core beneath till. Maximum age for moraine.
	AA-13707	38,329±1134	-27.8	Ditto, except different sample.
	AA-13709	43,705±2153	-28.1	Ditto, except different sample.
	AA-13708	43,134±2027	-24.3	Wood sheared into moraine core beneath till. Maximum age for moraine.
	UGA-6962	>48,400	-25.5	Wood in bed mechanically displaced into core of moraine. Maximum age for moraine.
	T-9661	$35{,}990^{+900}_{-800}$	-26.5	Ditto, except different sample.
2	A-6489	$41{,}100^{+1900}_{-1500}$	-26.9	Organic clast reworked into outwash. Maximum age for outwash.
3	QL-4539	23,020±280	-24.8	Organic clast reworked into outwash beneath till at outer margin of moraine. Maximum age for outwash and moraine.
	QL-4542	33,800±700	-27.0	Ditto, except different sample.
	QL-4541	>38,000	-28.5	Ditto, except different sample.
	QL-4540	>41,000	-27.7	Ditto, except different sample.
	Wk-2557	>40,000	-28.8	Ditto, except different sample.
	Wk-2558	>20,000	-26.3	Ditto, except different sample.
	Wk-2559	>35,000	-28.7	Ditto, except different sample.
	UGA-6934	$35{,}630^{+620}_{-510}$	-28.7	Ditto, except different sample.
4	QL-4527	20,840±400	-25.5	Organic clast reworked into outwash graded to outermost Llanquihue moraine. Maximum age for outwash and moraine..
	QL-4528	$40{,}900^{+2200}_{-1700}$	-26.5	Ditto, except different sample.
	Wk-2538	38,000±650	-28.0	Ditto, except different sample.
	Wk-2539	27,700±200	-27.0	Ditto, except different sample.
	Wk-2560	>30,000	-26.2	Ditto, except different sample.
	UGA-6944	$34{,}075^{+980}_{-875}$	-27.0	Large organic clast with stratified organic layers. Sample from top of clast. Clast reworked into outwash. Maximum age for outwash.
	UGA-6943	>48,000	-26.5	Same as UGA-6944, but from center of clast.
5	AA-9298	20,380±170	-29.9	Canal de Chanchán. Wood from 2.21 m depth in 2.44-m core to base of mire in Canal de Chanchán. Core located on channel bottom 60 m west of Route V-55-U.

Site No.	Lab. No.	Age ^{14}C yr BP	δ^{13}C (‰)	Description
	AA-9300	19,470±150	-28.7	Wood from 1.93 m depth in 2.09-m core to base of mire in Canal de Chanchán. Core site within 10 m of AA-9298.
	AA-9303	20,580±170	-29.9	Wood from 2.19 m depth in 2.34-m core to base of mire in Canal de Chanchán. Core site within 10 m of AA-9298.
	AA-15366	20,202±186	-29.2	Basal gyttja from a 2.0-m core from a mire in Canal de Chanchán. Core site within 10 m of AA-9298.
	AA-15365	19,305±149	-29.8	Basal organic matter from 2.2-m core located 10 m north of AA-15366.
	AA-15364	17,375±208	-30.2	Basal organic matter from 2.2-m core located 20 m north of AA-15366.
	AA-15363	16,252±146	-29.6	Basal organic matter from 2.2-m core located 30 m north of AA-15366.
	AA-15362	13,979±99	-28.9	Basal organic matter from 2.2-m core located 40 m north of AA-15366.
	AA-9304	18,025±200	-27.8	Basal organic matter from 2.0-m core in mire on floor of Canal de Chanchán 150 m east of Route V-55-U.
6	AA-9296	20,160±180	-27.2	Canal de la Puntilla. Wood from 4.35 m depth in 4.365-m core to base of mire in Canal de la Puntilla. See Moreno *et al.* (1999) for location and additional dates.
	Beta-60353	19,840±170	-29.2	Organic silt from 4.1 m in 4.1-m core to base of mire in Canal de la Puntilla. See Moreno *et al.* (1999) for location and additional radiocarbon dates.
7	A-7667*	$29{,}560^{+275}_{-265}$	-25.6	Puerto Octay. Organic silt and find sand from upper 2 cm of a 77-cm-thick bed of pyroclastic flow sediments between two units of ice-contact gravel on the north side of Route V-55-U near ice-contact slope. Fig. 27.
	A-7657	$33{,}045^{+315}_{-300}$	-27.3	Ditto, except sample collected 35 cm from top of organic bed.
	A-7666	$34{,}085^{+390}_{-375}$	-27.7	Check for reproducibility of A-7657.
	A-7665	$37{,}750^{+650}_{-600}$	-27.2	Ditto, except sample at 70 cm from top of organic bed.
	A-7658	$41{,}925^{+1330}_{-1140}$	-27.3	Check for reproducibility of A-7665.
	A-7664	$35{,}470^{+680}_{-625}$	-25.9	Ditto, except sample from base of organic bed.
	QL-1338*	29,600±350	—	Organic silt and fine sand from top of bed of weathered, organic pyroclastic flow sediments between two outwash units on the south side of Route V-55-U. Sample site on eastern end of exposure near ice-contact slope (Porter 1981), 75 m east of sample QL-4538.
	QL-1339	37,400±500	--	Organic silt and fine sand from near base of same organic layer and site as QL-1338 (Porter 1981).
	QL-4538*	29,030±540	-24.3	Organic silt and fine sand from upper 2 cm of a 90-cm-thick organic bed of weathered pyroclastic flow sediments between two outwash units on south side of Route V-55-U. Sample from near western end of section.
	UGA-6932*	$29{,}420^{+650}_{-600}$	-25.0	Organic silt and fine sand from upper 2 cm of a 90-cm-thick bed of organic pyroclastic flow sediments between two outwash units on south side of Route V-55-U. Sample collected 5 m east of sample QL-4538.
	UGA-6924	$38{,}550^{+800}_{-720}$	-27.2	Ditto, except sample from 45-50 cm depth.
	UGA-6926	$39{,}340^{+2130}_{-1680}$	-29.1	Ditto, except sample from 60-65 cm depth in organic bed.
	UGA-6930	$28{,}550^{+480}_{-450}$	-25.0	Organic silt and find sand from upper 2 cm of a 90-cm-thick bed of organic pyroclastic flow sediments between two outwash units on south side of Route V-55-U. Sample collected 15 m east of sample QL-4538.
	UGA-6928	33,415±700	-24.8	Ditto, except sample collected at 2-4 cm depth in organic bed.
	UGA-6929	$35{,}230^{+1110}_{-980}$	-25.0	Ditto, except sample collected at 44-46 cm depth in organic bed.
	QL-4537	33,900±102	-26.7	Ditto, except sample collected near base of organic unit.
8	AA-15900	19,993±257	-18.2	Fundo Liña Pantanosa. Gyttja from 3.30 cm depth in a 3.50-m core in mire in outer Llanquihue moraine belt. Mimimum age for moraine. See Heusser *et al.* (1999).
	AA-14774	19,768±397	-18.1	Ditto, except sample collected at 3.00 m depth.
9	A-7663	$29{,}265^{+210}_{-205}$	-24.9	Reworked organic clast in folded outwash distal to the outermost position reached by late Llanquihue piedmont ice. Maximum age for outwash and folding.

Site No.	Lab. No.	Age ^{14}C yr BP	δ^{13}C (‰)	Description
10	Wk-2554	25,100±420	-25.0	Organic clast reworked into outwash. Maximum age for outwash.
11	Wk-2537	29,800±300	-27.1	Frutillar Alto. Organic clast reworked into outwash graded to maximum Llanquihue moraine. Sample split and dated at two laboratories. Maximum age for outwash and moraine.
	A-6556	28,990±430	-27.4	Split of same sample as Wk-2537.
	A-6198	28,450±560	-27.0	Organic clast reworked into outwash graded to maximum Llanquihue moraine. Maximum age for outwash and moraine.
	QL-4549	27,250±250	-26.0	Organic clast reworked into outwash graded to maximum Llanquihue
		27,230±600	-26.0	moraine. Sample counted twice. Maximum age for outwash and moraine.
	QL-4547	24,250±250	-26.1	Large organic clast reworked into outwash graded to maximum Llanquihue moraine. Maximum age for outwash and moraine. Sample taken from top of clast.
	QL-4548	21,840±700	-27.1	Same clast as QL-4547, sample from middle of clast.
	A-6197	22,790±410	-26.6	Same clast as QL-4547, sample from base of clast.
	QL-4550	$36{,}000^{+1400}_{-1200}$	-27.3	Organic clast reworked into outwash graded to maximum Llanquihue moraine. Maximum age for outwash and moraine.
	AA-25374	21,120±180	-25.1	Ditto, except different sample.
	A-9512	$41{,}690^{+1490}_{-1260}$	-28.7	Ditto, except different sample.
	A-9510	$35{,}030^{+580}_{-540}$	-27.8	Ditto, except different sample.
	A-9513	$33{,}605^{+685}_{-630}$	-28.4	Ditto, except different sample.
	A-9514	$22{,}700^{+180}_{-175}$	-25.8	Ditto, except different sample.
	A-9515	$32{,}420^{+425}_{-405}$	-25.3	Ditto, except different sample.
	A-6787	$34{,}440^{+650}_{-600}$	-26.6	Ditto, except different sample.
12	A-6556	28,990±430	-27.4	Organic clast reworked into outwash graded to maximum Llanquihue moraine. Maximum age for outwash and moraine.
	A-6557	$38{,}280^{+1650}_{-1370}$	-25.7	Ditto, except different sample.
	A-6558	$43{,}960^{+3970}_{-2650}$	-26.1	Ditto, except different sample.
13	RL-116	20,100±500	—	Organic clast reworked into outwash beneath till of outer Llanquihue moraine. Maximum age for outwash and moraine. From Mercer (1976).
	UW-425	32,800±1600	—	Ditto, except sample from Porter (1981).
14	A-8534R	$19{,}760^{+250}_{-240}$	-29.7	Organic sand from 2.43-2.48 m in 2.70-m core through mire in channel between Llanquihue moraine ridges. Minimum age for moraines.
15	A-6199	>47,260	-28.9	Organic silt layer in lacustrine sediments in lakeside kame terrace.
16	A-7660*	$26{,}870^{+230}_{-225}$	-26.8	Frutillar Bajo. Small pieces of wood and fibrous organic matter from old land surface sealed intact on top of organic bed. See Figs. 25 and 26 for location of samples.
	A-7661*	26,560±165	-26.1	Ditto, except different sample.
	A-7656*	$27{,}900^{+195}_{-190}$	-25.6	Ditto, except different sample.
	UGA-6817*	27,425±215	-26.4	Ditto, except different sample.
	UGA-6818*	27,305±325	-25.9	Ditto, except different sample.
	UGA-6819*	27,855±325	-25.6	Ditto, except different sample.
	UGA-6820*	27,780±335	-26.8	Ditto, except different sample.
	UGA-6723*	26,530±300	-24.8	Ditto, except different sample.
	AA-13701*	26,151±303	-27.7	Ditto, except different sample.
	AA-13702*	26,809±310	-27.0	Ditto, except different sample.
	AA-13703*	26,444±290	-27.5	Ditto, except different sample.
	AA-13704*	25,853±273	-27.6	Ditto, except different sample.
	AA-13705*	26,159±371	-23.0	Ditto, except different sample.
	AA-13734*	25,357±245	-27.2	Ditto, except different sample.
	AA-13735*	25,764±335	-26.8	Ditto, except different sample.

Site No.	Lab. No.	Age ^{14}C yr BP	δ^{13}C (‰)	Description
	UGA-6915*	$28{,}910^{+510}_{-480}$	-26.2	Organic silt and fine sand from depth of 0-2 cm in Frutillar Bajo organic bed (Figs. 25 and 26). Sample from site of pollen profile in Heusser *et al.* (1999).
	UGA-6920	$32{,}600^{+960}_{-860}$	-25.4	Ditto, except sample from depth of 30-35 cm.
	UGA-6917	33,610±600	-26.1	Ditto, except sample from depth of 60-65 cm.
	UGA-6919	34,985±440	-25.5	Ditto, except sample from depth of 90-95 cm at base of organic bed.
	UGA-6723*	26,530±300	-24.8	Organic silt and fine sand from depth of 0-2 cm at site of pollen profile in Heusser *et al.* (1999).
	UGA-6724	36,960±550	-25.9	Ditto, except from depth of 90-95 cm at base of organic bed.
	UGA-6945	34,765±840	-25.0	Organic silt and fine sand from depth of 51-56 cm at base of organic bed 3 m north of pollen section in Heusser *et al.* (1999).
17	A-6196	22,870±310	-24.4	Organic clast from ice-contact stratified drift at top of ice-contact slope. Maximum age for drift.
18	UGA-6907	20,645±220	-20.8	Fundo Llanquihue. Gyttja from 6.00 m depth in 7.07-m core through mire just inside outermost Llanquihue moraine. See Heusser *et al.* (1999).
	UGA-6908	20,890±185	-21.2	Ditto, except sample from 6.20 m depth.
	UGA-6909	20,455±180	-25.4	Ditto, except sample from 6.40 m depth.
	UGA-6910	20,650±175	-23.1	Ditto, except sample from 6.60 m depth.
	UGA-6912	20,680±175	-23.5	Ditto, except sample from 7.00 m depth.
	UGA-6913	20,585±170	-24.9	Ditto, except sample was clayey gyttja from 7.01 m depth.
19	A-9423	14,650±75	-28.5	Puerto Phillippi. Top 1 cm of organic silt bed between two units of glaciolacustrine sediments. The top of the organic bed is sealed by glaciolacustrine sediments deposited in a lake dammed in front of the Lago Llanquihue piedmont lobe when it advanced to the western lakeshore.
20	A-8251	$16{,}930^{+265}_{-255}$	-26.6	Organic silt from 4.46-4.53 m depth in 4.60-m core through mire on Llanquihue moraine.
21	A-8254	$15{,}810^{+280}_{-270}$	-29.1	Gyttja at contact with laminated sediments at 3.58-3.63 m in 3.80-m core through mire on Llanquihue moraine system.
	A-8253	$14{,}885^{+260}_{-255}$	-24.7	Gyttja over laminated sediments from 3.30-3.40 m depth in 3.70-m core through mire on Llanquihue moraine belt.
22	A-8252	$15{,}790^{+265}_{-255}$	-28.8	Organic silt from 1.33-1.39 m depth in 1.40-m core through mire on Llanquihue moraine.
23	ETH-13529*	14,850±100	-25.5	Town of Llanquihue. Small wood piece in organic silt bed. See Fig. 18 for location of sample.
	ETH-13530*	14,670±120	-26.6	Ditto, except different sample.
	ETH-13531*	14,810±120	-22.9	Ditto, except different sample.
	ETH-13532*	14,780±120	-21.7	Ditto, except different sample.
	ETH-13533*	14,930±120	-24.1	Ditto, except different sample.
	ETH-13534*	15,120±140	-20.9	Ditto, except different sample.
	A-8174*	14,750±80	-27.9	Ditto, except different sample.
	A-8173*	15,120±95	-28.0	Ditto, except different sample.
	AA-21939	15,600±120	-28.7	Ditto, except different sample.
	AA-21940	15,140±110	-29.3	Ditto, except different sample.
	AA-21941	14,995±90	-27.1	Ditto, except different sample.
	AA-21942	14,765±90	-28.5	Ditto, except different sample.
	AA-21943	14,810±95	-28.3	Ditto, except different sample.

Site No.	Lab. No.	Age ^{14}C yr BP	δ^{13}C (‰)	Description
24	A-7712	$29{,}350^{+325}_{-310}$	-25.0	Weathered organic silt and fine sand composed of pyroclastic flow sediments. The sediments, about 50 cm to 3 m thick, rest on outwash and are overlain by thin (50 cm to 1 m) till. The weathered organic sediments were mobilized when overridden by ice that deposited the till, such that diapirs rise into the overlying till. A series of samples of organic sediments, none in place, was collected from near the till-organic interface. All the resulting dates afford maximum ages for the till. But none is a close limiting age because the organic sediment has been remobilized, the dates are widely varying, and a former land surface is not preserved.
	UGA-6939	25,020±290	-26.5	Ditto, except different sample.
	UGA-6821	26,150±220	-24.4	Ditto, except different sample.
	A-7662	$33{,}400^{+395}_{-375}$	-25.0	Ditto, except different sample.
	A-7659	$30{,}090^{+305}_{-290}$	-25.0	Ditto, except different sample.
	A-7688	$32{,}950^{+400}_{-380}$	-25.1	Ditto, except different sample.
	A-7706	$31{,}045^{+285}_{-275}$	-25.4	Ditto, except different sample.
	A-7718	$29{,}810^{+270}_{-265}$	-25.3	Ditto, except different sample.
	A-7731	$33{,}370^{+750}_{-685}$	-25.2	Ditto, except different sample.
	A-7715	$29{,}360^{+215}_{-210}$	-25.3	Ditto, except different sample.
	UGA-6938	>44,400	-25.8	Organic clast reworked into slightly weathered outwash that underlies the remobilized pyroclastic flow sediments.
25	ETH-13536	>45,460±1400	-29.5	Crossroad site. Small wood piece sheared from surface of weathered pyroclastic flow sediments in Section B of Fig. 23.
	ETH-11183	>35,120±310	-25.1	Small wood piece in weathered interdrift pyroclastic flow units in Section B of Fig. 23.
	ETH-11182	>36,020±340	-24.0	Ditto, except different sample.
	ETH-11187	>36,230±350	-29.4	Ditto, except different sample.
	ETH-11188	>38,450±380	-29.4	Ditto, except different sample.
	AA-8052	>48,900	-25 (est.)	Small wood piece from organic horizon in top 5 cm of interdrift weathered pyroclastic drift units, overlain by till at section C1 in Figure 23 on east side of Route 5.
26	AA-7459	12,840±90	-25 (est.)	Railroad bridge, Puerto Varas. Fibrous peat from upper of two thin peat layers that overlie the 26-cm-thick main organic bed in the railroad bridge section. Standard acid-base-acid pretreatment. See Fig. 22 for location.
	AA-7459B	13,940±85	-25 (est.)	Repeat of AA-7459 with strong acid-base-acid pretreatment.
	AA-7460	14,175±110	-25 (est.)	Fibrous peat from lower of two thin peat layers above the main organic bed in the railroad bridge section. Fig. 22.
	AA-7465	14,600±110	-25 (est.)	Small wood piece from lower of two thin peat layers above the main organic bed in the railroad bridge section. Standard acid-base-acid pretreatment. Fig. 22.
	AA-7465C	14,350±90	-25 (est.)	A split of same sample as AA-7465, with acid-base-acid pretreatment and then extraction of cellulose.
	ETH-13528	14,290±100	-24.8	Small wood piece from lower of two thin peat layers above the main organic bed in the railroad bridge section. Fig. 22.
	ETH-13528	14,460±85	-24.8	Same graphite target as ETH-13528. Fig. 22.
	ETH-13528	12,950±100	-24.8	Same sample as ETH-13528 and ETH-13528. Redated with separate pretreatments. Fig. 22.
	AA-21011*	14,600±100	-27.9	Peat from lower of two thin peat layers above the main organic bed in the railroad bridge section. Fig. 22.
	AA-21012*	14,360±100	-28.5	Ditto, except different sample.
	AA-21013*	14,570±150	-28.5	Ditto, except different sample.
	AA-21014*	14,680±100	-29.0	Ditto, except different sample.
	A-9193*	14,415±70	-27.9	Wood from upper 7 cm of 26-cm-thick main organic bed in the railroad bridge section. Fig. 22.
	A-8551*	$14{,}475^{+75}_{-70}$	-28.0	A split of same sample as A-9193.

Site No.	Lab. No.	Age ^{14}C yr BP	δ^{13}C (‰)	Description
	A-9194*	14,620±90	-28.3	Wood from upper 7 cm of 26-cm-thick main organic bed in the railroad bridge section. Fig. 22.
	A-8553*	14,735±75	-27.4	A split of same sample as A-9194.
	A-8554*	$14,570^{+80}_{-75}$	-28.2	Wood from upper 7 cm of 26-cm-thick main organic bed in the railroad bridge section. Fig. 22.
	A-9195*	$14,520^{+80}_{-75}$	-28.3	A split of same sample as A-8554.
	A-8552*	14,625±75	-27.9	Wood from upper 7 cm of 26-cm-thick main organic bed in the railroad bridge section. Fig. 22.
	A-8175*	14,930±80	-27.2	Ditto, except different sample.
	A-8775*	$14,285^{+110}_{-105}$	-27.9	Ditto, except different sample.
	QL-1335	15,050±100	—	Wood from 26-cm-thick main organic bed in the railroad bridge section. From Porter (1981, written communication, 1996).
	AA-23728	17,580±120	-27.8	Small wood piece 82 cm below top of organic silt unit that lies beneath the 26-m-thick main organic layer. Fig. 22.
	AA-23726	17,320±140	-27.2	Ditto, except 90 cm below top of organic silt unit.
	AA-23727	17,760±130	-28.4	Ditto, except 99 cm below top of organic silt unit.
	AA-23730	17,780±160	-28.9	Ditto, except 110 cm below top of organic silt unit.
	AA-23731	17,790±140	-28.7	Wood in vertical position at 116 cm below top of organic silt unit. This wood is part of the remnants of a small tree in growth position.
	AA-23729	17,520±140	-29.0	Wood from 120 cm depth from same tree as AA-23731.
	A-9526.1	17,505±150	-28.3	Wood from 126 cm depth from same tree as samples AA-23731 and AA-23729.
	A-9526.2	$17,405^{+500}_{-470}$	-29.0	A split of sample A-9526.1.
	AA-23733	17,770±150	-29.7	Small wood piece 132 cm below top of organic silt unit. Fig. 22.
	AA-23732	17,880±140	-28.5	Ditto, except 128 cm below top of organic silt bed.
	AA-23734	17,490±140	-29.1	Ditto, except 142 cm below top of organic silt bed.
27	I-5033	14,820±230	—	Calle Santa Rosa, Puerto Varas. Uppermost part of organic bed at 62 m elevation sealed intact by glaciolacustrine silt unit (Mercer 1976). By our interpretation, dates ponding of local lake by piedmont glacier in Puerto Varas embayment.
28	A-9523*	14,825±110	-27.1	Northwest Bluff, Puerto Varas. Upper 2 cm of a 23-cm-thick bed of gyttja, sealed at the top by laminated glaciolacustrine sediments at 63 m elevation.
	A-9524*	14,925±95	-27.3	Ditto, except different sample.
29	GX-5273	15,715±440	—	Bella Vista Park, Puerto Varas. Peat from within organic bed at 59.7-60.1 m elevation. Top of organic bed sealed by glaciolacustrine sediments (Porter 1981).
30	A-6322*	14,430±140	-24.8	Bella Vista Bluff, Puerto Varas. Wood in glaciolacustrine sediments 8 cm above the top of a prominent 23-cm-thick organic bed. The top surface of the organic bed is at 60.97 m elevation. See Fig. 20 for stratigraphy and sample location.
	A-8546*	14,655±75	-26.7	Wood in glaciolacustrine sediments 8 cm above the top of a prominent 23-cm-thick organic bed. The top surface of the organic bed is at 60.97 m elevation. Fig. 20.
	T-9656A*	14,560±95	-27.6	Organic silt from upper 1 cm of the prominent 23-cm-thick organic bed at 60.97 m elevation. Fig. 20.
	A-8549R*	14,715±85	-27.7	Organic trash layer of small wood pieces and macrofossils sealed by glaciolacustrine sediments on the surface of the prominent 23-cm-thick organic bed at 60.97 m elevation. Fig. 20.
	A-9187*	$14,595^{+80}_{-75}$	-27.7	Ditto, except different sample.
	A-9191*	14,585±80	-27.3	Ditto, except different sample.
	A-9185*	14,600±75	-27.6	Ditto, except different sample.
	A-9189*	$14,135^{+80}_{-75}$	-27.2	Ditto, except different sample.
	A-8547R	15,430±90	-29.2	Organic silt from within 23-cm-thick organic bed (Fig. 20).

Site No.	Lab. No.	Age ^{14}C yr BP	δ^{13}C (‰)	Description
	A-8548R	$15{,}075^{+140}_{-135}$	-28.2	Ditto, except different sample.
	A-8550	15,635±95	-28.3	Ditto, except different sample.
	A-9186	$14{,}980^{+95}_{-90}$	-27.1	Ditto, except different sample.
	A-9188	$15{,}070^{+150}_{-145}$	-27.4	Ditto, except different sample.
	A-9190	15,730±160	-27.6	Ditto, except different sample.
	A-9192	15,220±115	-27.7	Ditto, except different sample.
	A-9518	$15{,}035^{+210}_{-205}$	-27.1	Ditto, except different sample.
	A-9519	$15{,}205^{+210}_{-205}$	-27.6	Ditto, except different sample.
	A-9520	15,260±155	-27.0	Ditto, except different sample.
	A-9521	$15{,}360^{+195}_{-190}$	-27.0	Ditto, except different sample.
	A-9522	$15{,}250^{+165}_{-160}$	-27.4	Ditto, except different sample.
31	A-6775	$31{,}360^{+2850}_{-2100}$	-25.9	Organic clast reworked into outwash that passes beneath till of outermost Llanquihue moraine. Maximum age for outwash and moraine.
	Wk-2529	28,700±350	-24.8	Ditto, except different sample.
32	Wk-2536	22,250±220	-26.9	Organic clast reworked into outwash. Maximum age for outwash.
	Wk-2535	>25,000	-30.3	Ditto, except different sample.
	TUa-470A	22,985±235	-27.7	Ditto, except different sample.
33	A-6487	26,230±340	-27.0	Organic clast reworked into gravelly flow till in deformed core of moraine ridge. Maximum age for moraine ridge.
	A-6488	28,970±410	-26.6	Ditto, except different sample.
	A-8780	$28{,}060^{+160}_{-155}$	-26.1	Ditto, except different sample.
	A-8781	$27{,}405^{+350}_{-335}$	-27.0	Ditto, except different sample.
	A-8782	$36{,}865^{+505}_{-475}$	-26.6	Ditto, except different sample.
	A-8783	$29{,}410^{+315}_{-300}$	-25.8	Ditto, except different sample.
	UGA-6923	$32{,}740^{+520}_{-460}$	-26.7	Ditto, except different sample.
	UGA-6984	27,510±530	-26.7	Ditto, except different sample.
	UGA-6985	31,730±530	-26.6	Ditto, except different sample.
34	A-8530R	12,715±100	-29.0	Organic silt from 5.94-5.99 m depth in 6.20-m core through mire on Llanquihue moraine.
35	A-8531R	$18{,}265^{+185}_{-180}$	-28.7	Organic silty sand from 2.82-2.92 m depth in 3.30-m core through mire in small basin on Llanquihue moraine.
36	A-8529R	$12{,}225^{+165}_{-160}$	-26.1	Organic sand from 6.66-6.70 m depth in 6.90-m core through mire in depression between Llanquihue moraine ridges.
	A-8528R	$12{,}185^{+160}_{-155}$	-28.6	Organic sand from 6.39-6.42 m depth in 6.75-m core through mire in depression between Llanquihue moraine ridges.
	A-8527R	9660±80	-29.2	Organic sand from 5.90-5.94 m depth in 6.04-m core through mire in depression between Llanquihue moraine ridges.
37	A-8532	8060±160	-28.2	Gyttja from 5.35-5.40 m depth in 5.70-m core through mire on Llanquihue moraine.
38	A-8533R	13,165±120	-28.3	Organic fibers from 2.23-2.28 m depth from 2.30-m core through mire on Llanquihue moraine.
39	A-6490	$39{,}200^{+1500}_{-1300}$	-26.1	Organic clast reworked into outwash. Maximum age for outwash.
	QL-4544	>51,000	—	Ditto, except different sample.
40	A-6778	>27,160	-27.9	Organic clast reworked into outwash beneath outer edge of Llanquihue moraine. Maximum age for outwash and moraine.

Site No.	Lab. No.	Age ^{14}C yr BP	δ^{13}C (‰)	Description
	A-6777	29,080±360	-29.3	Ditto, except different sample.
41	A-6776	$34{,}420^{+9330}_{-4200}$	-28.6	Ditto, except different sample.
42	Wk-2531	23,300±220	-24.6	Organic clast reworked into outwash. Maximum age for outwash.
	Wk-2532	31,300±350	-27.1	Ditto, except different sample.
	Wk-2530	31,900±400	-26.8	Ditto, except different sample.
43	Wk-2548	31,600±550	-26.3	Ditto, except different sample.
	Wk-2549	32,700±600	-27.3	Ditto, except different sample.
	Wk-2550	31,460±470	-27.4	Ditto, except different sample.
44	A-6491	16,900±120	-25.9	Ditto, except different sample.
	A-6492	15,640±100	-27.2	Ditto, except different sample.
	UGA-6942	16,060±120	-25.0	Ditto, except different sample.
	QL-4545	28,550±500	-26.7	Ditto, except different sample.
45	A-6493	15,040±100	-25.2	Ditto, except different sample.
46	A-7626*	$23{,}120^{+130}_{-125}$	-27.9	Canal Tenglo. Fibrous peat and wood from top surface of peat layer. See Fig. 29 for sample location and site stratigraphy.
	T-11330A*	23,005±120	-27.3	Ditto, except different sample.
	A-7912	24,055±150	-27.2	Peat from base of peat layer. See Fig. 29 for sample location and site stratigraphy.
	A-8170*	$29{,}680^{+270}_{-260}$	-27.5	Fibrous peat and wood from top surface of peat layer. See Fig. 29 for sample location and site stratigraphy.
	A-8171*	$28{,}465^{+225}_{-245}$	-27.4	Ditto, except different sample.
	A-8172*	$30{,}610^{+290}_{-280}$	-27.0	Ditto, except different sample.
	A-7701*	$29{,}255^{+210}_{-200}$	-26.7	Ditto, except different sample.
	A-7705*	$29{,}655^{+230}_{-225}$	-27.4	Ditto, except different sample.
	A-7913*	$29{,}210^{+210}_{-205}$	-26.8	Ditto, except different sample.
	A-7703	$31{,}975^{+265}_{-255}$	-27.5	Ditto, except different sample.
	A-7914	$31{,}230^{+210}_{-205}$	-27.1	Ditto, except different sample.
	A-7625	$31{,}505^{+300}_{-290}$	-28.0	Ditto, except different sample.
	A-7915	$31{,}975^{+280}_{-270}$	-27.6	Ditto, except different sample.
	A-7734	$31{,}405^{+250}_{-245}$	-29.2	Ditto, except different sample.
	A-7696	$33{,}165^{+300}_{-285}$	-29.4	Ditto, except different sample.
	A-7700	$31{,}690^{+285}_{-275}$	-27.9	Ditto, except different sample.
	A-7721	$31{,}905^{+265}_{-260}$	-27.5	Ditto, except different sample.
	A-7694	$33{,}950^{+355}_{-340}$	-28.0	Ditto, except different sample.
	A-7695	$34{,}450^{+335}_{-320}$	-27.5	Remains of tree in growth position on top surface of peat layer. Fig. 29.
	A-7699	$39{,}660^{+640}_{-595}$	-28.6	Fibrous peat and wood from top surface of peat layer. Fig. 29.
47	T-10296A	15,940±315	-27.6	Punta Penas. Gyttja from top of 20-cm-thick organic bed. See Fig. 28 for sample location and site stratigraphy.
	T-10297A	16,275±440	-28.9	Organic silt from middle of 20-cm-thick organic bed. Fig. 28.
	T-10298A	16,000±275	-27.5	Organic silt from base of 20-cm-thick organic bed. Fig. 28.
	A-9019*	15,675±90	-27.8	Surface organic trash layer including leaves and wood, from the lower of the two prominent but thin organic layers higher in the section than the 20-cm-thick organic layer. Fig. 28.
	A-9020*	$15{,}665^{+110}_{-105}$	-26.9	Ditto, except different sample.
	AA-21009*	15,200±120	-28.6	Ditto, except different sample.

Site No.	Lab. No.	Age ^{14}C yr BP	δ^{13}C (‰)	Description
	AA-21010*	15,020±120	-29.4	Surface organic trash layer including leaves and wood, from the highest of the two prominent but thin organic layers higher in the section than the 20-cm-thick organic layer. Fig. 28.
	A-9017*	15,000±75	-27.2	Ditto, except different sample.
	A-9018*	$14{,}735^{+80}_{-75}$	-27.3	Ditto, except different sample.
	A-9506*	14,835±80	-27.1	Ditto, except different sample.
48	A-9508	$36{,}370^{+480}_{-450}$	-27.2	Punta Pelluco. Gyttja from organic layer in section at Punta Pelluco. See Fig. 30 for sample location and site stratigraphy.
	A-7722	$30{,}640^{+255}_{-250}$	-27.2	Gyttja from organic layer a same stratigraphic position as sample A-9508, but in gulfside cliff in embayment 500 m west of Punta Pelluco.
	A-7708	$33{,}855^{+340}_{-325}$	-29.0	Ditto, except different sample.
49	AA-15907	13,870±95	-26.0	Fundo Santa Elena. Gyttja from 4.35 m depth in 4.45-m core through mire on Llanquihue moraine belt.
50	Wk-2543	27,200±750	-27.8	Organic clast reworked into outwash. Maximum age for outwash.
	A-6781	$37{,}980^{+1090}_{-960}$	-26.2	Ditto, except different sample.
	A-6782	31,240±680	-26.5	Ditto, except different sample.
	A-6783	>26,030	-25.4	Ditto, except different sample.
	A-6784	$37{,}710^{+1670}_{-1390}$	-26.8	Ditto, except different sample.
	TUa-469A	25,000±275	-27.7	Ditto, except different sample.
	Wk-2542	>30,000	-27.5	Ditto, except different sample.
51	Wk-2544	>40,000	-29.5	Ditto, except different sample.
	Wk-2545	>45,000	-31.6	Ditto, except different sample.
	T-10303A	32,355±720	-26.1	Ditto, except different sample.
52	A-6785	$30{,}160^{+2650}_{-1990}$	-28.5	Ditto, except different sample.
53	AA-9791	26,280±295	-27.0	Organic clast reworked into gravelly outwash beneath outer edge of Llanquihue moraine. Maximum age for outwash and moraine.
	TUa-468A	19,820±185	-27.7	Ditto, except different sample.
54	A-6780	$24{,}325^{+1120}_{-985}$	-26.3	Organic clast reworked into outwash. Maximum age for outwash.
	T-10308A	24,280±360	-25.9	Redating of same clast as A-6780.
55	A-8526	$22{,}680^{+415}_{-395}$	-23.8	Organic silt from 4.77-4.82 m depth in 4.95-m core through mire on Llanquihue moraine belt.
	AA-24120	22,670±180	-24.0	Replicate of A-8526.
56	A-8525	$20{,}480^{+325}_{-315}$	-24.0	Organic silt from 4.46-4.50 m depth in 4.75-m core through mire on Llanquihue moraine belt.
	AA-24119	20,330±150	-24.0	Replicate of A-8525.
57	A-8266	$17{,}225^{+245}_{-240}$	-23.9	Gyttja from 4.16-4.23 m depth in 4.29-m core through mire on Llanquihue moraines.
58	A-8264	$18{,}655^{+515}_{-485}$	-17.4	Organic silt from 5.49-5.56 m depth in 5.72-m core through mire on Llanquihue moraines.
59	AA-21777	16,000±150	-27.6	Organic silt from 2.99-m depth in 3.10-m core through mire in Llanquihue moraines.
60	A-8784	$35{,}915^{+660}_{-610}$	-27.4	Organic clast reworked into outwash. Maximum age for outwash.
	A-8785	$32{,}780^{+390}_{-385}$	-27.5	Ditto, except different sample.
	A-8786	$41{,}660^{+905}_{-810}$	-27.8	Ditto, except different sample.
	A-8787	$26{,}475^{+265}_{-255}$	-27.0	Ditto, except different sample.

Site No.	Lab. No.	Age ^{14}C yr BP	δ^{13}C (‰)	Description
	A-8788	$38{,}180^{+625}_{-580}$	-26.3	Ditto, except different sample.
61	A-8789	$32{,}235^{+315}_{-300}$	-27.2	Ditto, except different sample.
62	A-8790	$26{,}560^{+240}_{-235}$	-28.1	Ditto, except different sample.
63	A-8791	$29{,}605^{+285}_{-275}$	-26.4	Ditto, except different sample.
	A-8792	$38{,}325^{+560}_{-525}$	-27.2	Ditto, except different sample.
	A-8793	$37{,}450^{+510}_{-480}$	-26.8	Ditto, except different sample.
	A-8794	$30{,}555^{+275}_{-270}$	-26.3	Ditto, except different sample.
64	A-8514	16,445±140	-28.5	Organic fibers from 5.20-5.26 m depth in 5.41-m core to base of mire in channels on outer Llanquihue moraine belt.
65	A-8515 R	$14{,}770^{+175}_{-170}$	-25.8	Organic matrix of gravel from 3.65-3.73 m depth in 3.83-m core to base of mire on outer Llanquihue moraine belt.
66	AA-16244	21,230±169	-21.4	Basal gyttja from 3.46-3.49 m depth in core to base of mire on outer Llanquihue moraine belt.
67	AA-15913	18,156±158	-26.4	La Campaña. Gyttja from 3.5 m depth in 3.85-m core to base of mire on outermost Llanquihue moraine belt. See Heusser *et al.* (1999).
	AA-15916	17,821±159	-26.2	Gyttja from 3.85 m depth in same core as AA-15913.
68	A-8263	$18{,}505^{+310}_{-295}$	-22.7	Organic silt from 3.59 m depth in 3.71-m core to base of mire on outermost Llanquihue moraine belt.
69	AA-13844	13,295±91	-28.3	Gyttja from 2.85 m depth in 2.98-m core to base of mire on Llanquihue moraine belt.
70	AA-13843	13,932±119	-28.7	Gyttja from 2.40 m depth in 2.44-m core to base of mire on Llanquihue moraine belt.
71	Wk-2541	25,300±300	-26.5	Organic clast reworked into outwash beneath outer edge of Llanquihue moraine. Maximum age for outwash and moraine.
72	Wk-2542	>30,000	-27.5	Reworked organic clast in outwash. Maximum age for outwash.
73	A-9507	15,220±80	-27.2	Isla Maillen. Gyttja from top of organic layer sealed by glaciolacustrine sediments that are overlain by till. Close maximum age for ice advance over site.
74	AA-13841	12,046±87	-26.3	Gyttja from 2.03 m depth in 2.31-m core to base of mire on Llanquihue moraine.
75	AA-13840	13,024±88	-27.3	Gyttja from 3.65 m depth in 3.77-m core to base of mire on Llanquihue moraine.
76	AA-13845	13,162±102	-27.9	Gyttja from 2.45 m depth in 2.80-m core to base of mire on Llanquihue moraine.
77	A-8255	$10{,}630^{+215}_{-210}$	-29.2	Organic silt from 3.59-3.62 m depth in 3.71-m core to base of mire on Llanquihue moraine.
78	A-8256	$14{,}545^{+265}_{-260}$	-26.2	Gyttja from 6.86-6.92 m depth in 7.20-m core to base of mire on Llanquihue moraine.
	AA-25369	15,045±130	-24.4	Basal gyttja from recoring of same mire, 3 m from site of A-8256.

Site No.	Lab. No.	Age ^{14}C yr BP	δ^{13}C (‰)	Description
79	A-8258	13,370±100	-28.4	Fibrous organic material in organic sand at 5.75-5.8 m depth in 5.90-m core to base of mire on Llanquihue moraine.
80	A-8259	12,115±115	-28.5	Fibrous organic material at 6.01-6.09 m depth in 6.20-m core to base of mire on Llanquihue moraine.
81	A-8261	$14{,}875^{+210}_{-205}$	-30.9	Huelmo. Gyttja from 5.88-5.94 m depth in 5.94-m core to base of mire in the coastal Llanquihue moraine belt. Core taken near edge of mire.
	AA-24121	15,590±110	-27.9	Gyttja from base of 5.94-m core taken beside core of sample A-8261.
	AA-23243	15,380±100	-29.4	Gyttja from 10.38 m depth in 10.52-m core in the center of the Huelmo mire. Core to base of mire. This date is part of a consistent sequence of ages in this core (Moreno 1988).
	AA-23244	16,410±110	-28.6	Gyttja from 10.50 m depth in the same 10.52-m core as AA-23243. This date is part of a consistent sequence of ages in this core (Moreno 1988).
82	A-8262	12,275±125	-29.2	Gyttja from 4.80-4.84 m depth in 4.84-m core to base of mire in coastal Llanquihue moraine belt.
83	A-8257	$14{,}135^{+180}_{-175}$	-20.0	Gyttja from 4.45-4.50 m depth in 4.75-m core to base of mire in Llanquihue moraine belt.
84	A-6661	12,330±130	-32.1	Lago Condorito. Gyttja from 9.29 m depth in 9.34-m core to base of lacustrine sediments in Lago Condorito.
85	A-8260	11,010±115	-26.9	Fibrous material in organic sand from 6.57-6.65 m depth in 6.59-m core to base of mire on Llanquihue moraine belt.
86	A-9525	$22{,}520^{+130}_{-125}$	-26.7	Wood and fibrous peat from upper surface of organic bed sealed by outwash that is overlain by Llanquihue moraine belt. The organic bed is about 500 m long and exposed in sea cliff 3.8 km south of Huelmo Date is close maximum for glacier advance over site.
	A-10079	$22{,}715^{+185}_{-180}$	-26.8	Ditto, except different sample.
	A-10080	$22{,}430^{+185}_{-180}$	-26.9	Ditto, except different sample.
	A-10081	$22{,}715^{+270}_{-260}$	-26.7	Ditto, except different sample.
87	A-8516	15,320±160	-25.2	Gyttja from 3.4-3.5 m depth in 3.9-m core through mire on Llanquihue moraine.
	A-8516 R	$15{,}330^{+280}_{-270}$	-25.2	Redating of sample A-8516.
	AA-25370	15,300±125	-25.0	Basal gyttja from 3.75-m core taken beside core of A-8516.
	AA-25371	15,660±100	-25.2	Basal gyttja from 3.85-m core taken beside core of AA-25370.
	AA-25372	29,085±350	-24.8	Small wood piece from within gyttja at base of 3.85-m core of AA-25371. This wood is retransported from numerous fossil wood pieces in Seno Reloncaví basin, because it is enclosed within gyttja dated to 15,660 ^{14}C yr B.P.
88	A-8265	9995^{+205}_{-200}	-23.7	Organic sand from 2.33-2.41 m depth in 2.65-m core to base of mire on Llanquihue moraine belt.
	A-8517 R	8270^{+155}_{-150}	-27.8	Organic sand from 2.58-2.65 m depth in 2.90-m core to base of mire on Llanquihue moraine belt.
89	AA-13842	13,582±94	-28.4	Basal gyttja from core to base of mire on Llanquihue moraine.
90	A-8520 R	$13{,}580^{+140}_{-130}$	-28.6	Organic fragments in sand matrix at 6.50-6.56 m depth in 6.60-m core to base of mire on Llanquihue moraine.
91	A-8518 R	$12{,}195^{+125}_{-120}$	-28.8	Organic-rich sand from 3.18-3.27 m depth in 3.30-m core to base of mire on Llanquihue moraine.
92	A-8519 R	11,885±90	-29.9	Peat from 3.08-3.13 m depth in 3.35-m core to base of mire on Llanquihue moraine.

Site No.	Lab. No.	Age ^{14}C yr BP	δ^{13}C (‰)	Description
93	A-8521 R	8515±85	-28.5	Organic silt from 5.92-5.95 m depth in 6.00-m core to base of mire on Llanquihue moraine.
	A-8522	13,895±175	-22.7	Organic silt from 6.82-6.87 m depth in 7.25-m core through mire on Llanquihue moraine.
	A-8523	$13{,}755^{+170}_{-165}$	-22.4	Organic silt from 7.05-7.11 m depth in 7.35-m core through mire on Llanquihue moraine.
94	A-7702	$15{,}285^{+150}_{-145}$	-25.8	Near Calbuco. Organic clast reworked into coarse foreset beds of a proglacial lacustrine delta that is capped by lodgement till. Maximum age for glacial advance across site.
	A-7698	15,500±85	-26.1	Ditto, except different sample.
	A-7697	15,535±85	-25.4	Ditto, except different sample.
	A-8776	16,160±80	-26.1	Ditto, except different sample.
	A-8777	15,730±70	-26.0	Ditto, except different sample.
	A-8778	15,365±85	-24.9	Ditto, except different sample.
	A-8779	$15{,}390^{+85}_{-80}$	-24.5	Ditto, except different sample.
	A-9426	$14{,}900^{+160}_{-155}$	-26.0	Ditto, except different sample.
	A-9425	15,130±125	-26.0	Ditto, except different sample.
	A-9427	15,110±100	-25.1	Ditto, except different sample.
	AA-25373	15,250±175	-26.4	Ditto, except different sample.
95	A-7627	20,925±115	+1.3	Shells in marine silt and clay bed mechanically dislocated into the core of a moraine and now 1 m above sea level.
96	AA-14770	>49,892	-30.0	Taiquemó. Woody peat from 6.0 m depth in 6.55-m core to base of Taiquemó mire on outermost Llanquihue moraine. This date is the oldest of a series of consistent dates in this core (Heusser *et al.* 1999).
97	AA-13731*	22,068±230	-26.1	Teguaco. Macrofossils from organic trash layer on surface of 28-cm-thick gyttja-and-organic silt bed sealed with glaciolacustrine unit. Dates flooding organic bed by proglacial lake.
	AA-13732*	23,126±207	-26.4	Ditto, except different sample.
	A-7623*	22,630±125	-26.6	Ditto, except different sample.
	AA-13733*	22,501±198	-24.6	Ditto, except different sample.
	A-7624*	22,500±120	-26.3	Ditto, except different sample.
	A-7687*	22,075±120	-28.1	Wood piece encased in laminated glaciolacustrine silt that rests on organic bed and seals the surface organic trash layer. The wood collected within 15 cm of the organic trash layer. The wood was probably washed into the proglacial lake, although it may have been floated from the land surface by rising lake waters. Dates flooding by proglacial lake.
	A-7729*	21,690±120	-28.3	Ditto, except different sample.
	A-7686*	$22{,}410^{+135}_{-130}$	-28.0	Ditto, except different sample.
	A-7732*	$22{,}350^{+205}_{-200}$	-28.4	Ditto, except different sample.
	A-7719*	$22{,}520^{+170}_{-165}$	-27.6	Ditto, except different sample.
	A-7710*	$21{,}955^{+120}_{-115}$	-27.9	Wood piece encased in massive lacustrine silt and fine sand that overlies the laminated glaciolacustrine silt. The wood was probably washed into the lake.
	QL-4534*	22,400±100	-26.8	Gyttja from upper 1 cm of 28-cm-thick silty gyttja bed, sealed by glaciolacustrine sediments.
	A-7693	$27{,}345^{+190}_{-185}$	-27.1	Organic silt from lowermost 2 cm of 28-cm-thick organic silt and gyttja bed.
	A-7692	26,620±175	-26.8	Ditto, except different sample.
	QL-4546	29,240±600	-25.8	Organic sand from the lowermost 2 cm of a 30-cm-thick organic sand unit that underlies the prominent 28-cm-thick silty-gyttja organic bed.
98	AA-13710*	14,458±98	-27.4	Dalcahue. Wood pieces (up to 15 cm long) lying on upper surface of organic layer, here 90 cm thick, that fills a small basin on a till surface. These wood pieces and associated plant fibers represent an intact old land surface preserved beneath glacial deposits that infill the basin. The collection sites are all within 1 m of location A in Fig. 31.

Site No.	Lab. No.	Age ^{14}C yr BP	δ^{13}C (‰)	Description
	AA-13711*	14,697±125	-28.6	Ditto, except different sample.
	AA-13712*	14,799±91	-28.8	Ditto, except different sample.
	AA-13713*	14,689±102	-28.7	Ditto, except different sample.
	AA-13714*	14,653±99	-28.3	Ditto, except different sample.
	AA-13715*	14,710±130	-27.9	Ditto, except different sample.
	AA-13716*	14,862±101	-26.9	Ditto, except different sample.
	AA-13717*	14,703±101	-27.2	Ditto, except different sample.
	AA-13718*	14,589±101	-28.3	Ditto, except different sample.
	AA-13719*	14,663±121	-27.3	Ditto, except different sample.
	AA-13720*	14,620±134	-28.5	Ditto, except different sample.
	AA-13721*	14,880±99	-27.8	Ditto, except different sample.
	AA-13722*	14,991±100	-27.1	Ditto, except different sample.
	AA-13723*	14,720±90	-27.6	Ditto, except different sample.
	AA-13724*	14,951±100	-28.4	Ditto, except different sample.
	AA-13725*	14,836±100	-26.7	Ditto, except different sample.
	AA-13726*	14,874±123	-26.7	Ditto, except different sample.
	AA-13727*	14,834±111	-27.1	Ditto, except different sample.
	AA-13728*	14,671±133	-27.2	Ditto, except different sample.
	AA-13729*	14,806±104	-26.5	Ditto, except different sample.
	AA-13730*	15,062±118	-28.2	Ditto, except different sample.
	A-7727*	14,915±75	-27.9	Ditto, except different sample.
	A-7716*	15,045±80	-26.7	Ditto, except different sample.
	UGA-6822*	14,610±180	-29.4	Ditto, except different sample.
	UGA-6921*	14,520±105	-26.0	Ditto, except different sample.
	UGA-6933*	14,915±105	-26.4	Ditto, except different sample.
	UGA-6983*	15,260±115	-28.4	Ditto, except different sample.
	UGA-6823*	15,050±180	-27.4	Large wood piece (25 cm) on old land surface on surface of Dalcahue organic bed at location A.
	UGA-6824*	14,700±170	-27.6	Same wood piece as UGA-6823.
	UGA-6825*	14,620±180	-27.6	Same wood piece as UGA-6823.
	UGA-6918*	14,480±180	-28.1	Organic silt and fine sand encasing wood of UGA-6823.
	UGA-6922*	14,995±100	-26.8	Uppermost 2 cm of organic silt from Dalcahue organic bed, 1 m south of location A (Fig. 31).
	UGA-6971	15,530±130	-26.6	Organic silt from 10-11 cm depth in Dalcahue organic bed 1 m south of location A (Fig. 31).
	UGA-6981	16,170±115	-26.4	Organic silt from 16-17 cm depth in Dalcahue organic bed 1 m south of location A (Fig. 31).
	UGA-6975	17,450±130	-25.3	Organic silt from 34-35 cm depth in Dalcahue organic bed 1 m south of location A (Fig. 31). Counted twice.
		16,810±130	-25.9	
	UGA-6982	17,595±130	-26.3	Organic silt from 42-44 cm at base of Dalcahue organic bed 1 m south of location A (Fig. 31).
	UGA-6977	18,305±190	-24.6	Organic silt from 42-44 cm at base of Dalcahue organic bed 1 m south of location A (Fig. 31).
	UGA-6978	18,085±135	-26.3	Organic silt from 45 cm at base of Dalcahue organic bed 1 m south location A (Fig. 31).
	UGA-7052	15,280±125	-28.3	Organic silt from 5 cm depth at location A in Dalcahue organic bed (Fig. 31). See Heusser *et al.* (1996).
	UGA-7053	15,975±145	-26.8	Organic silt from 10 cm depth at location A in Dalcahue organic bed (Fig. 31). See Heusser *et al.* (1996).
	UGA-7056	17,000±145	-28.0	Organic silt from 40 cm depth at location A in Dalcahue organic bed (Fig. 31). See Heusser *et al.* (1996).
	UGA-7058	17,365±130	-25.5	Organic silt from 50 cm depth at location A in Dalcahue organic bed (Fig. 31). See Heusser *et al.* (1996).
	UGA-7059	18,990±165	-25.6	Organic silt from 55 cm depth at location A in Dalcahue organic bed (Fig. 31). See Heusser *et al.* (1996).
	A-6189*	14,720±100	-27.8	Organic silt from uppermost 1 cm of Dalcahue organic bed at location B in Figure 31. See Heusser *et al.* (1996).
	A-6190	14,770±110	-27.7	Ditto, except different sample.
	UGA-6955	18,445±140	-25.7	Organic silt from 56-58 cm depth in the Dalcahue organic bed at location B (Fig. 31).

Site No.	Lab. No.	Age ^{14}C yr BP	δ^{13}C (‰)	Description
	UGA-6956	19,550±160	-26.9	Ditto, except different sample. Collected to check consistency of dates of organic silt samples collected at same depth.
	UGA-6957	17,965±135	-25.0	Ditto, except different sample.
	UGA-6958	18,675±145	-26.0	Ditto, except different sample.
	UGA-7004	18,365±145	-25.6	Ditto, except different sample.
	UGA-7005	18,865±180	-25.0	Ditto, except different sample.
	UGA-7006	18,910±145	-26.0	Ditto, except different sample.
	UGA-6960	18,295±150	-26.4	Ditto, except different sample.
	A-6191	21,070±280	-26.3	Organic silt from 60-62 cm depth at the base of the Dalcahue organic bed at location B (Fig. 31).
	A-6319	19,290±230	-26.1	Ditto, except different sample.
	AA-19423	15,742±100	-26.7	Organic silt from 14 cm depth in the Dalcahue organic bed at location B (Fig. 31). This sample, and all the others taken below, are from a section cut back 1.5 m from the original face, from which all the samples listed above from location B were collected. Here the organic bed is 154 cm thick.
	AA-19424	16,284±111	-26.1	Ditto, except sample from 18 cm depth.
	A-7689	$17{,}345^{+125}_{-120}$	-25.6	Ditto, except sample from 23 cm depth.
	AA-19425	19,577±162	-25.9	Ditto, except sample from 46 cm depth.
	A-7690	$20{,}645^{+225}_{-220}$	-25.8	Ditto, except sample from 58 cm depth.
	AA-19427 R	19,970±150	-25.5	Ditto, except sample from 64 cm depth.
	AA-19428 R	20,060±185	-25.5	Ditto, except sample from 72 cm depth.
	AA-19429	20,712±613	-25.2	Ditto, except sample from 80 cm depth.
	AA-19430	20,658±146	-26.0	Ditto, except sample from 81 cm depth.
	AA-19432	22,070±176	-25.5	Ditto, except sample from 98 cm depth.
	A-7683	22,690±135	-25.9	Ditto, except sample from 100 cm depth.
	AA-19433	21,434±199	-25.5	Ditto, except sample from 109 cm depth.
	AA-19434	21,972±229	-25.7	Ditto, except sample from 110 cm depth.
	AA-19435	21,027±186	-25.4	Ditto, except sample from 113 cm depth.
	AA-19436 R	25,176±237	-26.4	Ditto, except sample from 133 cm depth.
	AA-19438	28,558±366	-26.4	Ditto, except sample from 151 cm depth.
	A-7685	$30{,}070^{+225}_{-215}$	-26.5	Ditto, except sample from 151 cm depth.
	AA-19439	27,910±315	-26.5	Ditto, except sample from 152 cm depth.
99	A-8535R	$13{,}785^{+170}_{-165}$	-29.4	a. Organic silt with macrofossils from 6.24-6.29 m depth in 6.45-m core through mire in kettle on upper lip of ice-contact slope. Minimum age for ice recession from moraine on top of ice-contact slope.
	QL-4531	$27{,}550^{+1600}_{-1300}$	-22.7	b. Organic clast reworked into ice-contact stratified drift on upper lip of ice-contact slope. Maximum age for ice advance to top of ice-contact slope.
	QL-4532	14,820±450	-24.7	Ditto, except different sample.
	UGA-6972	21,080±220	-25.0	Ditto, except sample split and dated twice.
		20,030±160	-25.0	
	UGA-6979	19,840±180	-24.6	Ditto, except different sample.
100	AA-20370	14,941±97	-30.0	Mayol. Clay gyttja from 3.70 m depth in 3.75-m core to base of mire on Llanquihue moraine (Heusser *et al.* 1999).
101	TUa-258A	13,345±105	-25.8	Estero Huitanque. Organic matter from near base of core through mire on Llanquihue moraine. (Heusser *et al.* 1995).
	Beta-62029	14,350±240	—	Ditto, except different sample.
102	T-10307 A	13,560±95	-28.2	Peat from base of 3.0 m peat deposit in trough between two Llanquihue-age till flutes. (Lowell *et al.* 1995).
103	Beta-10481	13,040±210	—	Basal date of 2.80-m core at Puerto Cármen (Villagrán 1988).
104	Beta-10485	13,100±260	—	Date of peat from about 4.35 m depth in a 5-m core at Laguna Chaiguata (Villagrán 1988).
105	RL-1892	12,310±360	—	Cuesto Morenga. Peat over drift. Minimum date for deglaciation of site (Heusser 1990).